TWO DIMENSIONAL STRESS-STRAIN RELATIONSHIPS OF A FINE ASPHALT-AGGREGATE SYSTEM

JULY 1965
NO. 12

Joint Highway Research Project

by

N. B. LAL

PURDUE UNIVERSITY
LAFAYETTE INDIANA

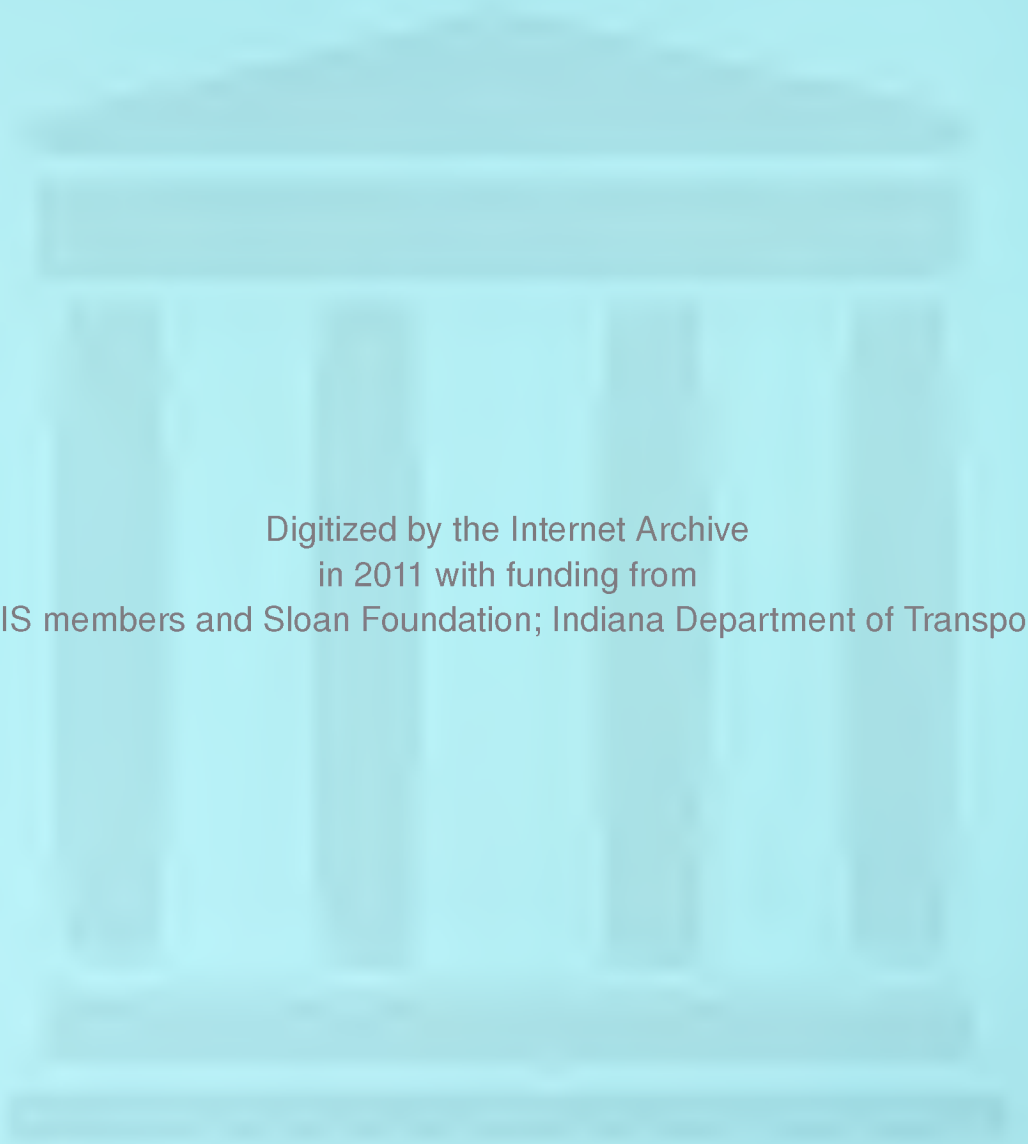

Digitized by the Internet Archive
in 2011 with funding from
LYRASIS members and Sloan Foundation; Indiana Department of Transportation

http://www.archive.org/details/twodimensionalst00laln

Final Report

TWO-DIMENSIONAL STRESS-STRAIN RELATIONSHIPS

OF A FINE AGGREGATE-ASPHALT SYSTEM

May 18, 1965

File: 2-4-22
Project: C-36-6V

To: K. B. Woods, Director
Joint Highway Research Project

From: H. L. Michael, Associate Director
Joint Highway Research Project

Attached is a report entitled "Two-Dimensional Stress-Strain Relationships of a Fine Aggregate-Asphalt System." The report was prepared by Mr. N. B. Lal under the direction of Professor W. H. Goetz and with the assistance of Professor M. E. Harr. Mr. Lal used this report as his thesis for the Ph. D. degree.

Respectfully submitted,

Harold L. Michael
Secretary

HLM:kr

Attachment

cc: P. L. Ashbaucher
J. R. Cooper
W. L. Dolch
W. H. Goetz
W. L. Grecco
F. F. Havey
F. S. Hill
G. A. Leonards
J. F. McLaughlin
F. B. Mendenhall
R. D. Miles
R. E. Hills
J. C. Oppenlander
W. P. Privette
M. B. Scott
J. V. Smythe
E. J. Yoder

Final Report

TWO-DIMENSIONAL STRESS-STRAIN RELATIONSHIPS OF A FINE AGGREGATE-ASPHALT SYSTEM

by

N. B. Lal
Research Assistant
Joint Highway Research Project

File: 2-4-22
Project: C-36-6V

Purdue University
May 1965

ACKNOWLEDGMENTS

The author expresses his sincere appreciation to Professor W. H. Goetz, his Major Professor and Professor M. E. Harr for their expert guidance and constant encouragement throughout the study.

Thanks are due to Professor E. O. Stitz and Mr. Egons Tons for their generous help in the experimental techniques involved in this study.

Last but not the least, the author is grateful to the Joint Highway Research Project, Professor K. B. Woods, Director, for providing financial support for this research program.

TABLE OF CONTENTS

	Page
LIST OF TABLES	v
LIST OF FIGURES	vi
ABSTRACT	ix
INTRODUCTION	1
REVIEW OF THE LITERATURE	4
OUTLINE OF THE INVESTIGATION	17
Purpose	17
Scope	18
Methods of Testing	18
Uniaxial Tension Tests	19
Simple Shear Tests	22
Axial Compression Tests	26
PROCEDURE AND EQUIPMENT	27
Uniaxial Tension Tests	27
Simple Shear Tests	35
Axial Compression Tests	40
TEST RESULTS AND DISCUSSION	47
Uniaxial Tension Test Results	49
Discussion of Uniaxial Tension Test Results	58
Simple Shear Test Results	64
Discussion of Simple Shear Test Results	69
Axial Compression Test Results	71
Discussion of Axial Compression Test Results	71
SUMMARY OF TEST RESULTS	79
DISCUSSION OF STRESS-STRAIN EXPRESSIONS	82

Page

CONCLUSIONS 86

SUGGESTIONS FOR FURTHER RESEARCH 88

LIST OF REFERENCES 90

APPENDIX A. Equations of Motion in Two Dimensions 93

APPENDIX B 96

Uniaxial Tension Tests 96
Preparation of Specimens 96
Curing of Specimens 97
Capping of Specimens 98
Testing of Specimens 99
Simple Shear Tests 103
Preparation of Specimens 103
Curing of Specimens 103
Cementing of Specimens 103
Testing of Specimens 104
Axial Compression Tests 105
Preparation of Specimens 105
Curing of Specimens 105
Testing of Specimens 106

APPENDIX C. Derivation of Stress-Strain Expressions 107

Derivation of Normal Tensile Stress-Axial Strain Relationship as Function of Time and Temperature 107
Derivation of Normal Tensile Stress-Circumferential Strain Relationship as Function of Time and Temperature 116
Derivation of Shear Stress-Shear Strain Relationship as Function of Time and Temperature 120

APPENDIX D. Materials Used in the Study 126

VITA 130

LIST OF TABLES

Table — Page

1. Axial Strain - Time Relationships for Uniaxial Tension Tests 53

2. Circumferential Strain - Time Relationships for Uniaxial Tension Tests 57

3. Shear Strain - Time Relationships for Simple Shear Tests 68

4. Sieve Analysis of Sheet-Asphalt Mixture Percent by Weight 128

LIST OF FIGURES

Figure — Page

1. Simple Shear Test Results, Deformation of Moveable Plate at Different Times Under Constant Load vs. Specimen Thickness 25
2. Uniaxial Tension Test Specimen with Split Mold and Plungers 28
3. Double Plunger Compaction Device with Mold and Plungers in Position 29
4. Capped Tension Test Specimen with Split Aligning Block, Caps and Hand Level 30
5. Diagrammatic Sketch Showing Instrumentation of a Uniaxial Tension Test 31
6. Uniaxial Tension Test in Progress 32
7. Typical Data Sheet for Uniaxial Tension Test 33
8. Deformations at Different Points Along Height of Specimen . . 34
9. Typical Simple Shear Test Specimens with Forming Mold and Plungers 36
10. Diagrammatic Sketch Showing Instrumentation of a Simple Shear Test 37
11. A Simple Shear Test in Progress 38
12. Typical Data Sheet for Simple Shear Test 39
13. Hollow Cylindrical Specimen for Axial Compression Test with Split Mold and Plungers 42
14. Diagrammatic Sketch Showing Instrumentation for Change in Thickness Measurements in Axial Compression Test 43
15. Hollow Cylindrical Specimen with Appurtenances Used for Axial Compression Test 44

Figure Page

16. Axial Compression Test in Progress 45

17. Typical Data Sheet for Axial Compression Test 46

18. Uniaxial Tension Test Results, Axial Strain vs. Time Curves, Temperature 40°F 50

19. Uniaxial Tension Test Results, Axial Strain vs. Time Curves, Temperature 77°F 51

20. Uniaxial Tension Test Results, Axial Strain vs. Time, Temperature 100°F 52

21. Uniaxial Tension Test Results, Circumferential Strain vs. Time Curves, Temperature 40°F 54

22. Uniaxial Tension Test Results, Circumferential Strain vs. Time Curves, Temperature 77°F 55

23. Uniaxial Tension Test Results, Circumferential Strain vs. Time Curves, Temperature 100°F 56

24. Poisson's Ratio (ν) at 40°F 61

25. Poisson's Ratio (ν) at 77°F 62

26. Poisson's Ratio (ν) at 100°F 63

27. Simple Shear Test Results, Shear Strain vs. Time Curves, Temperature 40°F 65

28. Simple Shear Test Results, Shear Strain vs. Time Curves, Temperature 77°F 66

29. Simple Shear Test Results, Shear Strain vs. Time Curves, Temperature 100°F 67

30. Axial Compression Test Results, Axial Strain vs. Time Curves, Temperature 40°F 72

31. Axial Compression Test Results, Axial Strain vs. Time Curves, Temperature 77°F 73

32. Axial Compression Test Results, Axial Strain vs. Time Curves, Temperature 100°F 74

33. Axial Compression Test Results, Circumferential Strain vs. Time Curves, Temperature 40°F 75

Figure Page

34. Axial Compression Test Results, Circumferential Strain vs. Time Curves, Temperature 77°F 76

35. Axial Compression Test Results, Circumferential Strain vs. Time Curves, Temperature 100°F 77

36. Uniaxial Tension Test Results $1/k_2$ vs. σ_z 109

37. Uniaxial Tension Test Results Log $[I(T)/S(T)]$ vs. Log (T) . . 111

38. Uniaxial Tension Test Results Log $[1/S(T)]$ vs. Log (T) . . . 113

39. Uniaxial Tension Test Results $1/k_2'$ vs. σ_z 117

40. Uniaxial Tension Test Results Log $[I'(T)/S'(T)]$ vs. Log (T) 118

41. Uniaxial Tension Test Results Log $1/S'(T)$ vs. Log (T) ... 119

42. Simple Shear Test Results $1/k_2''$ vs. σ_z 122

43. Simple Shear Test Results Log $[I''(T)/S''(T)]$ vs. Log (T) . . 123

44. Simple Shear Test Results Log $[1/S''(T)]$ vs. Log (T) 124

45. Gradation Curve for Sheet Asphalt Mixture 129

ABSTRACT

Lal, Narindra Bansi. Ph.D., Purdue University, June 1965. Two-Dimensional Stress-Strain Relationships of a Fine Aggregate-Asphalt System. Major Professor: William H. Goetz.

The study was undertaken to provide the equations necessary to solve a two-dimensional deformable system for a sheet-asphalt mixture knowing the boundary conditions imposed on the material. Whereas the two general two-dimensional equations of motion involve five unknowns, three independent equations were sought to solve the system completely.

The required three equations were determined on the basis of experimental data obtained from two different types of laboratory tests. Uniaxial Tension and Simple Shear tests were chosen for this purpose.

The Uniaxial Tension tests were performed on cylindrical specimens by subjecting them to constant stress at constant temperature and observing the axial and circumferential strains with time. The tests were repeated under different stresses at three temperatures. On the basis of the data obtained from these tests, an equation relating stress (σ_z) to axial strain (ϵ_z) was derived. The equation had the following form:

$$\sigma_z = \left(\frac{T}{c_1}\right)^{-c_2} - \left(\frac{T}{p_1}\right)^{-p_2} \frac{\epsilon_z}{t\,\frac{\partial \epsilon_z}{\partial t}} \; ; \; 40^\circ F \leq T \leq 100^\circ F$$

where t stands for time, T for temperature and c_1, c_2, p_1, p_2 are four material constants. A similar expression relating stress (σ_z) to

circumferential strain (ϵ_y) was also obtained from the results of these tests.

The Simple Shear tests were performed on thin rectangular specimens by subjecting them to constant shear stress at constant temperature and observing the shear strain with time. The tests were repeated under different stresses at three temperatures. On the basis of these tests, an expression relating shear stress to shear strain was obtained in the same form as given above for Uniaxial Tension tests.

The four material constants as found from the stress-strain expressions derived from the above two types of tests were independent of time and temperature. Since the values of these material constants as determined from the two series of tests were in close agreement, it was indicated that these are independent of the type of test.

Axial Compression tests were performed on hollow-cylindrical specimens to compare the results with those predicted on the basis of the corresponding Uniaxial Tension tests. It was found that for small strains of less than about 0.4 percent, the two tests gave very close results. For large strains, whereas the strain (ordinate)-time (abscissa) plot on log-log scales tended to curve upward at the beginning of failure conditions in Uniaxial Tension tests, the corresponding plots for Axial Compression tests tended to curve downward to lesser slopes, at about the same time.

It was concluded that three independent stress-strain relationships exist as functions of time and temperature. These expressions contain four basic material constants which are independent of time and temperature and type of test.

INTRODUCTION

Bituminous concrete has long been used as a part of the section of flexible pavements. However, in the past it has been used principally for the upper layer or layers of the system. Until fairly recently, even when the bituminous portion was of substantial thickness, it was looked upon as part of the surfacing. Therefore, its load distribution value has been relegated to a secondary consideration and strength design of the material has been considered principally with respect to its internal stability. However, with the expanding use of bituminous mixtures as load-distributing layers, i.e., the use of asphalt in the lower layers of the system, it becomes imperative to be able to evaluate them in regard to all aspects of their strength properties.

The current testing methods for bituminous concrete are very much restricted in scope in the sense that they do not take into account the fundamental properties of a mix. In most cases, the criteria for design is based on empirical test values obtained by arbitrarily assigned deformation rates and temperatures. As a consequence, the resultant test values do not relate the properties of the mix even as well as do the modulus of elasticity and Poisson's ratio for steel. However, the principles of elasticity have been used by engineers for designing flexible pavements (1).

It is now well-known that bituminous concrete is neither purely elastic nor purely plastic but is viscous as well as elastic, and that the stress-strain relationships are functions of time and temperature.

Those parts of these stress-strain relationships which are independent of time and temperature are material constants, and if these are true material constants, should be independent of the size and shape of the specimen and also of the type of test.

Considerable work has been done (2, 3, 4) to show that asphalt cements when loaded show elastic,retarded elastic and viscous behavior. Based on the evidence that elastic response as well as viscous behavior is exhibited by asphalts, several attempts have been made during the last decade to predict the behavior of bituminous concrete by one-dimensional mechanical models consisting of elastic springs and viscous dashpots. So far, no single model, even in a one-dimensional sense, has been found to predict accurately the behavior of bituminous mixtures.

Instead of such a one-dimensional approach to the study of the behavior of bituminous mixtures it appears much more realistic to approach the problem by starting from the completely general equations of equilibrium (Appendix A) of a two-dimensional system. These equations of motion follow directly from Newton's second law of motion and this approach is completely general in the sense that it is applicable to any homogeneous and isotropic material. To render a two-dimensional system solvable, in addition to these two equations of motion which contain five unknowns, three more equations are needed. It is the purpose of this investigation to determine if these three equations can be obtained from relevant experimental data relating stress to strain as a function of time and temperature.

Any true material constants should be reflected in these stress-

strain relationships. For a particular bituminous mix, these constants should be independent of the type of test.

This study was undertaken to determine and verify such material constants and to obtain the three equations necessary for a system of five equations containing five unknowns.

REVIEW OF THE LITERATURE

This review of the literature is concerned mainly with the deformation characteristics of bituminous mixtures, for pre-failure conditions, and the test methods adopted for determining these characteristics. While reviewing the research done in this area, only the work aimed at an understanding and prediction of the behavior of bituminous mixtures has been considered pertinent.

Milburn (6) describes a deformation test for proportioning mineral aggregate and asphalt so that the mixture may best withstand high temperature. The test consists in subjecting specimen, 1-inch high by 1 1/4-inch in diameter to a constant load at a constant temperature for a definite length of time, and determining the decrease in height of the specimen. It was concluded that the correlation of specific gravity results of the compressed specimens with deformation results can be used for the design of bituminous mixtures of the sheet asphalt type.

Emmons and Anderton (7) describe a test developed to correlate service behavior with laboratory evaluation. Specimens were compressed by means of a power tamping device and were 8 x 6 x 2 1/4 inches in size. The specimen, heated to 140°F and confined in a mold, was subjected to pressure that caused a portion of the material to be extruded from openings in the bottom and ends of the mold. Curves indicate that the test is sensitive to variations in composition of bituminous mixtures and is suitable for the investigation of both fine and coarse-graded mixtures.

Kriege and Gilbert (8) deal with factors controlling the deformation of bitumen-aggregate mixtures under traffic conditions. Emphasis is laid on having moving loaded wheels as deforming agents rather than static loads. For this purpose, a modified Dorry Hardness Machine was used for a study of the resistance of such mixtures to deformation. The depth and location of deformation was recorded. Failure was considered to occur when the gradually increasing tendency to rut was suddenly greatly accelerated.

Vokac (9) gives a test method which he claims will produce a definite measure of a mixture's tendency to deform i.e., shove in service. The method consists in compacting specimens between opposed plungers in a 2-inch cylinder using a load of 500 psi and testing with a Page Impact testing machine. It was found that the number of blows required to cause failure when plotted against the height from which the hammer falls gives a straight line on a log-log plot. The slope of this straight line is the "Index of Deformation" which is an indication of the tendency the mixture will have to shove in a surface under traffic.

Vokac (10) also gives data showing the usefulness of compression testing of asphalt paving mixtures. With the data given by him, the fundamental characteristics such as modulus of elasticity in compression, compressive strength and elastic limit may be evaluated. Specimens were tested by applying loads at a uniform rate of deformation, and also by applying a uniform rate of increase of load. A rate of deformation of 0.05 in.per minute was found practical in the application of loads for a uniform rate of deformation. The author states that, with appropriate treatment of the data, "it is indicated that the stress characteristics of samples with miscellaneous heights and densities as

obtained in coring a pavement surface, may be evaluated on a strictly comparable basis."

Lee and Markwick (11) found that three stages occurred during the process of deformation of bituminous mixture specimens subjected to tensile and shear tests. The first stage related to the initial rapid rate, the second to the decreased rate with time and the third one, the almost constant rate of deformation, was taken as a measure of resistance of the material to deformation. The one-dimensional Burgers' model of elastic springs and viscous dashpots was found to have a qualitative agreement in its behavior to the behavior of bituminous surfacing mixtures under load. Three types of tests, viz. uniform tension, uniform shear and bending of beams, were performed at constant stress; deformation-time curves were obtained in each case. Since, for any one material, similar curves were obtained by the three tests, the authors considered it reasonable to infer that the same property of the material was measured in each case.

Lee, Warren and Walters(12) discuss their work on the flow properties of bitumen and bitumen-aggregate mixtures. The tensile test was selected for studying the flow properties of mixtures because the material is subject to constant uniform stress, the test results are independent of the dimensions of the specimen and they can be expressed quantitatively. A relationship between stress and minimum rate of strain (11) is given by $R = ks^p$, where R is the minimum rate of strain, S is the applied stress and k and p are constants. The above relationship gives parallel straight lines on a log-log plot over the investigated temperature range and p is thus considered a fundamental material property termed "plastic flow index." The value of k represents the minimum rate of deformation

at unit stress and is thus termed the "mobility." An equation giving the relationships between "k" and temperature over a range of about 25°C is given.

Pfeiffer (13) explains the underlying theory of the so-called "cell test" in which the plastic nature of bituminous mixes is fully taken into account. According to the author, "little value can be attached to the figures found by determining the compressive strength of cubes in the usual way." As to Vokac's paper (10), the author says, "the conclusion in the synopsis of his article, viz. 'that the stress characteristics of samples with miscellaneous heights and densities may be evaluated on a strictly comparable basis,' is evidently invalid."

As to the tensile and bending tests, the author says, "the behavior of a bituminous composition on elongation is a property which is at least as important in judging the suitability of bituminous road mixtures as the compressive strength. It was shown by Lee and Markwick, among other investigators, that when a road sample is bent, which is the most frequent cause of rupture in road carpets, tensile stresses are the most important factors. Bending tests have the drawback, however, that they produce such a complicated distribution of stresses that even with normally elastic materials, it is impossible satisfactorily to analyze the symptoms in question. Any attempt to do so with such a complicated mixture as a bituminous road carpet is, therefore, doomed to fail."

Hillman (14) uses the flexure test to study the essential characteristics of bituminous paving mixtures. The objective of his investigation was to study the effect of different variables upon test results obtained with laboratory specimens subjected to bending tests. The machine used for these bending tests is described in detail.

These flexure tests of bituminous mixtures under a constant rate of loading show that the modulus of rupture and modulus of elasticity both increase as rate of stress increases.

Mack (15) presents the theoretical aspects of the mechanical properties of bituminous pavements comprising load-carrying capacity, flow property and elasticity. He used a compression machine to investigate the deformation of cylindrical specimens under constant load as a function of time. A straight line relationship on a log-log plot was found to exist between height of the compression specimen at any time and time. However, only short times were considered. The determination of the rheological properties of bituminous mixtures was also carried out by subjecting the specimen to successive compressive loads. It was found that each successive loading renders bituminous mixtures more resistant to flow indicating work-hardening due to repeated compressions. He found that increasing the degree of plasticity of asphalts increases the resistance to flow of bituminous mixtures, increases the stresses obtained at a given deformation, decreases the rate of dissipation of stresses, and decreases elasticity at 50°F but has practically no effect on elasticity at 60°F and higher.

Nijboer (16 and 17) describes a bitumen-aggregate mixture as a plastic material with viscous properties and analyzes its resistance to plastic flow. The triaxial test is used to measure magnitudes of the physical properties describing the material. Simple rules have been given on the basis of relevant experimental work showing the variation in mixture properties as a result of composition variables. Regarding practical applications, in some cases the viscous property of the material cannot be used to meet external stresses, whereas in

others it would lead to permissible deformations. Bituminous mixtures, according to the author, can be designed accordingly.

Mack (18) emphasizes the importance of taking the time function into consideration for the measurement of the load-bearing capacity of road structures. Results from compression tests carried out on cylindrical briquettes indicate the bearing strength of bituminous pavements under the influence of load and time. "The non-recoverable part of deformation obeys the following equation: $\frac{S}{S_o} = \left(\frac{Vt}{V_o t_o}\right)^b$

where S = stress, either compressive, tensile or shearing,

V = strain or shear rate,

S_o = stress which brings about the lowest observable strain rate V_o,

t = time,

t_o = time at V_o

b = a numerical constant."

The results illustrate the known hardening of asphalt pavements under the influence of traffic. To further illustrate the deformation mechanism of bituminous mixtures, the author gives data from bending tests performed by Hillman (14). According to the equations given, the author says "the stress is a function of the strain-rate and time, hence the strain-rate depends not only on the stress but also on the time and the deformation of an asphalt pavement is influenced by previous operations, because the number of particles moving decreases with each deformation." Equations have been given by the author for the recoverable deformation as a function of time and also of the non-recoverable deformation as a function of time.

Van der Poel (19) describes a simple general system in the form of a nomograph by means of which the deformation of bitumens can be calculated as a function of stress, time and temperature. Both static creep tests as well as dynamic tests with an alternating stress of constant amplitude were performed in this work. Two log-log plots 1) stiffness modulus for static creep tests against time and 2) stiffness modulus for dynamic tests against $\frac{1}{w}$, where $w = 2\pi \times$ frequency, were drawn using the same scales. In both cases, almost identical curves were obtained. To quote the author, "Thus, for practical purposes, the difference between the two loading procedures largely disappears and we will, therefore, not distinguish between them further."

Nijboer (20) describes the characteristics of asphalts and aggregates which affect both the elastic and plastic behavior of mixtures. He compares test results under short duration loadings with those derived from long-duration loadings. The mixture was found to show plastic properties on long-term loading in triaxial tests, while asphalt properties on short-duration loadings seemed to approach those of an elastic material. The compressive and tensile strengths increased with increasing rate of deformation and the maximum stress was obtained at a constant deformation of material amounting to 2.5 to 3.5% in compression and 1.5 to 2.0% in tension, both at higher temperatures. These values decreased by one-third at lower temperatures. It was further found that elastic recovery of the material was fairly complete up to 1% deformation and independent of temperature and hardness of binder.

Mack (21 and 22) observed that the deformation of bituminous mixtures consists of an instantaneous elastic strain, independent of

time, and retarded elastic deformation followed by a plastic deformation, whose rate decreases with time, and which determines the mechanical behavior of a mixture. The "coefficient of plastic traction" (i.e., stress divided by strain rate) increases with increasing compressive strength and time as a result of a hardening process which accompanies the plastic deformation of a mixture. The author emphasizes the importance of the consideration of time in the testing methods for bituminous mixtures, for the deformation of bituminous pavements is a function of time.

Wood (23) in the first part of his study on stress-deformation characteristics of asphaltic mixtures, gives a general relationship between maximum unconfined compressive strength, temperature and rate of deformation, as a result of unconfined compressive strength tests on sand-asphalt. In the second part of his study, unconfined repeated load tests were performed and according to the author "the data suggest that the elastic portion of the deformation takes place principally in the polymolecular film of asphalt which surrounds the aggregate particles." It was found that a stress, termed "Endurance Limit" could be cycled a number of times without causing excessive shear deformations. This concept of "Endurance Limit" was confirmed by performing confined, repeated-load tests.

McLaughlin (24) deals with some load-carrying characteristics of a bituminous concrete overlay. Relationships between strength and rate of deformation and temperature were investigated by compression tests on laboratory specimens compacted by different methods as well as by compression tests on pavement cores. As a result of repeated-load tests on pavement cores, it was found that the cumulative permanent

deformation, y, is given by $y = kx^{1/n}$ where x is the number of load repetitions and k, n are constants; i.e., cumulative permanent deformation and the number of load repetitions show a straight line relationship on a log-log plot.

Goetz, McLaughlin and Wood (25) give "relationships among the factors governing the load--carrying characteristics of bituminous mixtures that should provide a basis for the better understanding of the properties of the material." For sheet-asphalt mixtures, a relationship between maximum unconfined compressive strength and rate of deformation and temperature was found, which was also applicable for bituminous concrete mixes. Also, repeated-load tests were performed on laboratory-prepared specimens as well as pavement cores. Relationships between cumulative permanent deformation and number of load applications are given as a straight line on a log-log plot, for slow-cycle tests as well as for rapid-cycle tests. The authors observe that "the results of repeated-load tests on bituminous mixtures suggest that this type of test might provide valuable information concerning the plastic nature of the mixture and, in addition, give a measure of its endurance limit (18)."

Wood and Goetz (26) give data on compressive creep loading of sand-asphalt mixture specimens which indicate the same trend as observed by Mack (21, 22). On unloading, instantaneous recovery, retarded recovery and permanent deformation were observed. A Burgers' model was used to find that, in a restricted sense, the laws of linear viscoelasticity were obeyed.

Secor and Monismith (27, 28) give data from triaxial compression test results in creep, stress relaxation and repeated load for one

bituminous mixture. Comparisons between predicted data using a four-element model consisting of Hookean springs and Newtonian dashpots, and actual test data showed errors less than 30 per cent.

Hargett and Johnson (29) performed Tension and Compression tests on specimens 4 inches in diameter and 4 inches high, compacted by a mechanical compactor. They found that the two bituminous mixtures were quite sensitive to elongating deformation. It was found that an elongating deformation of 1 inch in 60 produced failure, whereas a deformation of 1 inch in 20 produced failure in compression.

Krokosky (30) presents curves for the non-linear characteristics (for linear characteristics, the mechanical model should consist of only linear springs and dashpots filled with a Newtonian fluid) of asphalt/aggregate compositions. He attempted to separate the non-linear effects from the linear effects.

Pister and Monismith (31) emphasize the importance of time-dependent material properties and loading conditions in pavement design methods. Data are given showing visco-elastic behavior of bituminous mixtures under different types of loading. Some mechanical models are discussed in representing the visco-elastic material properties.

Monismith and Secor (32) in continuation of their earlier work in the field, applied viscoelastic analysis to the prediction of deflections of slabs made of a test mixture and placed under static loading on an elastic foundation. Discrepancy was found to exist between theory and experimental data, but it was attributed to the fact that the analysis was based on a simple extension of elastic theory.

Papazian (33) expresses visco-elastic stress-strain laws with the coefficients called the complex moduli of the material, considered

fundamental material constants, based on the assumption that asphaltic concrete is linearly visco-elastic. Regarding his data, the author says "for the levels of stress used in these tests, asphaltic concrete is a reasonably linear material." Dynamic tests were run on unconfined cylindrical specimens by subjecting them to sinusoidal stresses of several amplitudes and frequencies and the resultant axial and circumferential strains studied. Electrical strain gages (SR-4) were used to measure the axial and circumferential strains. Also, static tests were run on unconfined specimens to determine the complex moduli. Under "Interpretation," the author says "when the stresses become excessive, or when the deformations are not small, ultimate strength concepts may have to be used in the evaluation of a given material. Such an evaluation may involve the determination of the shearing strength of the material, as defined by cohesion and angle of internal friction."

Davis, Krokosky and Tons (34) give the rheological properties of asphaltic concrete by tension tests at constant strain rates. Tension tests were run on cylindrical specimens 2 inches in diameter and 5 inches high at three asphalt contents, four temperatures ranging from -20°F to +120°F and three different strain rates. It was concluded by the authors that the bituminous mixtures showed non-linear visco-elastic behavior. A method of evaluation of non-linearity is presented.

Huang (35) continued the work of Wood and Goetz (26) to find the influence of type and amount of bitumen, level of stress and density on the deformation characteristics of sand-bitumen mixtures under constant compressive stress. A hypothesis is put forward which says that the deformation of a bituminous mixture under constant stress is

comprised of two parts, 1) "work-hardening deformation" which strengthens the specimen and which is present under low levels of stress or short loading times and 2) "work-softening deformation" which weakens the specimen and which is present under high levels of stress and long loading times. Expressions for these two types of deformations are given separately in terms of stress, time and constants. An expression for the total deformation is also given.

Monismith, Secor, and Secor (36) in this study deal with the investigation of the development of thermal stresses and deformations in asphalt concrete, under controlled conditions. Creep tests in tension at constant temperature as well as variable temperatures were performed, among other tests. It was found that the material can be considered thermorheologically simple (i.e., the relaxation modulus curves are shifted only along the time axis by a temperature change), at least to a first approximation. It was found possible to predict stresses or deformations resulting from temperature changes by creep data using visco-elastic theory. Also, thermal stresses in a slab were determined knowing the temperature distribution, coefficient of thermal expansion and relaxation modulus for various temperatures.

It appears from this review of the literature that the determination of fundamental properties of bituminous mixtures, independent of any boundary conditions on the material, is being increasingly emphasized. This is a step in the right direction towards a rational design of bituminous mixtures to replace the current empirical methods.

However, most of the research work done recently, with the objective of finding the fundamental properties of the material, is based on the theory of visco-elasticity. Various attempts have been

made, assuming the asphalt-aggregate mixture as a linearly visco-elastic material to find stress-strain laws by fitting data in one-dimensional models consisting of Hookean springs and Newtonian dashpots. It is now well-known that an asphalt-aggregate mixture is not a linearly visco-elastic material, and no single model has thus far been found which predicts the behavior of bituminous mixtures accurately.

At this stage of our knowledge of the material, a more fundamental approach to the problem seems desirable. One can start from the completely general two-dimensional equations of motion derived from Newton's second law of motion. These two equations contain five unknowns. Hence, if three more equations relating the unknowns can be found, a two-dimensional deformable system of any bituminous mixture may be rendered completely solvable.

OUTLINE OF THE INVESTIGATION

This investigation was undertaken with a view to finding basic material constants for bituminous mixtures under load which would be independent of the type of test and any boundary conditions imposed on the material.

A fundamental approach to the problem, by starting with the completely general equations of motion of a two-dimensional deformable system (Appendix A), appeared to be the most appropriate line of attack. To render this two-dimensional deformable system solvable, relevant experimental data had to be obtained for which some preliminary investigations as to the type of tests and the measurements involved therein had to be carried out.

This section deals with the precise purpose of the study, its scope and the various testing methods used in the preliminary investigation.

Purpose

The precise purpose of this study was to determine and verify material constants which would be independent of the type of test and to derive independent stress-strain relationships which are necessary to render a two-dimensional system of the sheet-asphalt mixture solvable.

Starting with the two equations of motion in two dimensions containing five unknowns, three more independent equations relating the unknowns needed to be obtained. To achieve this, relevant experimental data were obtained and applied to relate stresses with strains as functions

of time, temperature and material constants.

The material constants obtained in this way, if indeed they are constants, should be independent of the type of test or any boundary conditions imposed upon the material, and therefore, capable of verification.

Scope

This investigation is limited to a laboratory study of a sheet-asphalt mixture (Appendix D). This fine-graded mixture was selected to approach, as closely as possible, a homogeneous and isotropic condition required for the application of the afore-mentioned theory.

The material was tested for the evaluation of constants, at three temperatures: 40°F, 77°F and 100°F. These temperatures cover the range which available equipment provided. From a practical standpoint, tests at these three temperatures should be sufficient for the evaluation of theoretical considerations.

The material constants as determined from one type of test are compared with those determined from other tests.

Methods of Testing

In order to obtain three equations required for completely solving the afore-mentioned two-dimensional deformable system, relevant experimental data had to be obtained from different types of tests. For this purpose two different laboratory tests, viz. Uniaxial Tension and Simple Shear tests, were chosen. To verify the material constants, as obtained from these tests, a third type of test, viz. Axial Compression test, was chosen. The considerations for the choice of these tests and the experimental techniques employed therein are given

below under separate headings for each test.

Uniaxial Tension Tests

To evaluate the material constants expected to be found in the relationships between normal stress and strains along and at right angles to the direction of application of stress, a Uniaxial Tension test was chosen. This was done because in such a test the shear stresses are zero and the material is intended to be subjected to normal tensile stresses only.

Under constant* tensile stress, at a constant temperature, the strains in the material were determined with time. A cylindrical specimen two-inches in diameter and four-inches high was subjected to constant stress and the elongation per inch as well as decrease in radius per inch was noted with time. To avoid the end-effects, the measurement of strains in the middle portion of the specimen was desirable. Also, to minimize the errors due to any possible eccentricity in the application of load, both the strains were measured at locations 180° apart in the middle portion of the specimen and their mean taken. In this way, by measuring the elongation of the middle one-inch portion and the reduction in diameter at the middle, plots of the axial strain versus time and lateral strain versus time, at constant tensile stress, were obtained. By repeating the above procedures for different

---

*In the absence of information about the actual stress distribution in the specimen, a uniform stress distribution over the cross-section has been assumed. Under a constant tensile load, as the diameter of specimen decreases with time, the tensile stress increases correspondingly. This increase in tensile stress, however, is very slight as is discussed under "Discussion of Uniaxial Tension Test Results." In the following pages, by "Stress" is meant the nominal stress i.e., total load divided by original cross-sectional area of the specimen.

temperatures, the relationships betweeen normal stress and the axial and lateral strains were obtained as functions of time and temperature and material constants evaluated.

The measurement of strains had to be done very carefully so as to make sure that the observed strains were really the actual strains in the material. As a preliminary study, the following techniques of measuring strains (37) were explored:

1. Electrical strain gage (SR-4)
2. Optical strain gage (Tuckerman strain gage)
3. Printing a grid on specimen
4. "Photostress" technique
5. Mechanical strain gages

The electrical strain gages (SR-4) were found not to be satisfactory for the following reasons: First, it was found that the portion of the specimen treated with cementing material was considerably stiffened compared to the rest of the specimen surface. Since the strain is measured over this stiffened material, it is not the true strain in the actual material as desired. Second, strains over 3/4 percent could not be measured satisfactorily because the gages seemed to start peeling off at that strain.

The Tuckerman optical strain gage was found to be much more satisfactory and accurate (readings up to 2×10^{-6} inch could be observed). It had the advantage over the electrical strain gage in the fact that the material over which the strain was to be measured was unaffected. For the axial strain measurements, a base length of one inch was used, while for lateral strain, the maximum base length that could be used was one-half inch. A base length of one-fourth inch was found to be

unstable at least for the specimen tested. The gages were mounted on the specimen by springs or rubber bands. Thus, to have four gages (two for the axial strain, 180° apart, and two for lateral strain 180° apart) in the middle portion of the specimen was not possible. Hence the use of Tuckerman optical strain gages was given up.

In the grid method of strain analysis a grid with 100 or more lines per inch is printed on the specimen so that the change in length of sides of a printed square along and at right angles to direction of application of stress can be noted. The grid is printed on the specimen by spraying a photosensitive material over the specimen; putting a negative of the grid in contact with the specimen and thus printing it by a photographic process. This method seems to have some promise and has the advantage of possibly measuring the relative movement of discreet aggregate particles in the mix compared to the matrix. The observations with time could be recorded as a series of pictures of the deforming grid on the loaded specimen. However the method could not be adopted for this study as the process of printing a grid on a circular surface is a highly specialized one and could not be accomplished locally.

The photostress method consists in applying a reflective aluminum paint over the surface of the specimen and putting a photo-elastic transparent material over it. Polarized light is thrown over the photo-stress material and the amount of strain determined by matching the observed color with standard colors. This method has the disadvantage of giving only the difference between the axial and the lateral strains and not these strains independently.

Of the mechanical methods available, Huggenberger Extensometers were tried but were found unsuitable for this material and for this particular

set-up which required four extensometers in the middle portion of the specimen.

A new simple mechanical device was developed, as explained in detail later, which worked very satisfactorily. This consisted of levers with pointed ends contacting the specimen and hinged for minimum friction. The hinges acted as fulcrums for the levers. Deformation of the specimen at the point in contact with the pointed end of the lever was recorded by a dial indicator attached to the lever end away from the specimen. Axial strain in the middle portion of the specimen was determined by the difference in deformations recorded by dial indicators attached to the levers 1 inch apart vertically. The readings of the dial indicators were estimated up to 0.00005 inch. Change in diameter at mid-height of specimen was recorded by dial indicators with their extensions, machined to fit the curved surface, resting directly on the specimen surface.

Simple Shear Tests

To evaluate the material constants expected to be found in the relationships between shear stress and shear strain, a Simple Shear test was chosen. This was done because in a Simple Shear test the normal stresses are zero, and the material is intended to be subjected to shear stress only. Under constant shear stress, at a constant temperature, the shear strains in the material can be determined with time.

By definition, shear strain is the change which a right angle undergoes from the unstrained position. Based on this, the first attempt to conduct a Simple Shear test was to make a specimen two inches square in cross-section with a 3/16 inch square hole in the center.

The specimen was subjected to pure shear by cementing two opposite faces to steel plates, fixing one and pulling the other with a constant load. The measurement was to be made by observing the change in the right angle of the hole with time. However, it was found extremely difficult to measure the angle with an accuracy of even one minute of arc because the sides of the square hole were not smooth enough. The change in the angle also could be measured indirectly by measuring the change in the lengths of the sides and the diagonal of the square hole. This involved very cumbersome calculations for each of the many observations to be taken at frequent intervals of time for each test.

A simpler and more direct means of determining shear strain as a function of time under constant stress was achieved by forming a specimen of appropriate thickness, fixing one face, and pulling the other parallel face under constant load. In deciding upon the thickness of specimens for these Simple Shear tests, the following points were considered:

1. Minimum amount of bending while the specimen is being subjected to simple shearing stress.
2. Non-interference of particles within the specimen.
3. Practicability of fabricating specimens with uniformity or homogeneity of compacted materials.
4. Ability to record the dilation of the specimen while undergoing shearing strain.

To take the above-mentioned points into consideration, specimens four inches long and two inches wide with varying thicknesses, viz. 2, 1, 1/2, 3/8, 5/16 and 1/4 inches were subjected to constant shear stress. This was done by cementing a steel plate to each face of the specimen with a formulation of epoxy resins and curing agent (See Appendix B).

One of the steel plates was held in a fixed position and the other was pulled by a constant dead load. The deformation with time of the movable plate in the direction of load application was recorded in 1/10,000 inches. A plot of the deformation of the movable plate vs. thickness at different times is shown in Figure 1.

It can be seen from this plot that the amount of bending moment induced in the specimen increases with increasing thickness. Thus, to minimize bending and approach the conditions of a pure shear test as closely as possible, the minimum practical thickness of specimen should be adopted.

For many purposes it is considered that the minimum dimension of a test specimen should be no less than three times the maximum size of aggregate in the text mixture. The largest size fraction of aggregate in the test mixture passed a No. 8 sieve (with an opening of 0.0937 inch) and was retained on a No. 16 sieve. This fraction constitutes only 7 percent by weight of mixture. With a specimen thickness of 1/4 inch, the maximum size of aggregate, according to the above rule, comes out to be 0.0833 inch. Since only 1 1/2 percent of the particles in the test mixture were above this size, which is not significant as far as the interference of particles is concerned, and since it did not seem practicable to compact material uniformly at thicknesses less than 1/4 inch, this thickness was used.

Dilation measurements of the test specimen were attempted by measuring the movement of the plate in a direction at right angles to the direction of load application. In case of the 1/4 inch thick specimen, this deformation was considered to be negligible.

SIMPLE SHEAR TEST RESULTS

DEFORMATION OF MOVEABLE PLATE AT DIFFERENT TIMES UNDER CONSTANT LOAD vs. SPECIMEN THICKNESS

TEMP. = 77 °F

STRESS = 1.73 PSI

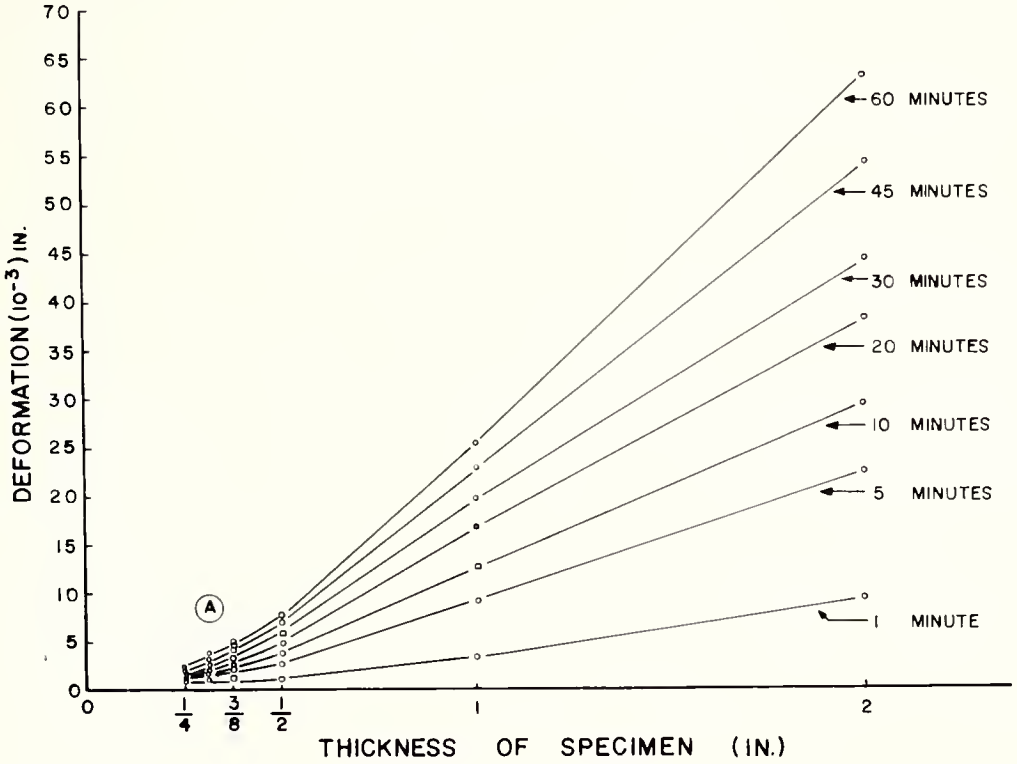

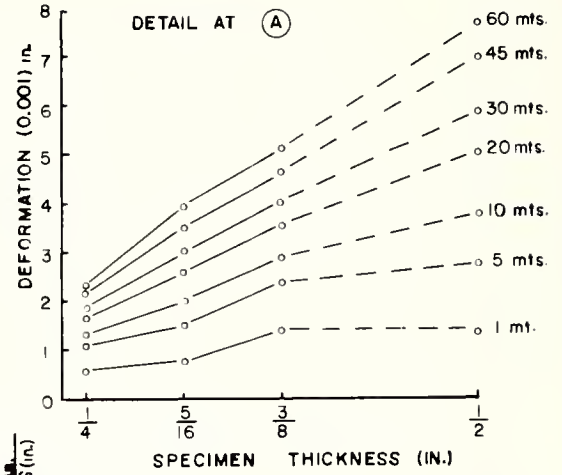

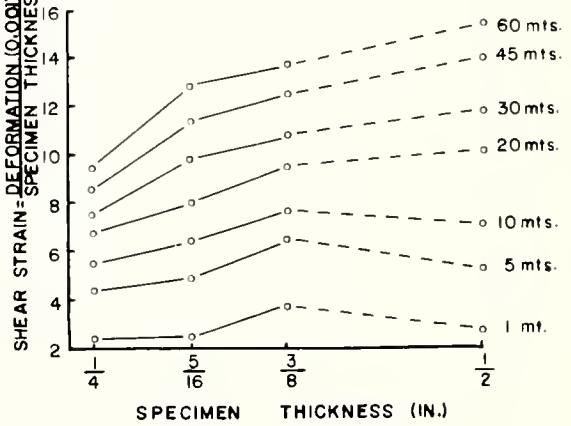

FIG. 1

Axial Compression Tests

In an attempt to verify the material constants, as obtained from the Uniaxial Tension and Simple Shear tests, a direct compression test was performed. In order to study the deformation of an element of the material, it seemed desirable to subject a hollow cylinder of the same mixture as used for tension and shear specimens to constant* compressive stress. The deformations of the material can be observed both in the axial as well as the lateral direction by noting the deformations on the inside as well as the outside of the hollow cylinder. The same instrumentation as developed for measuring axial deformations for specimens in Uniaxial Tension tests was applicable for axial deformation in these tests also. For measuring the change in inside diameter, a modification of this lever system using dial indicators was used.

---

*The compressive stress distribution over the cross-section of a specimen has been assumed to be uniform in the absence of information about the actual distribution. Under constant load, the area of cross-section increases with time, the increase being maximum in the middle, with the result that the magnitude of the compressive stress decreases. This decrease in compressive stress, however, is very small, as discussed under the "Discussion of Axial Compression Test Results". By "Stress" is meant "Nominal Stress", i.e., total load divided by the original area of the cross-section.

PROCEDURE AND EQUIPMENT

The procedures followed and the equipment used in this study are divided into:

1. Uniaxial Tension Tests
2. Simple Shear Tests
3. Axial Compression Tests

The details concerning the preparation of specimens, their capping or cementing to steel plates, curing and testing are given in Appendix B. In this section, a general description of the specimens and their testing is given for the above-mentioned tests.

Uniaxial Tension Tests

The Uniaxial Tension tests were performed on 2 inch diameter by 4 inch high cylindrical specimens of the sheet asphalt mixture. The specimens were compacted by the double-plunger method in a hydraulic compaction device. A typical cylindrical specimen, together with the split mold and two plungers used for molding the specimen, are shown in Figure 2. The compaction of a specimen in the hydraulic compaction device is shown in Figure 3. The specimen was cemented to caps at its ends by a formulation of epoxy resins the composition of which is given in Appendix B. In the capping operation, special care had to be taken so the caps would be properly aligned, vertically and horizontally, with the axis of the specimen so as to avoid eccentricity in loading. This was done by keeping the specimen within a tight-fitting split block, machined to fit the specimen with caps in position, while the epoxy was

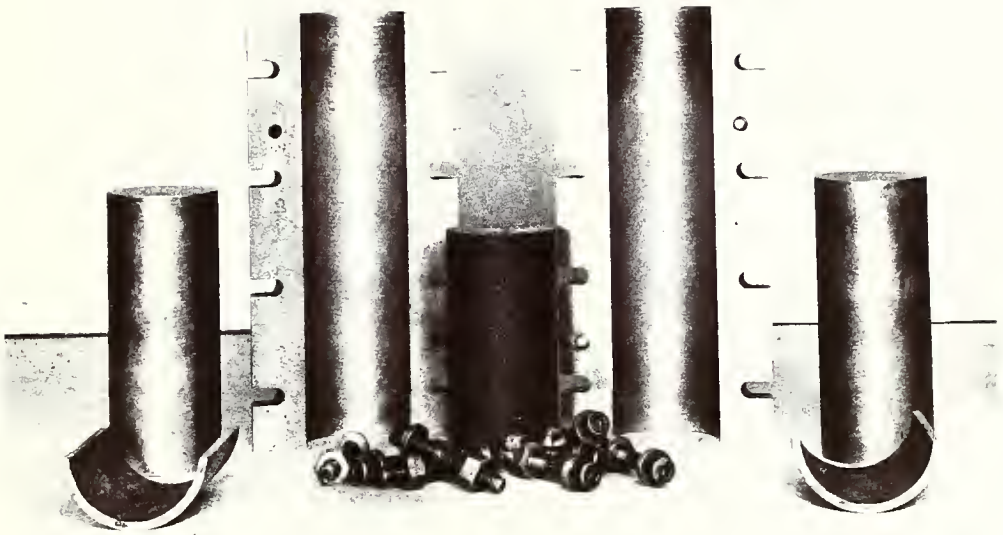

FIG. 2 UNIAXIAL TENSION TEST SPECIMEN WITH SPLIT MOLD AND PLUNGERS

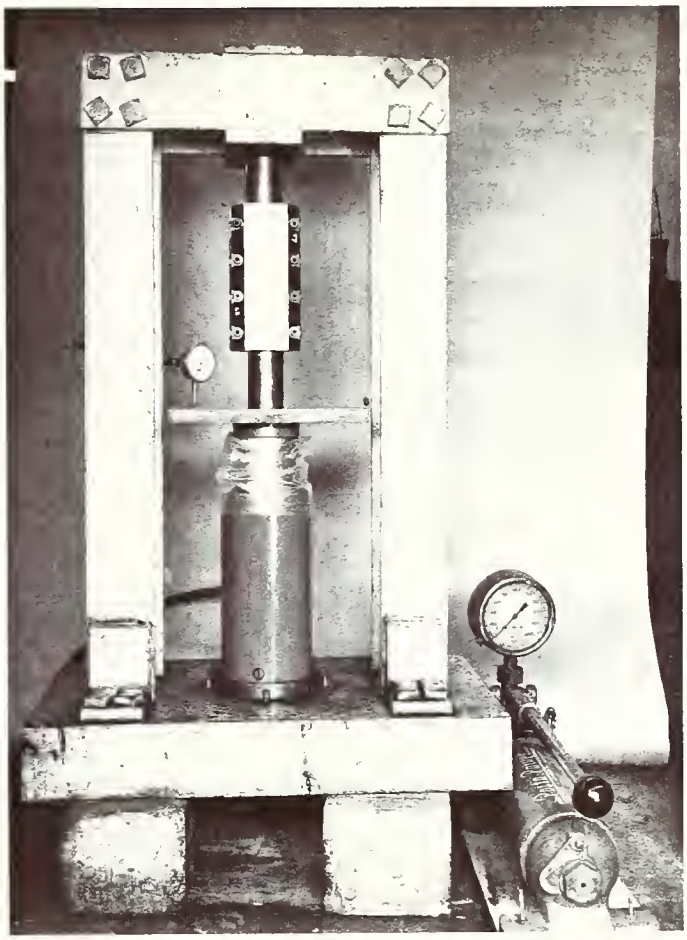

FIG. 3. DOUBLE PLUNGER COMPACTION DEVICE WITH MOLD AND PLUNGERS IN POSITION

FIG. 4. CAPPED TENSION TEST SPECIMEN WITH SPLIT ALIGNING BLOCK, CAPS AND HAND LEVEL

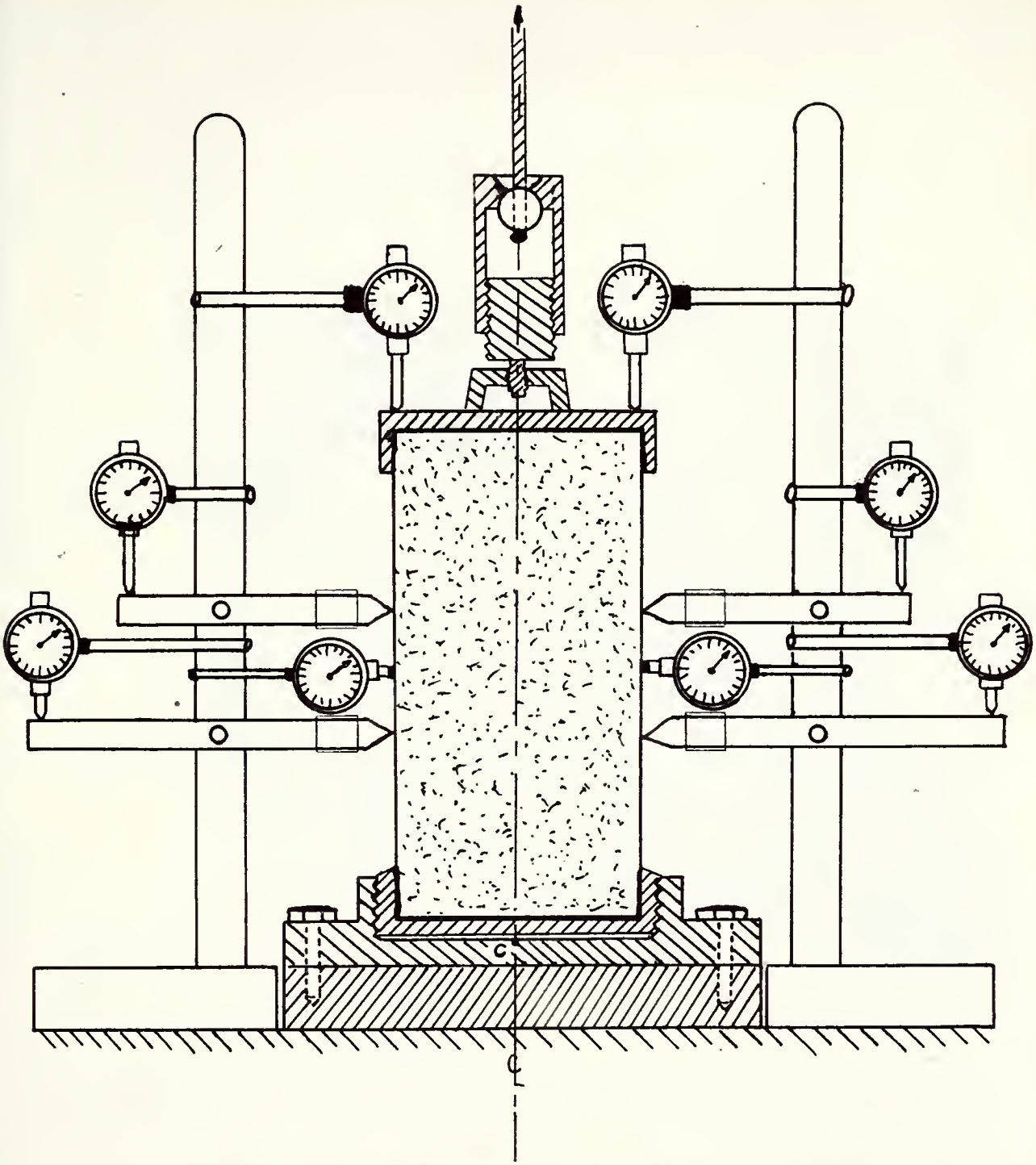

Figure 5. Diagrammatic Sketch Showing Instrumentation of a Uniaxial Tension Test.

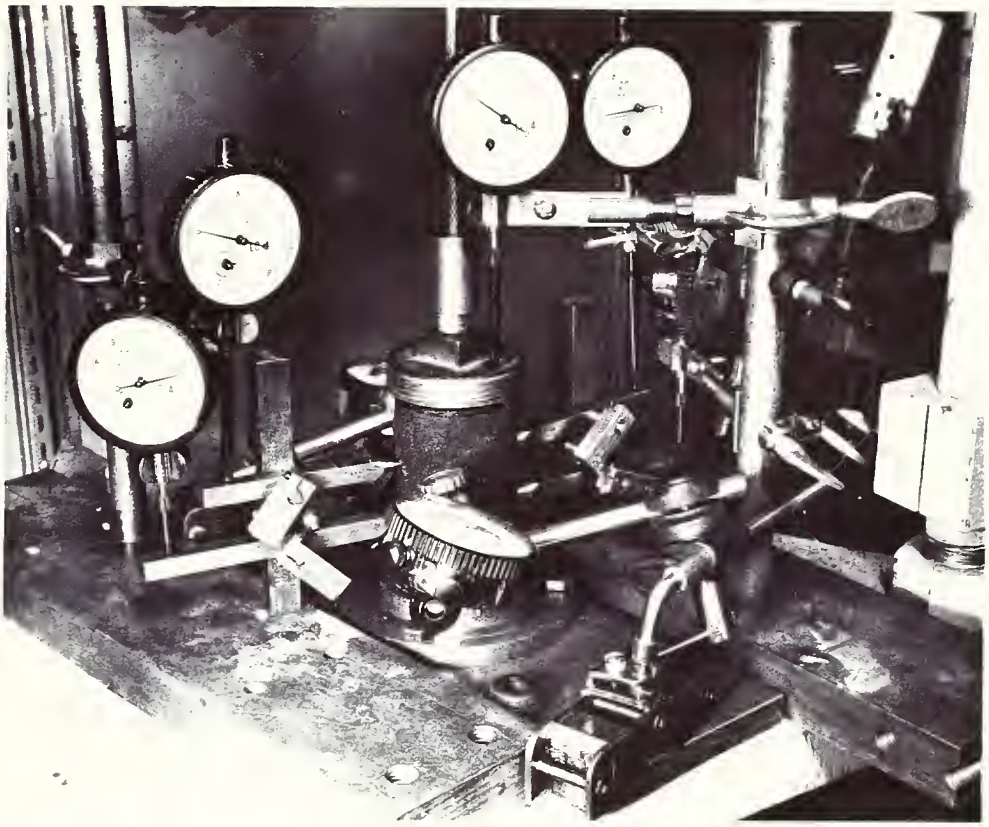

FIG. 6. UNIAXIAL TENSION TEST IN PROGRESS

Data Sheet

Uniaxial Tension Test

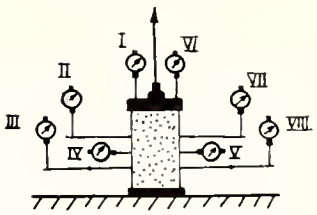

Temp. = 100°F

Stress = 2.43 psi

Time in Min.	Dial Indicator Readings (0.001 inch)							
	I	II	III	IV	V	VI	VII	VIII
0.0	10.20	59.30	47.20	34.35	34.05	9.90	64.10	51.00
0.5	23.05	55.20	43.60					
1.0				32.50	31.90			
1.5						28.50	58.90	47.35
2.0	34.50	52.50	41.45					
2.5				31.75	31.30			
3.0						36.30	57.00	46.40
3.5	41.60	50.80	40.05					
4.0				30.90	30.80			
4.5						42.55	55.60	45.60
5.0	47.60	49.40	39.15					
5.5				30.50	30.40			
6.0						48.00	54.50	44.85
7.0	55.10	47.90	38.10					
7.5				30.00	30.00			
8.0						55.50	53.25	44.00
10.0	66.60	45.40	36.50					
10.5				29.40	29.40			
11.0						67.00	51.60	42.95
12.0	75.00	43.85	35.45					
12.5				28.80	28.80			
13.0						75.70	50.05	42.20
15.0	90.10	41.05	34.35					
15.5				28.25	28.30			
16.0						92.20	47.75	41.15
19.0	107.50	36.10	32.60					
19.5				27.75	27.40			
20.0						108.50	42.60	39.20

Note: Deformations recorded by dial indicatore II and VII are to be multiplied by 2.

Figure 7. Typical Data Sheet for Uniaxial Tension Test

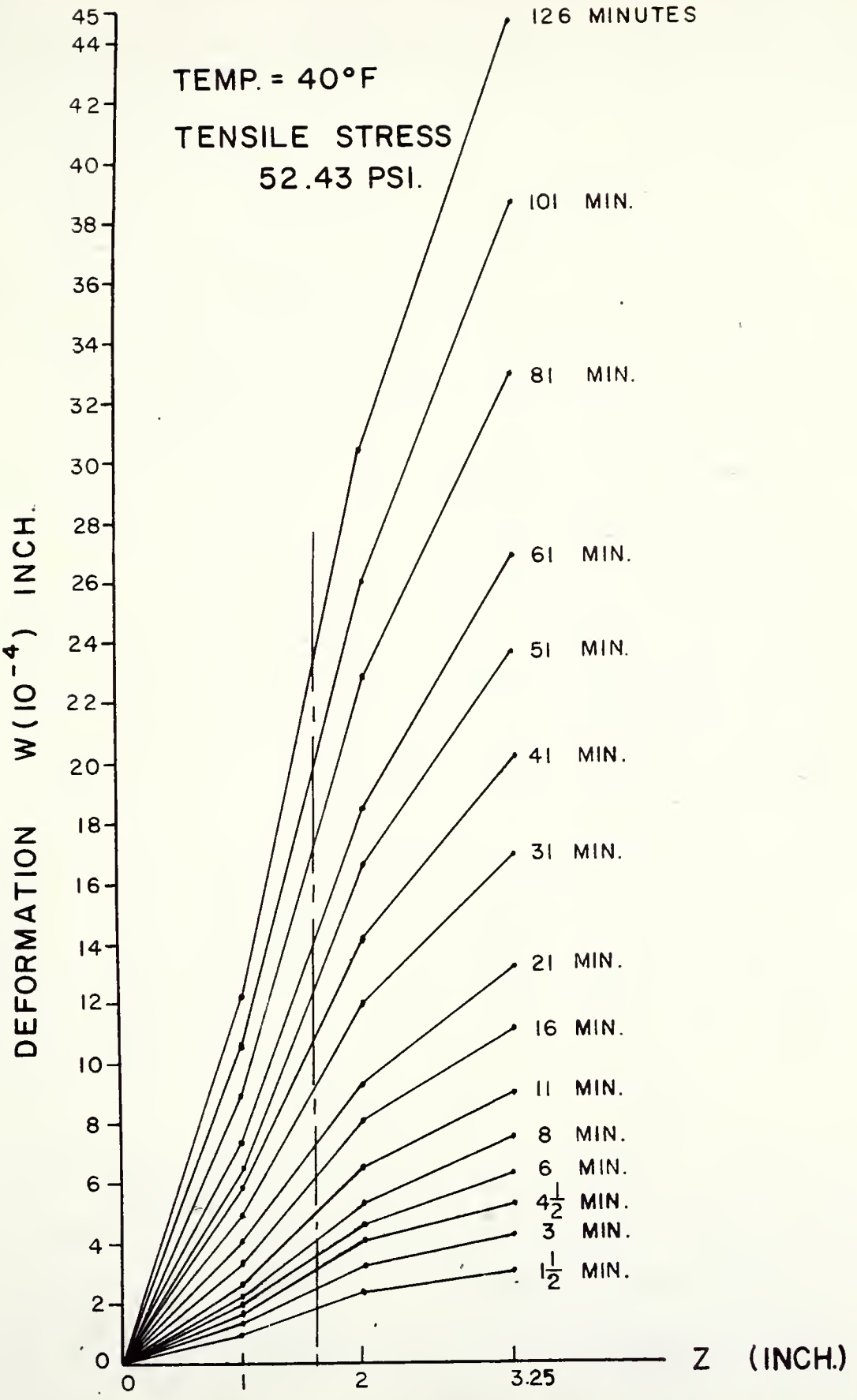

Figure 8. Deformations at Different Points Along Height of Specimen.

in the process of setting. The lower cap was machined to fit in the testing set-up and the upper cap had a hole machined exactly in the center to receive a swivel for loading the specimen. A capped specimen, along with the split block and caps is shown in Figure 4.

A diagrammatic sketch of the testing set-up is given in Figure 5 and a test in progress is shown in Figure 6.

The axial deformations in the specimen subjected to a constant tensile stress were measured by dial indicators and hinged levers with pointed ends contacting the specimen, as shown in Figures 5 and 6. The deformations of the levers, capable of rotating about the hinge acting as a fulcrum, were measured by dial indicators with a 0.0001 inch least division with readings estimated to one-half of these. The total axial deformations were also measured by dial indicators of the same accuracy. The decrease in diameter of the specimen was measured by similar dial indicators but had their extension ends machined to fit the curved surface of specimen.

The typical data sheet shown in Figure 7 gives the readings of different dial indicators at various intervals of time (without the deformations calculated from them). A typical plot of the deformations at different points along the height of specimen Z, at different times during the test is given in Figure 8.

Simple Shear Tests

The Simple Shear tests of the sheet asphalt mixture were performed on rectangular specimens 4 inches long, 2 inches deep and 1/4 inch thick. The specimens were compacted by the double-plunger method in the same hydraulic compaction device and to the same density as used for

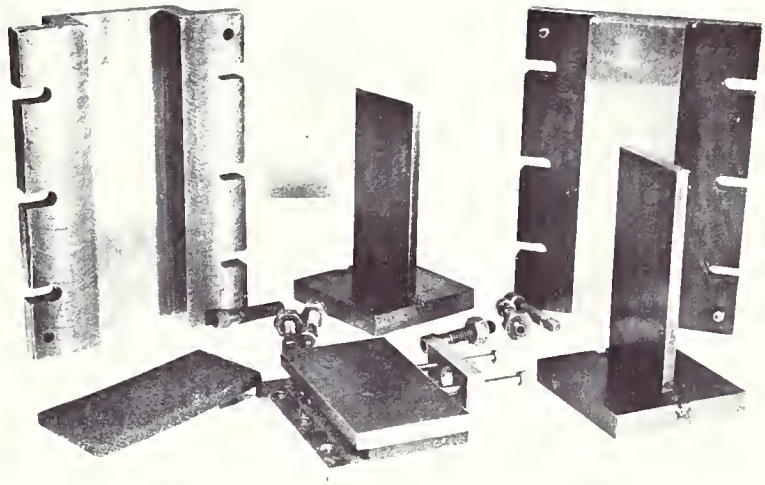

FIG. 9. TYPICAL SIMPLE SHEAR TEST SPECIMENS WITH FORMING MOLD AND PLUNGERS

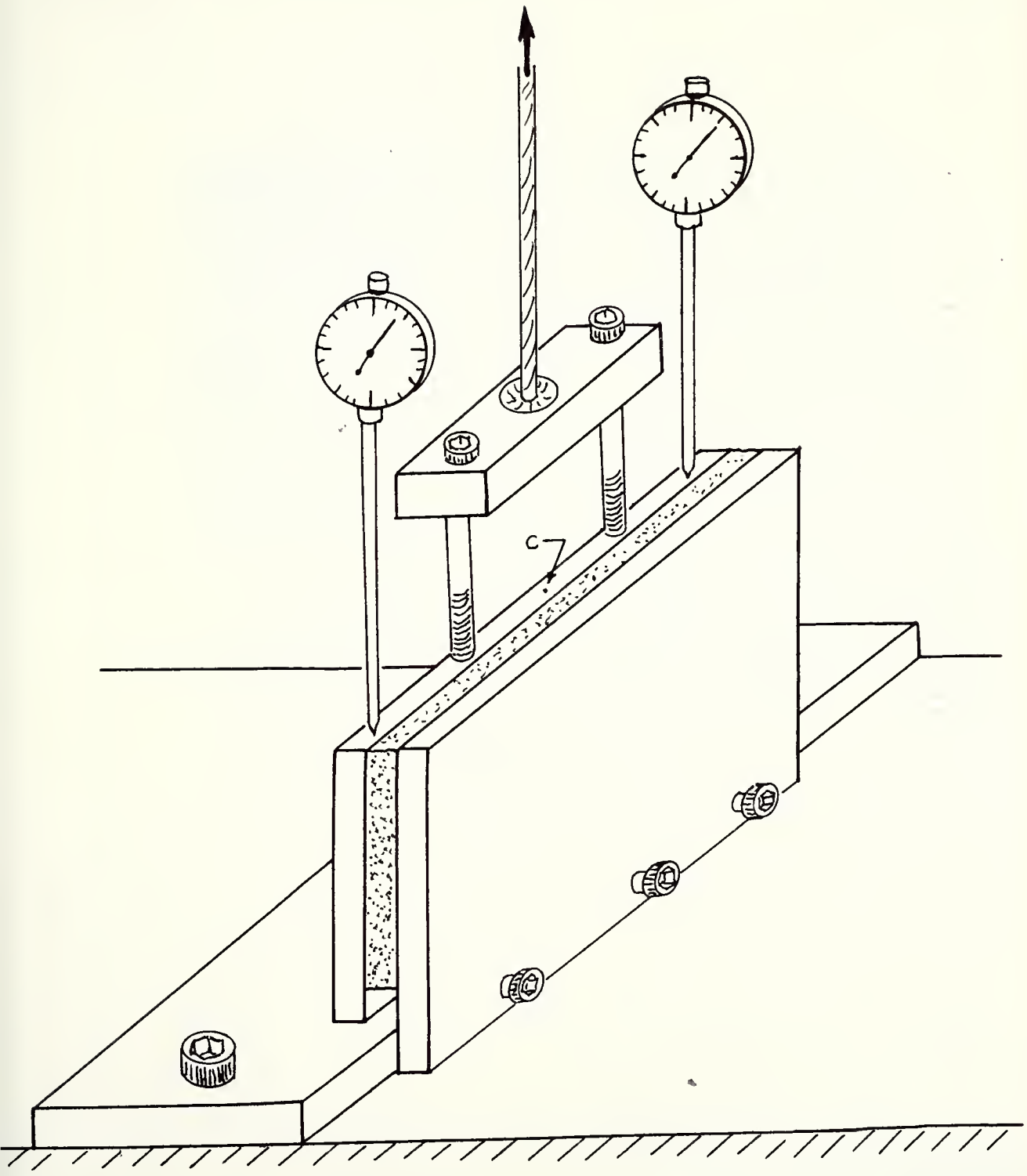

Figure 10. Diagrammatic Sketch Showing Instrumentation of a Simple Shear Test.

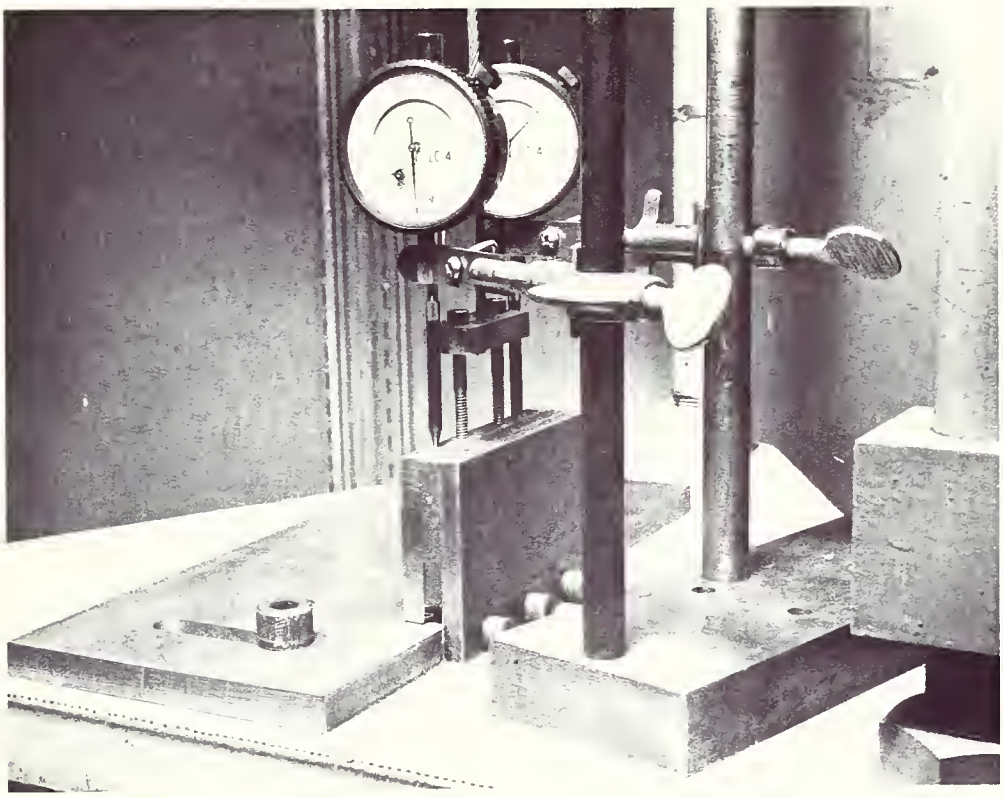

FIG. 11. A SIMPLE SHEAR TEST IN PROGRESS

Data Sheet

Simple Shear Test

Dial indicators I and II were placed equally distant from the center of the movable plate as shown in Figure 11.

Temp. = 100°F

Stress = 1.73 psi

Time in Minutes	Reading of Dial Indicator I	Deformation of Movable Plate 0.001 in.	Reading of Dial Indicator II	Deformation of Movable Plate 0.001 in.
0.0	14.0		17.70	
0.5	11.70	2.30	15.50	2.20
1.0	11.20	2.80	14.90	2.80
1.5	10.90	3.10	14.50	3.20
2.0	10.70	3.30	14.20	3.50
2.5	10.50	3.50	14.00	3.70
3.0	10.30	3.70	13.80	3.90
3.5	10.10	3.90	13.65	4.05
4.0	9.90	4.10	13.50	4.20
4.5	9.70	4.30	13.35	4.35
5.0	9.60	4.40	13.20	4.50
6.0	9.30	4.70	12.80	4.90
7.0	9.00	5.00	12.45	5.25
8.0	8.75	5.25	12.10	5.60
9.0	8.45	5.55	11.85	5.85
10.0	8.05	5.95	11.50	6.20
11.0	7.65	6.35	11.10	6.60
12.0	7.30	6.70	10.70	7.00
13.0	6.80	7.20	10.20	7.50
14.0	6.30	7.70	9.70	8.00
15.0	5.50	8.50	9.05	8.65

Figure 12. Typical Data Sheet for Simple Shear Test

Uniaxial Tension test specimens. A typical specimen along with the split mold and plungers, is shown in Figure 9. The specimen was cemented to steel plates on its parallel faces using the same composition of epoxy resins as used for Uniaxial Tension tests. A specimen so prepared also is shown in Figure 9. The steel plates were made parallel to each other by the use of a hand level.

A diagrammatic sketch of the testing set-up for the Simple Shear test is shown in Figure 10. One of the steel plates was fixed in position by bolting it to the fixed base plate. The other movable steel plate was subjected to a constant load applied through a swivel to avoid any bending. The deformation of the movable plate was recorded by two 0.0001-inch dial indicators placed at equal distance from the center of the plate or point of application of load. A test in progress is shown in Figure 11. A typical data sheet is shown in Figure 12. Each test was carried out for about two hours or until the time when failure was first indicated by the observation of cracks, whichever was shorter.

Axial Compression Tests

The Axial Compression tests were performed on hollow cylinders of the sheet asphalt mixture compacted to the same density as that of Uniaxial Tension or Simple Shear test specimens. The specimens were 4 inches high with a 2-inch outside diameter and 1-inch diameter hole. The split mold and plungers as used for Uniaxial Tension test specimens were used for these specimens also with slight modifications. One plunger was fitted with a 1-inch diameter rod coming out of it in the center and the other was provided with a corresponding hole to

accommodate the rod. The specimen was compacted by the double-plunger method. A compacted hollow cylindrical specimen with split-mold and plungers is shown in Figure 13.

A diagrammatic sketch of the testing set-up for the compression test is shown in Figure 14. The hollow cylindrical specimen was placed on a hollow steel cylinder, fitted with two levers hinged at their mid-lengths symmetrically about the axis. The upper ends of these levers were machined to fit the curved surface of the hole and the lower ends were located in front of small circular holes provided in the steel cylinder. Dial indicators, with their extensions going into these holes pressed against the lower ends of the levers. This made the upper ends of the levers press against the curved surface of hole at mid-height of specimen. Increase in the internal diameter of the specimen at its mid-height was thus recorded by the dial indicators. Change in the outside diameter was recorded by dial indicators in the same way as described for the Uniaxial Tension tests. The change in the external and internal diameters gave the change in thickness of specimen per inch which in turn, gave the circumferential strain. The axial strain in the middle 1-inch length of specimen was determined exactly in the same way as described for Uniaxial Tension tests.

The hollow steel cylinder with hinged levers is shown in Figure 15. Also shown are the steel discs with lubricated steel balls used at the ends of the assembly and a clamp to hold the specimen in position with the steel cylinder.

In Figure 16, the entire assembly is shown ready for test. A typical data sheet for an Axial Compression test is given in Figure 17.

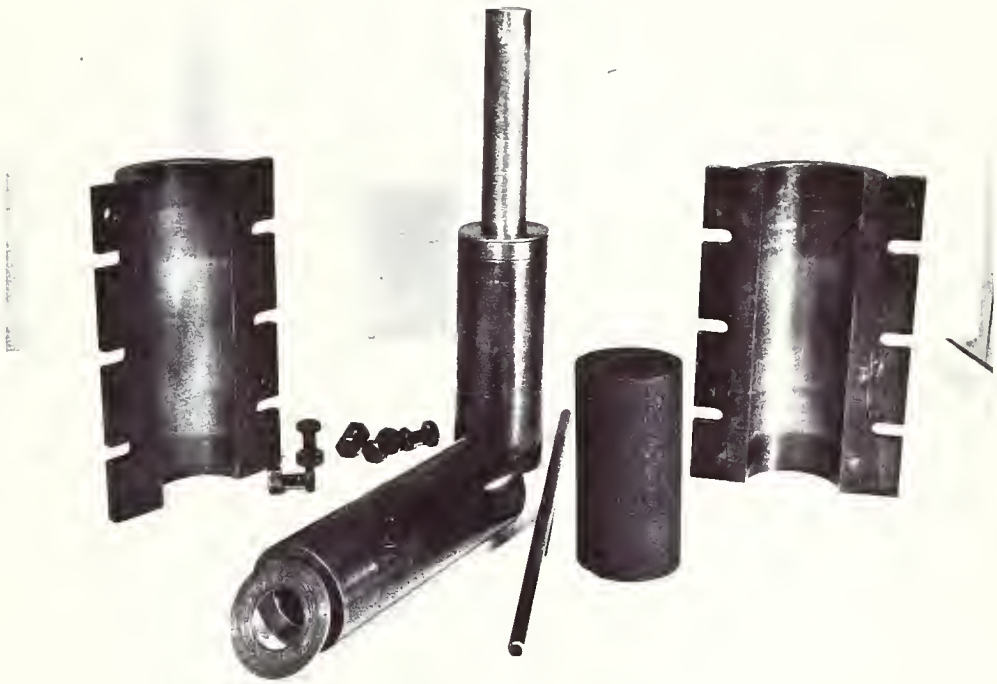

FIG. 13. HOLLOW CYLINDRICAL SPECIMEN FOR AXIAL COMPRESSION TEST WITH SPLIT MOLD AND PLUNGERS

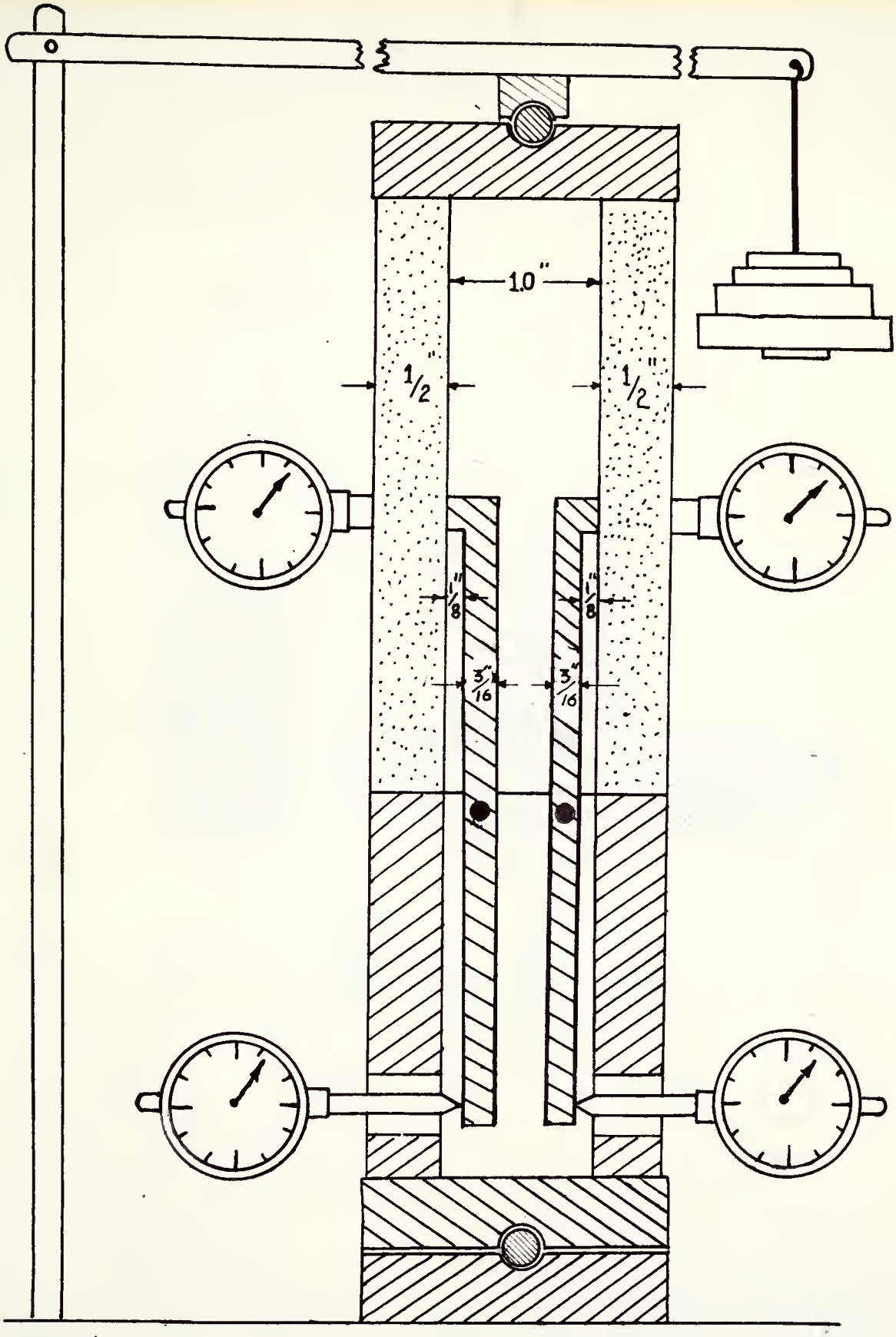

Figure 14. Diagrammatic Sketch Showing Instrumentation for Change in Thickness Measurements in Axial Compression Test.

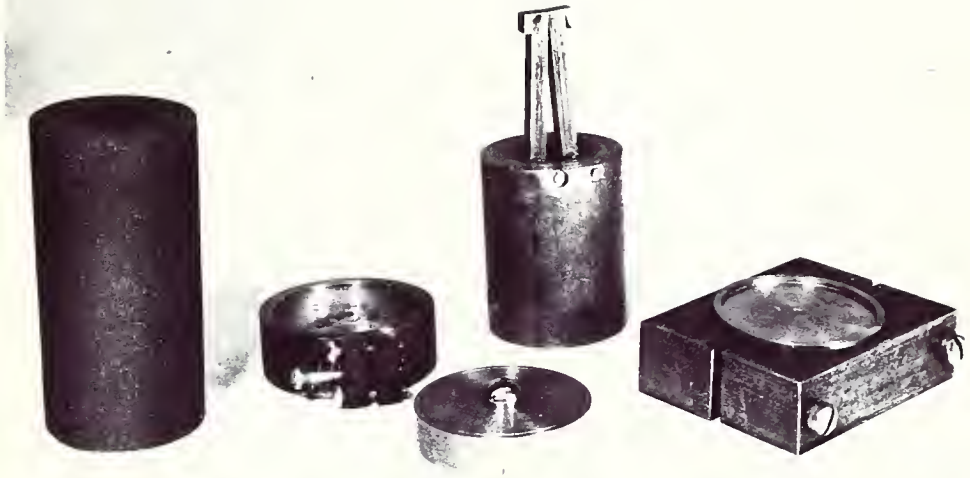

FIG. 15. HOLLOW CYLINDRICAL SPECIMEN WITH APPURTENANCES USED FOR AXIAL COMPRESSION TEST

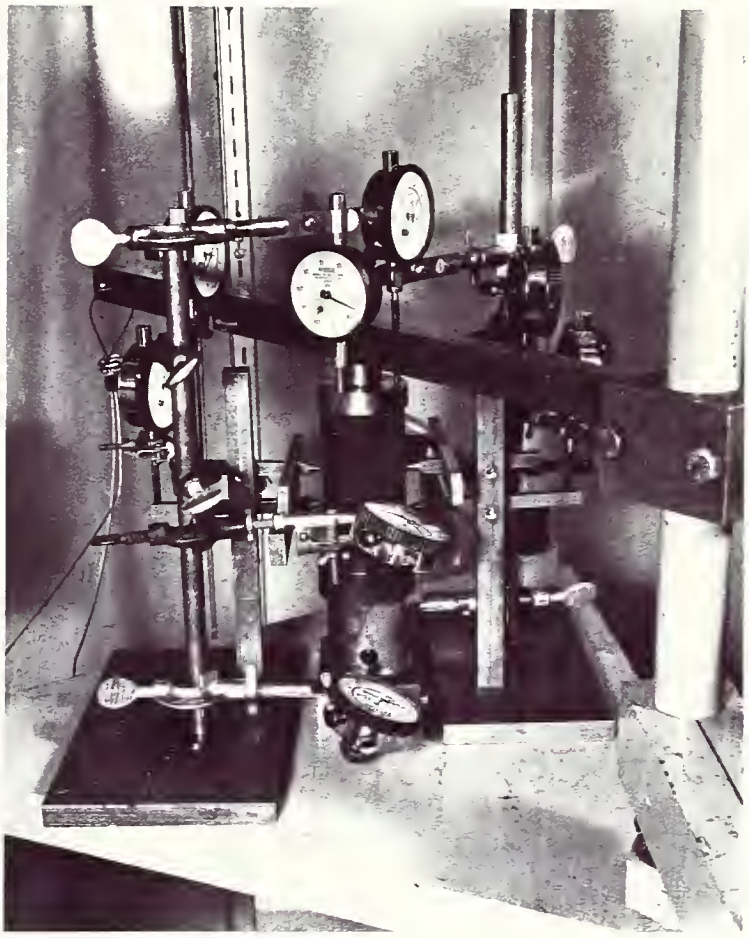

FIG. 16. AXIAL COMPRESSION TEST IN PROGRESS

Data Sheet

Axial Compression Test

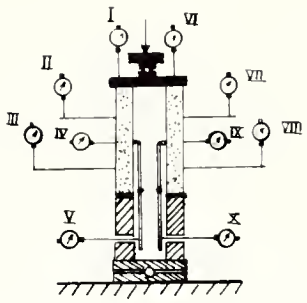

Temp. = 100°F Stress = 3.8 psi

Time in Min.	Dial Indicator Reading (0.001 inch)									
	I	II	III	IV	V	VI	VII	VIII	IX	X
0.0	67.80	23.40	35.80	21.80	14.70	59.00	42.30	59.45	35.30	28.70
0.5	51.00	29.30	41.00							
1.0				23.60	14.50					
1.5						37.00	49.30	45.45		
2.0									37.80	28.50
2.5	43.85	31.60	43.10							
3.0				24.90	14.45					
3.5						33.30	50.60	46.75		
4.0									38.90	28.40
4.5	41.15	32.40	43.80							
5.0				25.80	14.35					
5.5						31.00	51.55	47.50		
6.0									39.40	28.30
6.5	39.70	32.85	44.00							
7.0				26.50	14.20					
7.5						29.90	52.40	47.90		
8.0									39.90	28.10
10.0	37.90	33.45	44.80							
10.5				26.85	14.00					
11.0						28.00	52.55	48.45		
11.5									40.10	27.90
15.0	36.15	34.00	45.15							
15.5				27.10	13.75					
16.0						27.80	53.10	48.35		
16.5									40.40	27.70
20.0	35.15	34.40	45.75							
20.5				27.60	13.60					
21.0						25.50	53.55	49.35		
21.5									40.60	27.50
25.0	33.90	34.65	45.90							
25.5				27.80	13.45					
26.0						24.00	54.00	49.80		
26.5									40.80	27.40
31.0	32.90	35.05	46.50							
31.5				28.20	13.20					
32.0						23.00	54.15	50.10		
32.5									41.10	27.30
40.0	31.75	35.40	46.80							
40.5				28.55	12.95					
41.0						21.50	54.70	50.65		
41.5									41.30	27.20

Note: Deformations recorded by dial indicators II and VII are to be multiplied by 2.

Figure 17. Typical Data Sheet for Axial Compression Test

TEST RESULTS AND DISCUSSION

The following is the outline of different types of tests performed in this investigation including observations recorded under the influence of different variables:

I. Uniaxial Tension Tests

   a. Axial deformations observed with the following variables:

      1. Applied tensile stress

      2. Temperature

      3. Time

   b. Circumferential deformations observed with the following variables:

      1. Applied tensile stress

      2. Temperature

      3. Time

II. Simple Shear Tests

   a. Shearing strain observed with the following variables:

      1. Applied shear stress

      2. Temperature

      3. Time

III. Axial Compression Tests

   a. Axial deformations observed with the following variables:

      1. Applied compressive stress

      2. Temperature

3. Time

b. Circumferential deformations observed with the following variables:

1. Applied compressive stress

2. Temperature

3. Time

This outline is followed in presenting results in both graphical and tabular forms.

Uniaxial Tension Test Results

In the Uniaxial Tension tests, the axial and circumferential deformations, under different constant applied stresses and at different temperatures, were observed with time. Strains in the middle portion were calculated from deformations.

In Figures 18, 19 and 20, the axial strains have been plotted against time on a log-log scale for the constant tensile stresses, as indicated on the figures and at $40^{\circ}F$, $77^{\circ}F$ and $100^{\circ}F$, respectively. The results plotted on these figures are tabulated in Table 1. In this Table, the axial strain at one minute and the slope of the plot are given to characterize each log-log plot. This has been done because the relationship between axial strain (ϵ_z) and time (t) for the straight line portion of the plot can be written as $\log \epsilon_z = \log k_1 + k_2 \log t$ where constant k_2 is the slope of the line and constant $k_1 = \epsilon_z$ at $t = 1$ min.

The ratio of the change in diameter to the original diameter being equal to the ratio of change in circumference to original circumference, the observed change per inch of diameter of the specimen has been termed "circumferential strain".

The log-log plots of circumferential strain vs. time for the constant tensile stresses as indicated on the figures and at $40^{\circ}F$, $77^{\circ}F$ and $100^{\circ}F$ are given in Figures 21 to 23 and the results are tabulated in Table 2. The circumferential strain at one minute and the slope of the straight line portion of the log-log plot have been used to characterize each plot for the same reasons as explained for Table 1.

UNIAXIAL TENSION TEST RESULTS

AXIAL STRAIN vs. TIME CURVES

TEMPERATURE = 40°F

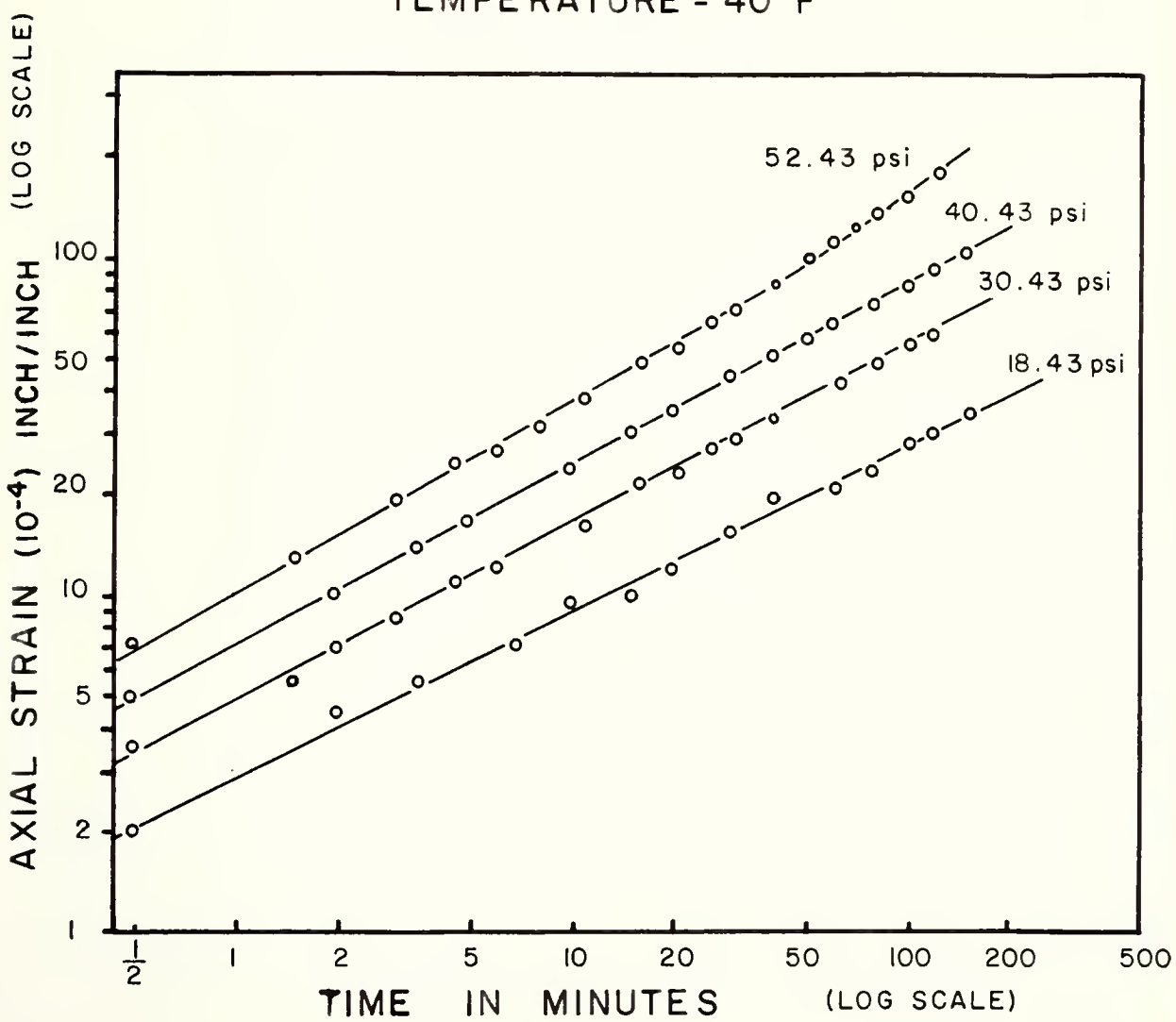

FIG. 18

UNIAXIAL TENSION TEST RESULTS

AXIAL STRAIN vs. TIME CURVES

TEMPERATURE = 77° F

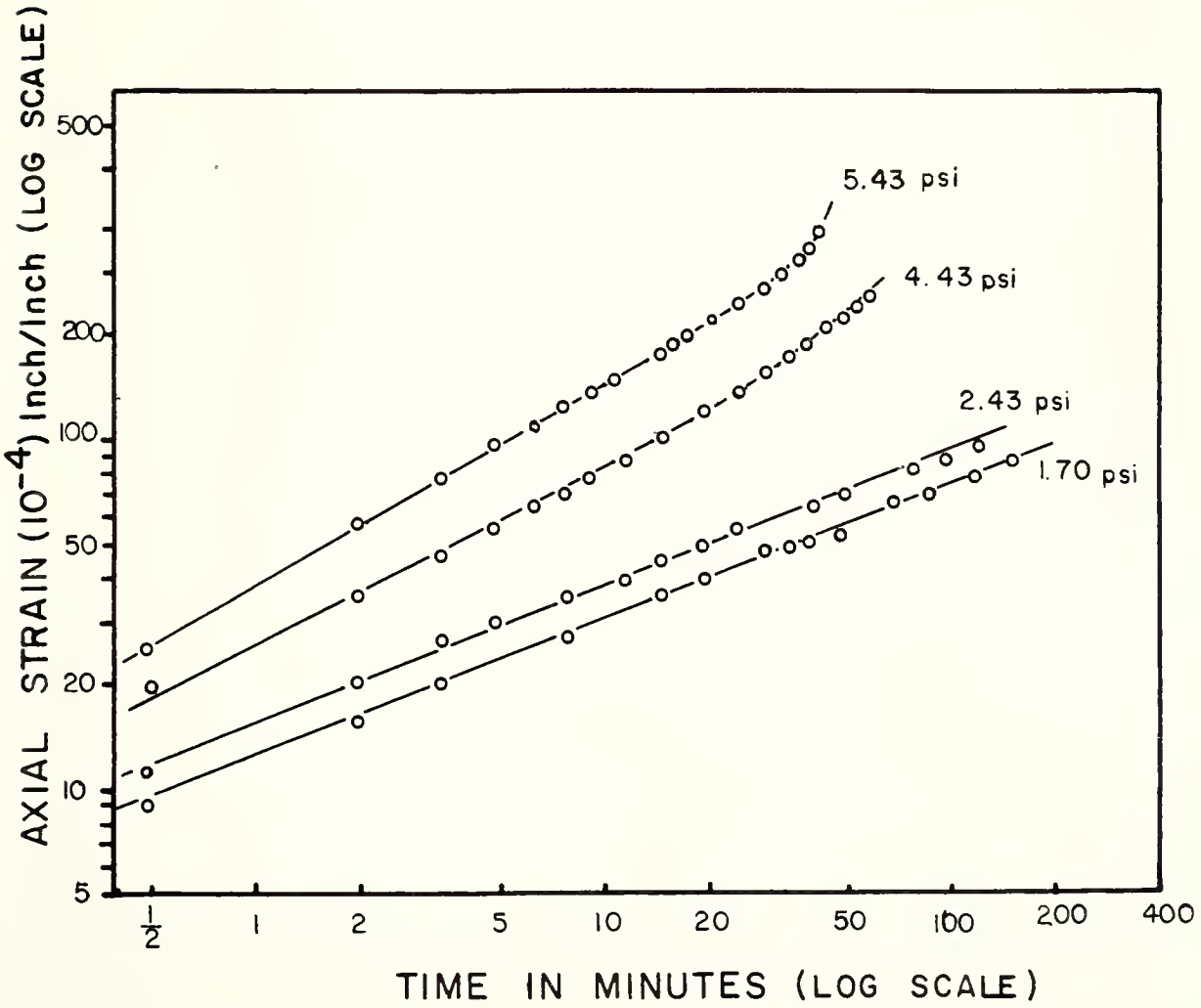

FIG. 19

UNIAXIAL TENSION TEST RESULTS

AXIAL STRAIN vs. TIME CURVES

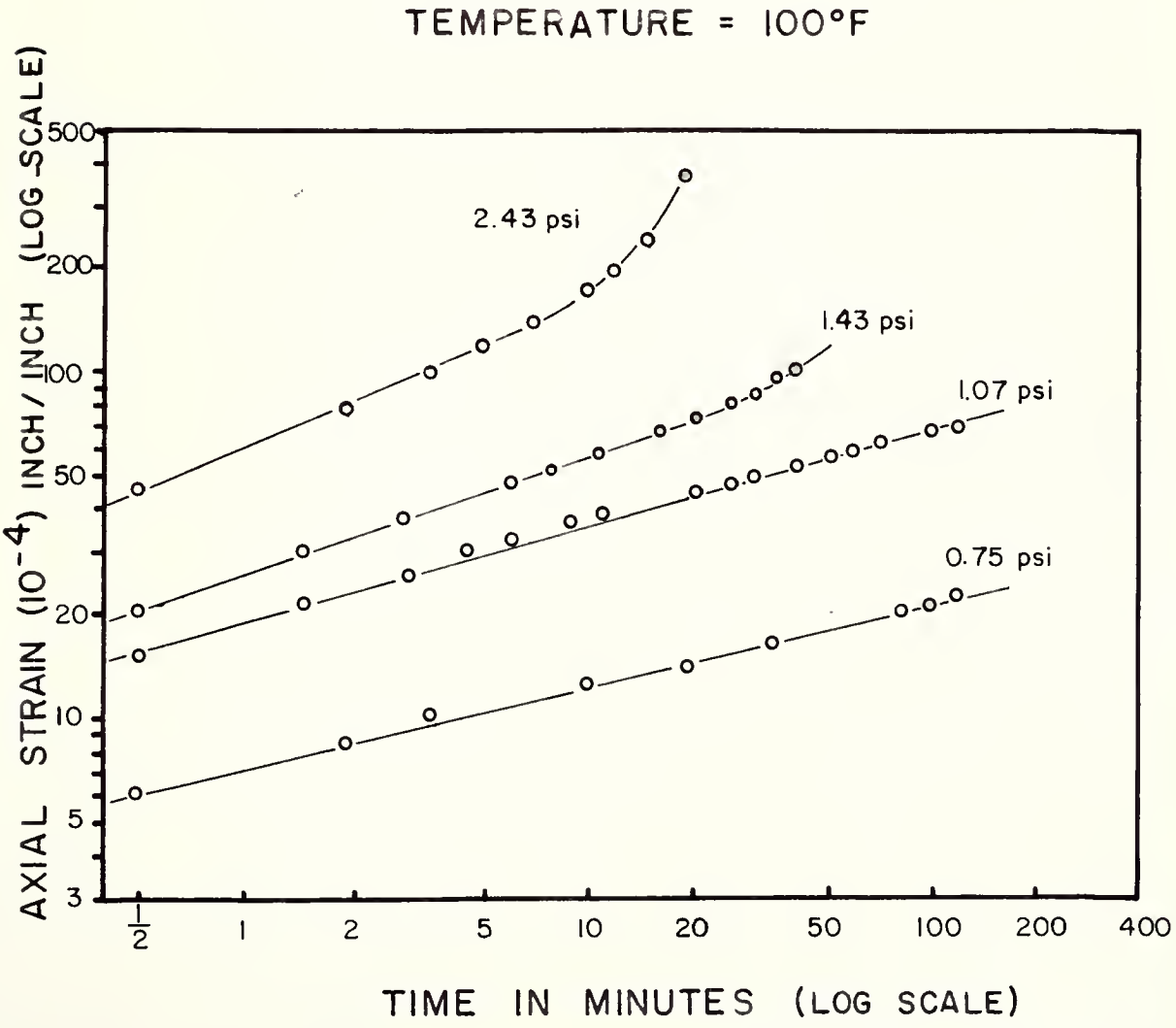

FIG. 20

Table 1

Axial Strain - Time Relationships
For
Uniaxial Tension Tests

40°F			77°F			100°F		
Applied Tensile Stress Psi	Axial Strain at One-Minute 0.0001 in./in.	Slope of Axial Strain vs. Time Plot (log-log)	Applied Tensile Stress Psi	Axial Strain at One-Minute 0.0001 in./in.	Slope of Axial Strain vs. Time Plot (log-log)	Applied Tensile Stress Psi	Axial Strain at One-Minute 0.0001 in./in.	Slope of Axial Strain vs. Time Plot (log-log)
18.43	2.55	1:1.95	1.70	11.5	1:2.80	0.75	7.2	1:4.40
30.43	4.40	1:1.90	2.43	15.0	1:2.50	1.07	18.5	1:3.70
40.43	6.60	1:1.85	4.43	28.5	1:2.00	1.43	26.0	1:3.20
52.43	9.60	1:1.80	5.43	39.0	1:1.80	2.43	60.0	1:2.40

UNIAXIAL TENSION TEST RESULTS

CIRCUMFERENTIAL STRAIN vs. TIME CURVES

TEMPERATURE = 40°F

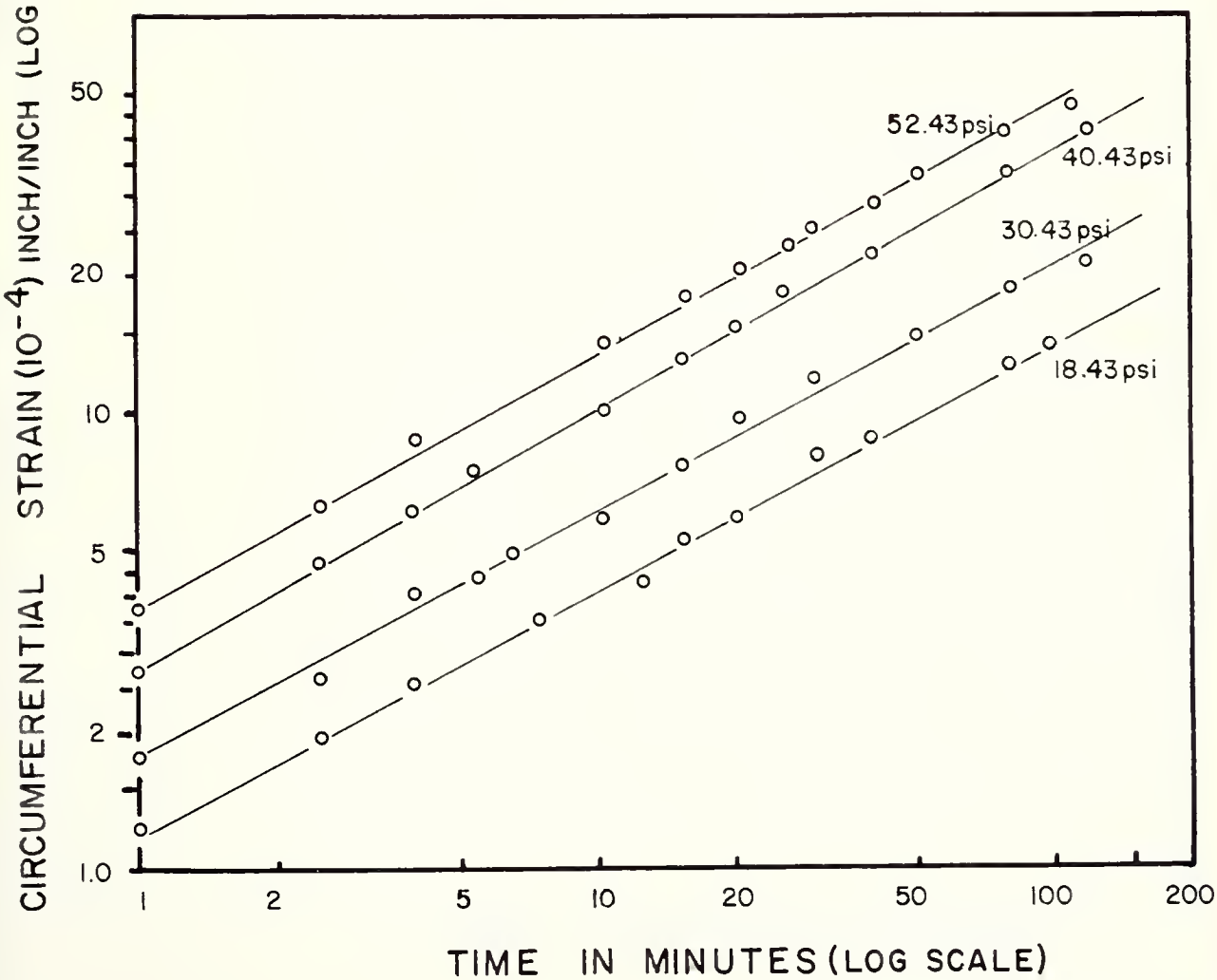

FIG. 21

UNIAXAL TENSION TEST RESULTS

CIRCUMFERENTIAL STRAIN vs. TIME CURVES

TEMPERATURE = 77°F

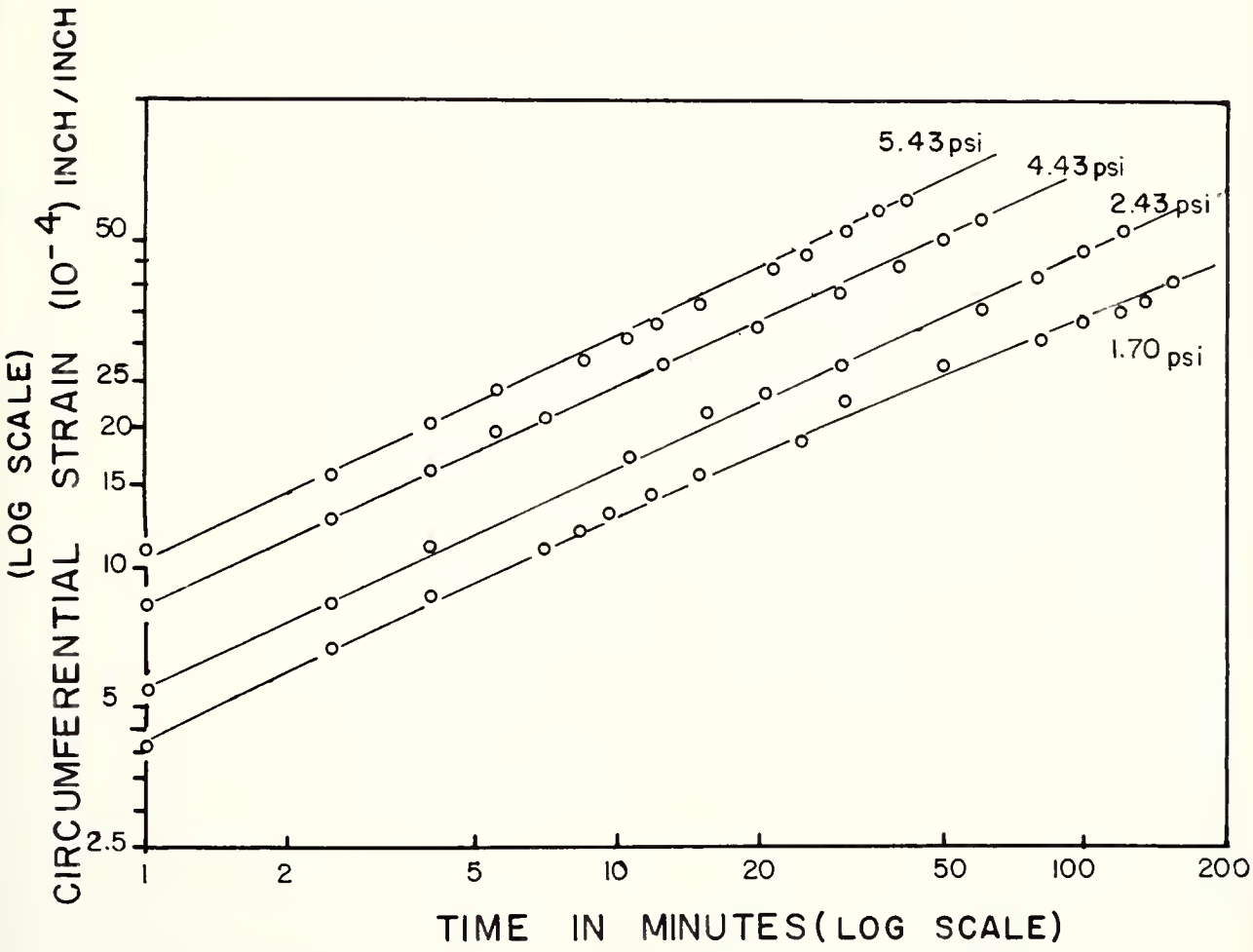

FIG. 22

UNIAXIAL TENSION TEST RESULTS

CIRCUMFERENTIAL STRAIN vs. TIME CURVES

TEMPERATURE = 100°F

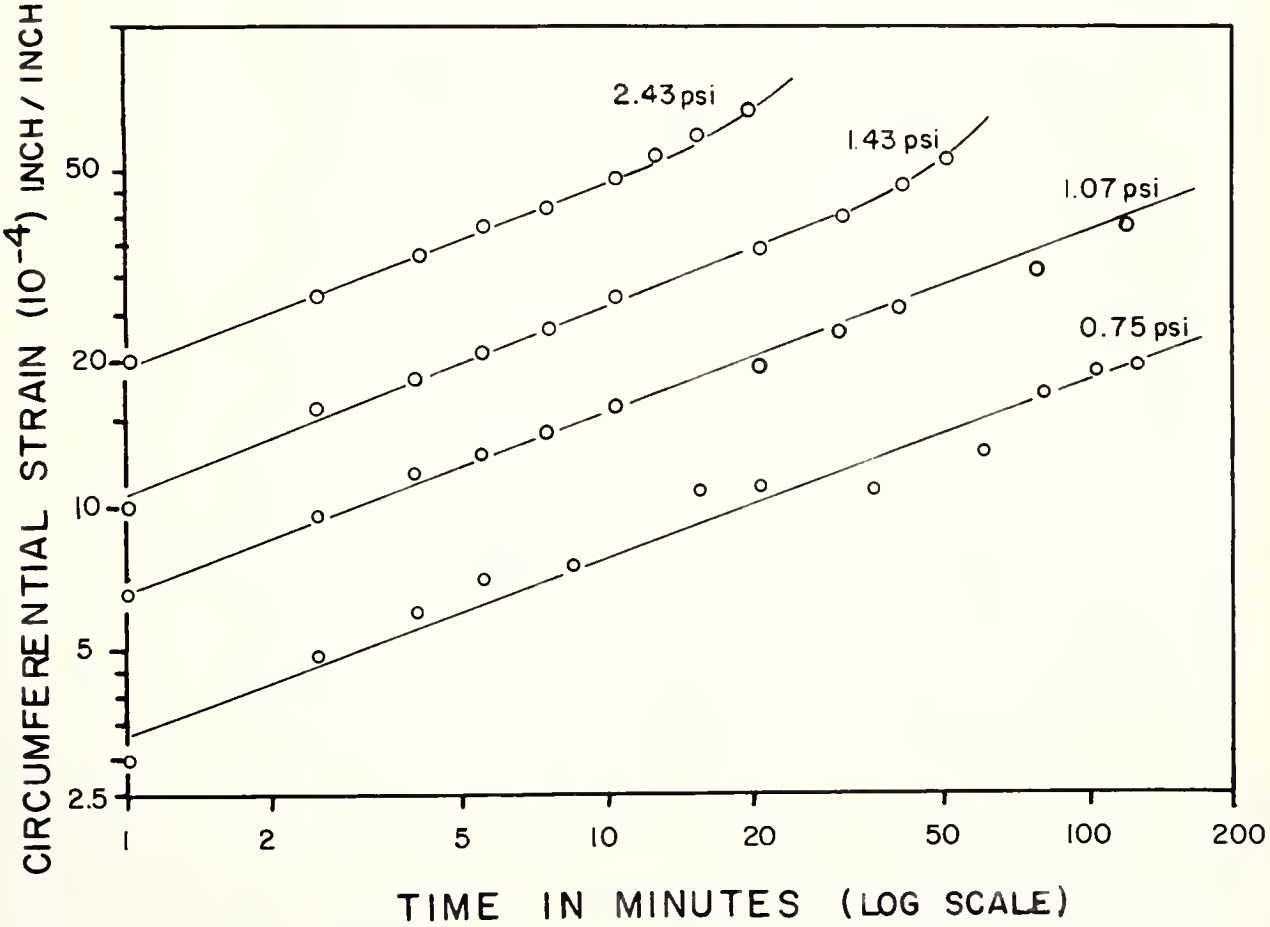

FIG. 23

Table 2

Circumferential Strain - Time Relationships
For
Uniaxial Tension Tests

40°F			77°F			100°F		
Applied Tensile Stress Psi	Circumferential Strain at One-Minute 0.0001 in./in.	Slope of Circumferential Strain vs. Time Plot (log-log)	Applied Tensile Stress Psi	Circumferential Strain at One-Minute 0.0001 in./in.	Slope of Circumferential Strain vs. Time Plot (log-log)	Applied Tensile Stress Psi	Circumferential Strain at One-Minute 0.0001 in./in.	Slope of Circumferential Strain vs. Time Plot (log-log)
18.43	1.18	1:2.00	1.70	4.25	1:2.40	0.75	3.25	1:3.00
30.43	1.75	1:1.95	2.43	5.50	1:2.30	1.07	6.5	1:2.85
40.43	2.75	1:1.90	4.43	8.50	1:2.20	1.43	10.0	1:2.75
52.43	3.75	1:1.85	5.43	11.0	1:2.12	2.43	20.0	1:2.50

Discussion of Uniaxial Tension Test Results

The log-log axial strain vs. time curves as given in Figures 18, 19 and 20 are straight lines in the pre-failure region and start to curve upward as the specimen starts to fail and cracks appear in the central portion of the specimen. Other researchers, for example Lee, Warren and Walters (12), have obtained similar deformation - time curves on a log-log plot. They, however, plotted only the over-all specimen deformation under tension and did not measure the strain in the material without the end effects influencing the results.

The results tabulated in Table 1 give some interesting points about the behavior of the material under constant stress. First, at constant temperature, the axial strain at one minute does not vary proportionally with the tensile stress. This becomes very apparent by comparing the strains at one minute under the highest and lowest stresses to which the specimen had been subjected at any constant temperature. With increasing stress, at constant temperature, the deviation of proportionality between stress and strain at one minute also increases.

With increasing temperature, the deviation from proportionality of stress to strain at one minute increases also. As can be seen from results of tests carried out at $40^{\circ}F$, the strain at one minute under 18.43 psi is 2.55×10^{-4} in/in. while the strain at one minute under 52.43 psi is 9.60×10^{-4} in/in., showing little deviation from proportionality. However, at $100^{\circ}F$, the strain at one minute under 0.75 psi is 7.2×10^{-4} in/in. while the strain at one minute under 2.43 psi is 60×10^{-4} in/in., showing considerable deviation from proportionality between stress and strain at one minute at this higher temperature.

These results indicate that the sheet asphalt mixture under test, is a non-linear visco-elastic material, the deviation from linearity increasing with temperature.

Second, the slopes of the axial strain vs. time curves on a log-log plot vary with the applied tensile stress at constant temperature and also with temperature. As can be observed from the tabulated results in Table 1. the slopes become steeper with increasing stress at constant temperature.

Also, the change in slope for a unit change in stress, at constant temperature, increases with the increasing temperatures. Whereas at $40^{\circ}F$, the slope changes from 1 in 1.80 at 52.43 psi to 1 in 1.95 at 18.43 psi, the slopes change from 1 in 1.80 at 5.43 psi to 1 in 2.80 at 1.70 psi at $77^{\circ}F$, and from 1 in 2.40 at 2.43 psi to 1 in 4.40 at 0.75 psi at $100^{\circ}F$. This further goes to show that the test mixture is a non-linear visco-elastic material, the deviation from linearity increasing with temperature.

A study of the change in slope of these strain-time curves on log-log scales, as a function of applied tensile stress and at different temperatures, seems to be a desirable line of investigation in determining the stress-strain relationship as a function of time and temperature.

It must be mentioned here that the tensile stress over the specimen cross-section during the test increases with time due to a decrease in diameter, but the change is very small as indicated below. The maximum circumferential strain recorded before failure is about 0.5% i.e., a decrease of 2 x 0.0050 inches in diameter. The minimum area of cross-section, therefore, is $\pi/4\ (2 - 2 \times 0.005)^2 = \pi/4 \times (1.99)^2 = \frac{3.96}{4}\ \pi$ sq. in.

Maximum increase in stress = $(4/3.96 - 1) = 1\%$ which is negligible.

The circumferential strain (or change in radius) vs. time curves (log-

log scales) as given in Figures 21, 22 and 23, are straight lines. As the specimen starts to fail with cracks appearing in its middle portion, the straight line tends to curve upward if measurements for change in diameter are made at points where cracks do not open first. If, however, the measurements for changes in diameter are made at points where cracks first start opening, the specimen begins to fail without further reduction in diameter. Only in Figure 23, do the upper two straight lines (for stresses 2.43 and 1.43 psi) tend to curve upward. The rest of the straight lines remain straight for reasons explained above.

The data of Table 2 show that the deviation from proportionality between applied tensile stress and circumferential strain at one minute is very distinct at 100°F, but the results at 40°F and 77°F do not show any marked deviation.

The slope of the log-log plot of the circumferential strain vs. time under constant tensile stress and temperature is seen to become steeper with increasing stress. This change is not as marked as it was in the case of the slopes of axial strain vs. time curves on a log-log plot, for results at 77°F and 100°F. For example, at 77°F, whereas the slopes of the axial strain vs. time curves on the log-log plot vary from 1 in 2.80 to 1 in 1.80 for stresses from 1.70 psi to 5.43 psi, the corresponding figures for circumferential strain-time curves are 1. in 2.40 to 1 in 2.12. The comparable figures at 100°F are 1 in 4.40 to 1 in 2.40 for axial strain-time curves and from 1 in 3.00 to 1 in 2.50 for circumferential strain curves.

The data from Uniaxial Tension tests were examined to learn how the Poisson's ratio for the sheet asphalt material varies with applied stress, time and temperature. In Figures 24, 25 and 26, axial

POISSON'S RATIO (ν)

AT
40°F

POISSON'S RATIO(ν) = $\frac{\text{CIRCUMFERENTIAL STRAIN}}{\text{AXIAL STRAIN}}$

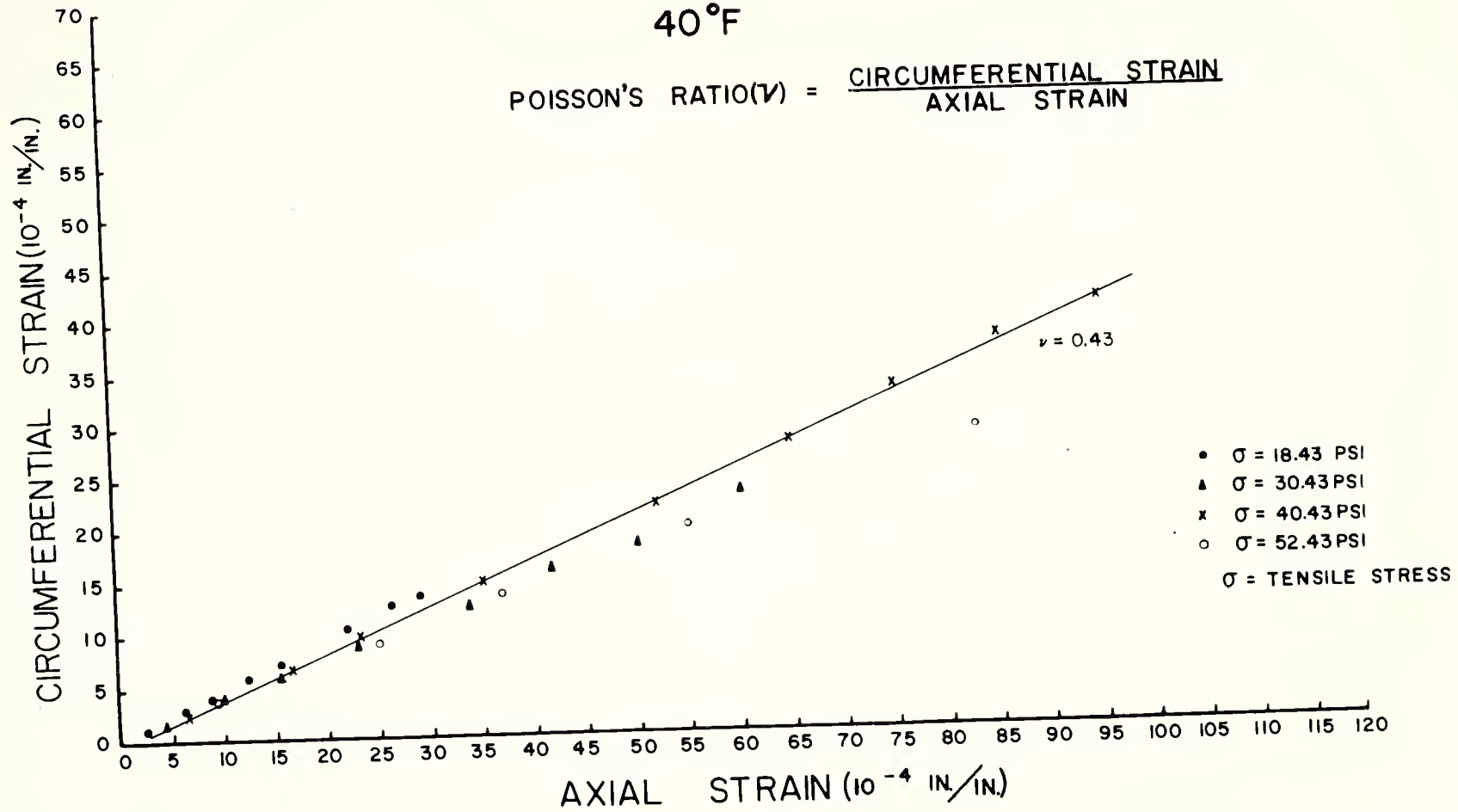

FIG. 24

POISSON'S RATIO(ν)
AT
77°F

POISSON'S RATIO(ν) = $\frac{\text{CIRCUMFERENTIAL STRAIN}}{\text{AXIAL STRAIN}}$

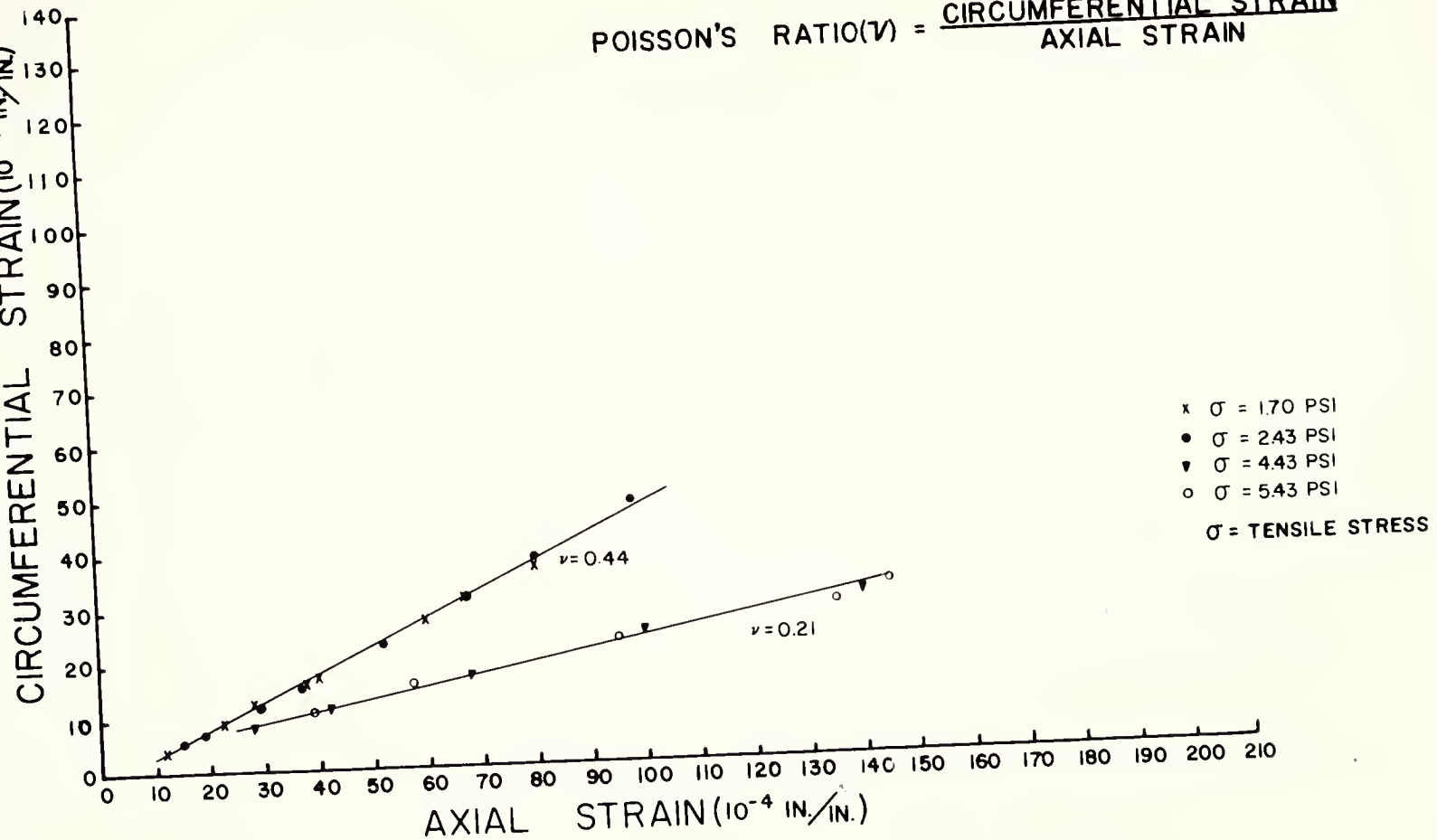

FIG. 25

POISSON'S RATIO (ν)

AT
100°F

$$\text{POISSON'S RATIO}(\nu) = \frac{\text{CIRCUMFERENTIAL STRAIN}}{\text{AXIAL STRAIN}}$$

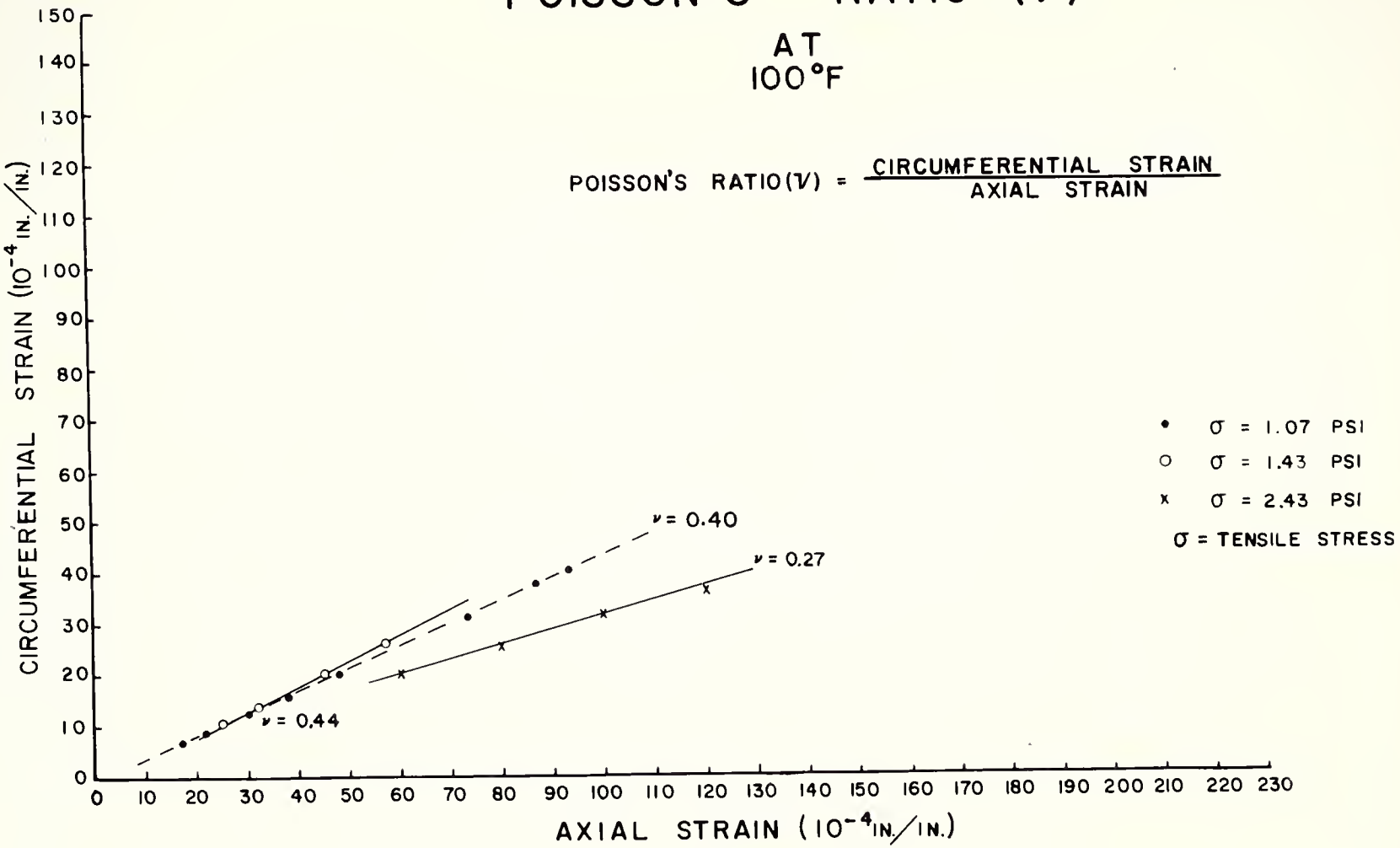

FIG. 26

strain is plotted against the corresponding circumferential strain at different times under various applied stresses at 40°F, 77°F and 100°F, respectively. It can be seen from these plots that at 40°F the Poisson's ratio does not vary much with the applied stress. However, the Poisson's ratio can be seen to decrease with increasing applied stress at 77°F and 100°F

The above data show that the deformation characteristics of the mixture are greatly different at different temperatures. At 40°F, the mixture behaves almost like an elastic material in the sense that the Poisson's ratio seems to be independent of applied stress and time. At higher temperatures, however, the Poisson's ratio is dependent upon applied stress and time.

The decrease in Poisson's ratio with increasing stress is probably due to the lack of time for asphalt, present as films on aggregate in the mixture, to deform laterally as it is being pulled axially at a relatively faster rate due to the higher applied stress. This means that the higher the axial strain rate, the lower will be the Poisson's ratio. Thus, whereas the Poisson's ratio for the material at 40°F is almost constant at 0.43, it varies from 0.44 at 1.70 psi to 0.21 at 5.43 psi at 77°F and from 0.44 at 1.07 psi to 0.27 at 2.43 psi at 100°F, at one minute. Therefore, these results show that the Poisson's ratio is a function of applied stress, time and temperature.

Simple Shear Test Results

In the Simple Shear tests, the deformation of the movable plate, from which the shearing strain can be calculated, was observed with time under different constant applied stresses and temperatures.

SIMPLE SHEAR TEST RESULTS

SHEAR STRAIN vs. TIME CURVES

TEMPERATURE = 40°F

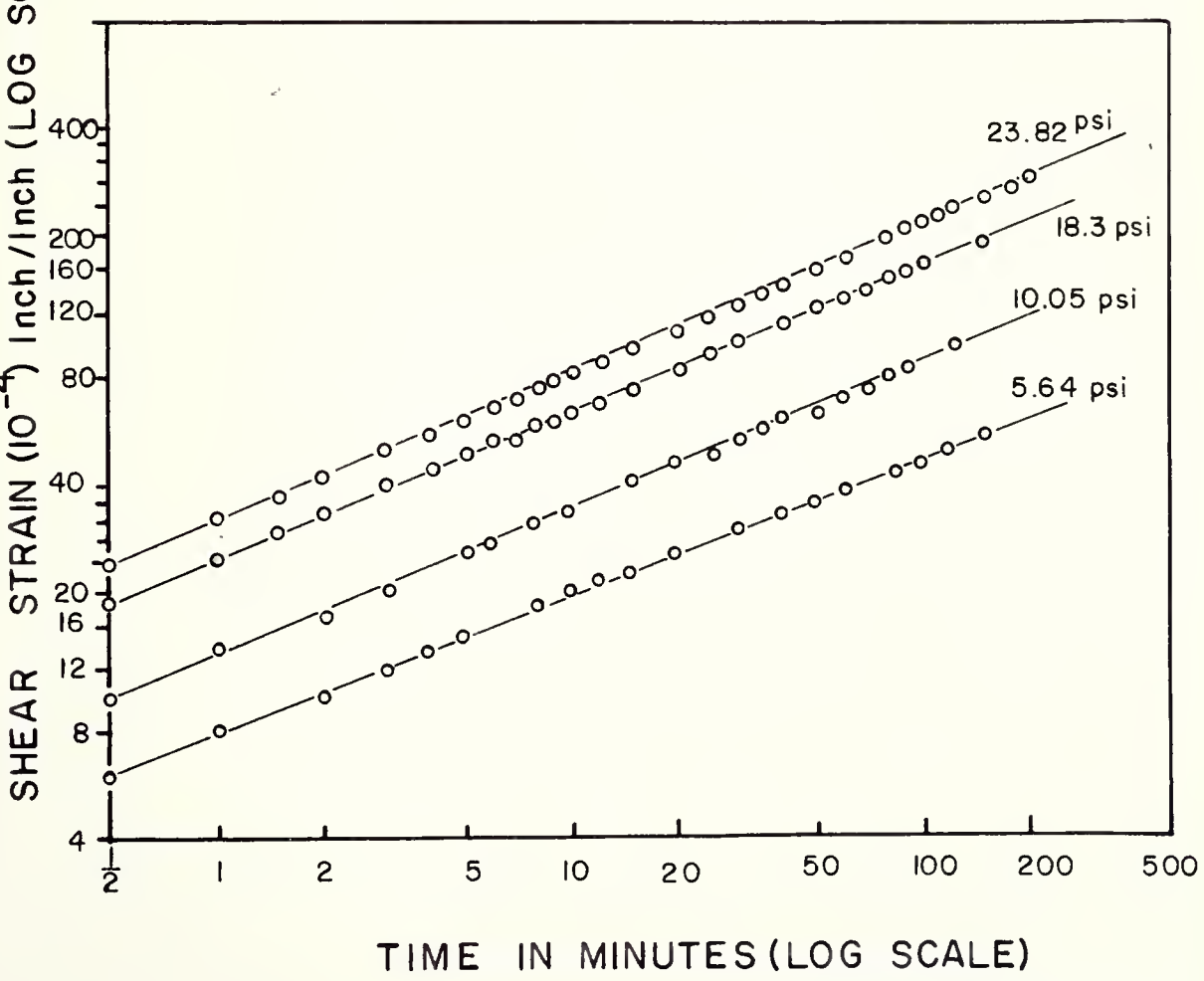

FIG. 27

SIMPLE SHEAR TEST RESULTS

SHEAR STRAIN vs. TIME CURVES

TEMPERATURE = 77°F

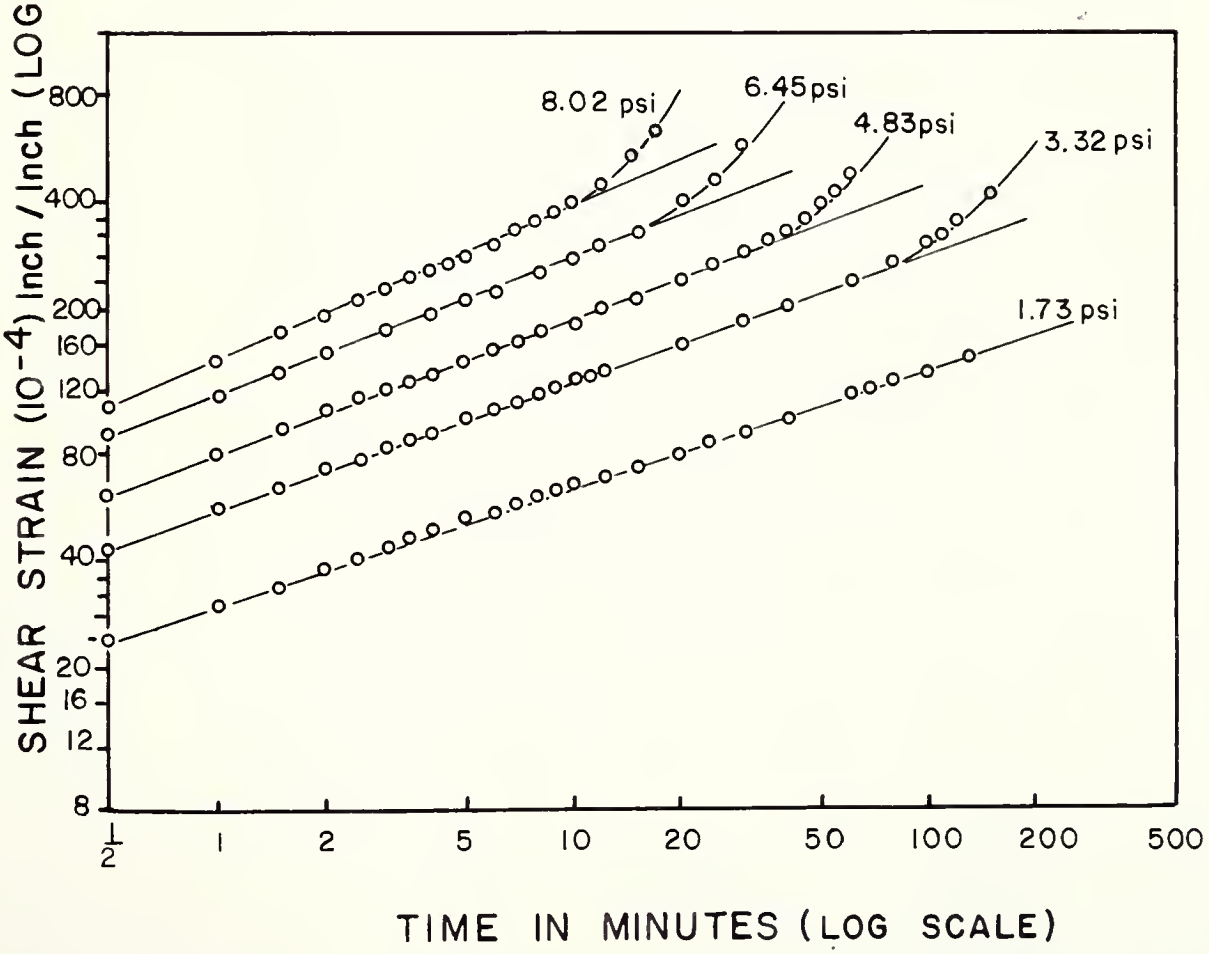

FIG. 28

SIMPLE SHEAR TEST RESULTS

SHEAR STRAIN vs. TIME CURVES

TEMPERATURE = 100°F

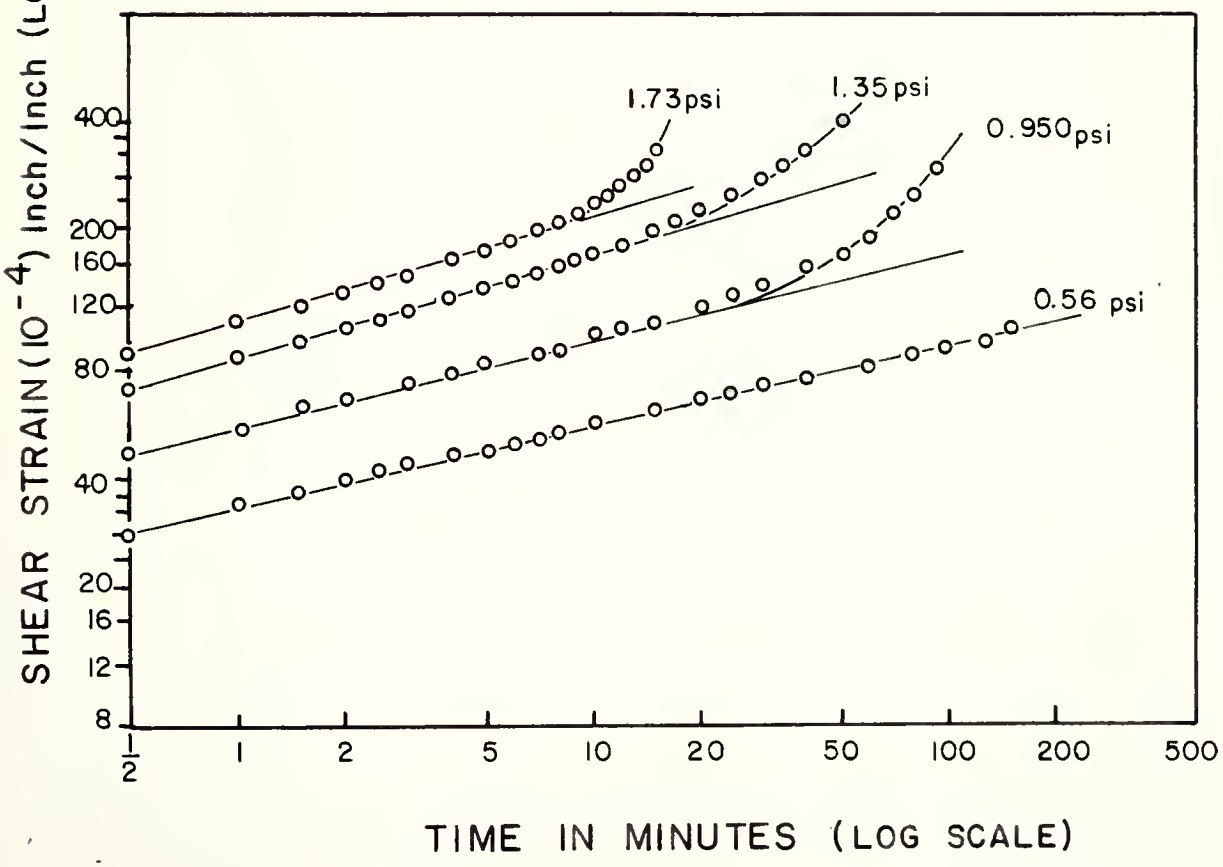

FIG. 29

Table 3

Shear Strain - Time Relationships
For
Simple Shear Tests

40°F			77°F			100°F		
Applied Shear Stress Psi	Shear Strain at One-Minute 0.0001 in./in.	Slope of Shear Strain vs. Time Plot (log-log)	Applied Shear Stress Psi	Shear Strain at One-Minute 0.0001 in./in.	Slope of Shear Strain vs. Time Plot (log-log)	Applied Shear Stress Psi	Shear Strain at One-Minute 0.0001 in./in.	Slope of Shear Strain vs. Time Plot (log-log)
5.64	8.0	1:2.55	1.73	30	1:3.00	0.563	34.0	1:4.50
10.05	13.6	1:2.50	3.32	56.0	1:2.80	0.950	56.0	1:4.00
18.3	24.4	1:2.45	4.83	80.0	1:2.60	1.35	88.0	1:3.50
23.82	32.0	1:2.40	6.45	114.0	1:2.50	1.732	110.0	1:3.38
			8.02	146.0	1:2.30			

In Figures 27, 28 and 29 shearing strains at indicated constant shearing stresses have been plotted against time on a log-log scale for tests at 40°F, 77°F and 100°F, respectively. The results as plotted on these figures are tabulated in Table 3. In this table, the slopes of the strain-time curves pertain only to the straight line portion of the curve. The shearing strain at one minute and the slope of the straight line portion of the plot have been used to characterize each plot for same reasons as explained for Table 1.

Discussion of Simple Shear Test Results

The shear strain of the specimen, under constant load and temperature, plotted against time on log-log scales is given for different applied stresses at 40°F, 77°F and 100°F, respectively in Figures 27, 28 and 29. As in the case of axial strain vs. time plots on log-log scales for Uniaxial Tension tests, the deformation of the movable plate or shear strain under constant stress vs. time plots are straight lines for pre-failure conditions and tend to curve upward just as the material begins to fail. Similar curves were obtained by Lee and Markwick (11) who tested 1-inch thick specimens and also plotted the dilation of the specimen with time. As explained earlier, the specimens for simple shear test were made 1/4-inch thick and it was not possible at this thickness to record the lateral deformation of the movable plate accurately because of its very small magnitude.

Neglecting dilation, the deformation of the plate at any time divided by the thickness of specimen can be taken as the shear strain at that time. Thus, shear strain at any time when the thickness of the specimen is 1/4-inch, is four times the deformation of the movable plate at that time.

It is interesting to note that the results for Simple Shear tests tabulated in Table 3 show the same trends as noted in the Uniaxial Tension rest results tabulated in Tables 1 and 2. The deviation from proportionality betweeen applied shear stress and the shear strain at one minute can be observed from the results at 100°F, but the results at 40°F and 77°F do not show any marked deviation. As in the case of Uniaxial Tension test results, the slopes of shear strain-time curves on log-log plots become steeper with increasing stress. The rate of change of slope with stress varies with temperature. For example, at 40°F, the slope is 1 in 2.55 at 5.64 psi and is 1 in 2.40 at a stress more than four times greater whereas at 100°F the slope is 1 in 4.50 at 0.563 psi and at a stress more than three times greater it is 1 in 3.38.

In order to determine the shear stress-shear strain relationship as a function of time and temperature, a study of the change of slope of the log-log plots of deformation vs. time with varying applied stress and temperature seems to be useful. At this point, it is to be noted that since the shear strain-time plots for Simple Shear tests show the same trends with applied stress and temperature as shown by the axial strain-time and circumferential strain-time plots for Uniaxial Tension tests, it appears valid to conclude that the basic material constants of the mixture may be reflected in stress-strain relationships derived from the data of these two tests.

Axial Compression Test Results

In the Axial Compression tests, the axial deformations as well as circumferential deformations on the inside and outside of the hollow specimens under different constant applied stresses and temperatures were observed with time.

In Figures 30, 31 and 32, the axial strains have been plotted against time on a log-log plot under constant compressive stresses, as indicated on the figures and at 40°F, 77°F and 100°F, respectively. The corresponding circumferential strain-time curves on log-log plots are given in Figures 33, 34 and 35. The Axial Compression tests were performed to compare the results obtained with the corresponding results predicted from Uniaxial Tension tests. For this purpose, the strain-time curves as predicted by Uniaxial Tension tests are shown dotted alongside the actual curves obtained from the Axial Compression tests in the following figures.

Discussion of Axial Compression Test Results

The axial strain vs. time plots on log-log scale in Figures 30 to 32 show that these are not continuous straight lines as obtained in the Uniaxial Tension tests, but are straight only up to some deformation after which they curve downward to lesser slopes. The same trend can be observed from the circumferential strain vs. time plots in Figures 33 to 35 on log-log scales. The circumferential strain was calculated by finding the change in the thickness per inch of the wall of the hollow specimen.

The same general trend of the slope on the log-log plot becoming steeper with the increasing stress, as was observed in the case of Uniaxial Tension tests, can be observed in the case of compression test results also, but only for the straight line portions of curves.

AXIAL COMPRESSION TEST RESULTS

AXIAL STRAIN vs. TIME CURVES

TEMPERATURE = 40° F

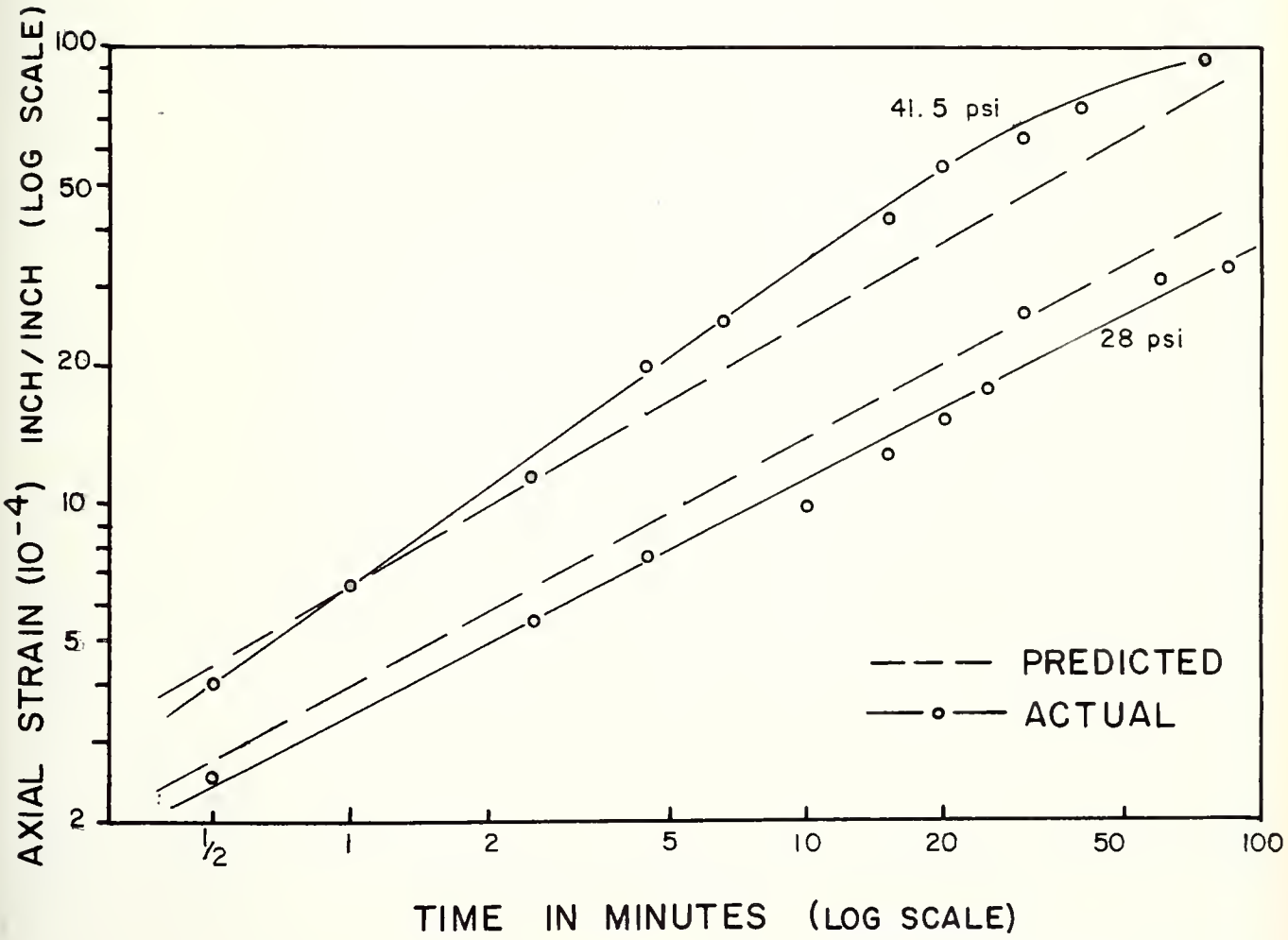

FIG. 30

AXIAL COMPRESSION TEST RESULTS

AXIAL STRAIN vs. TIME CURVES

TEMPERATURE = 77°F

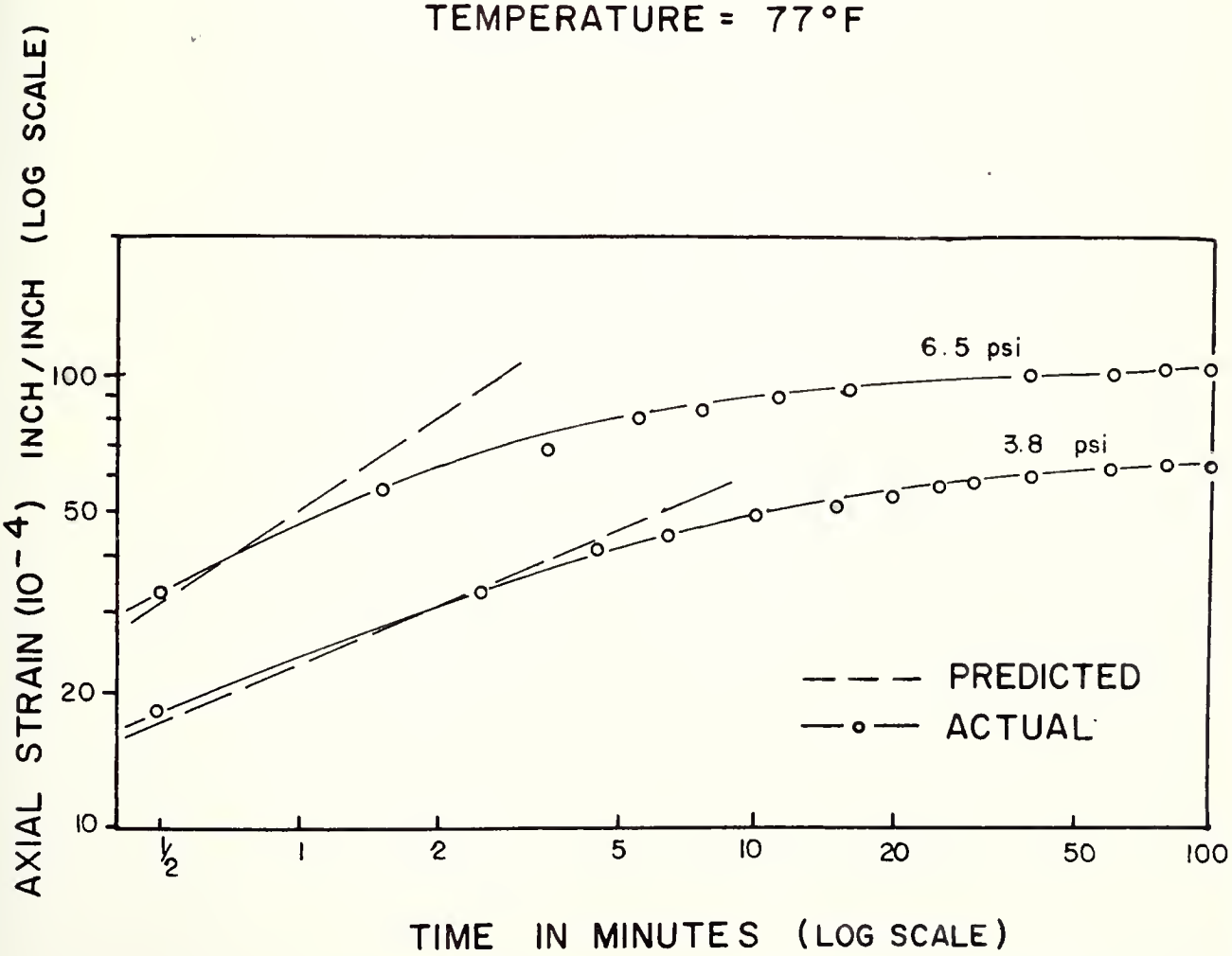

FIG. 31

AXIAL COMPRESSION TEST RESULTS

AXIAL STRAIN vs. TIME CURVES

TEMPERATURE = 100°F

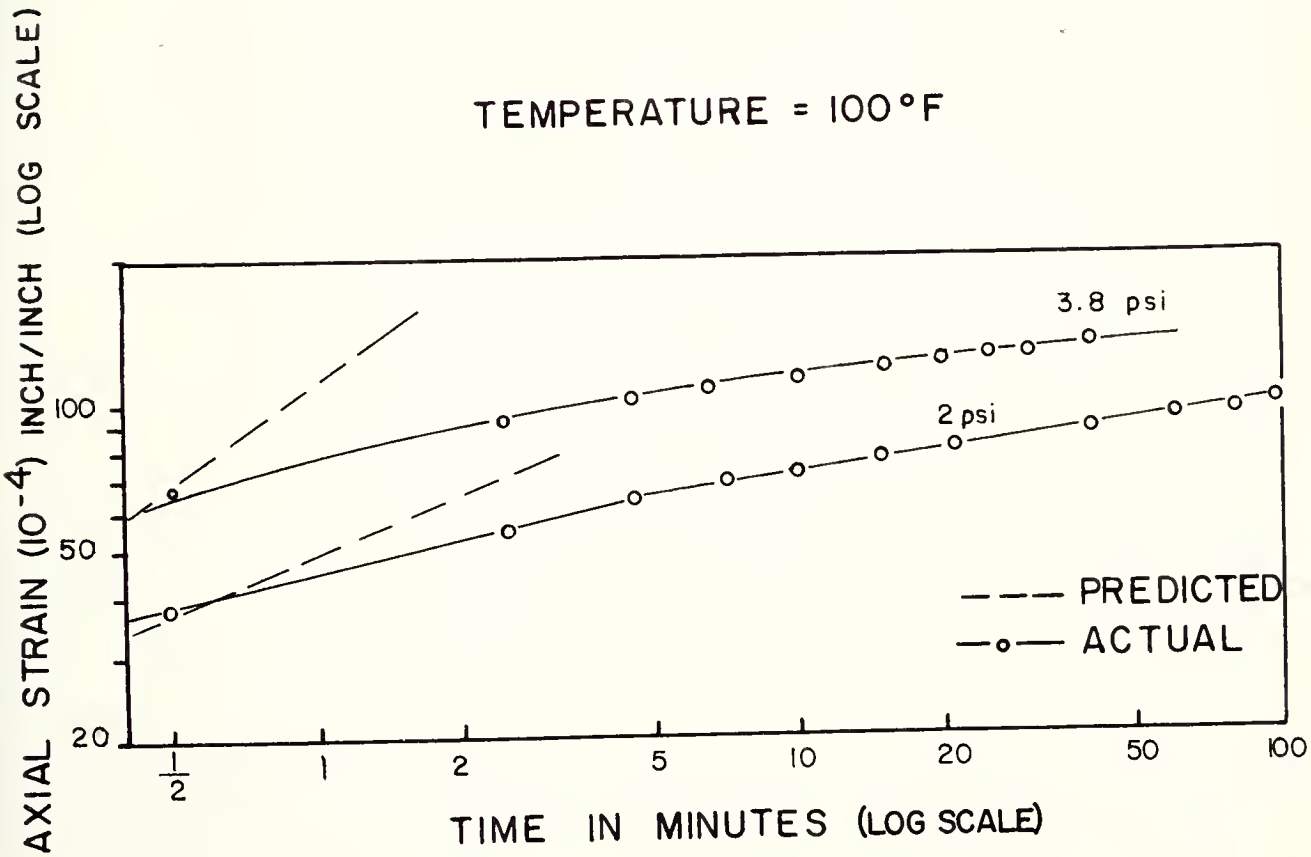

FIG. 32

AXIAL COMPRESSION TEST RESULTS

CIRCUMFERENTIAL STRAIN vs. TIME CURVES

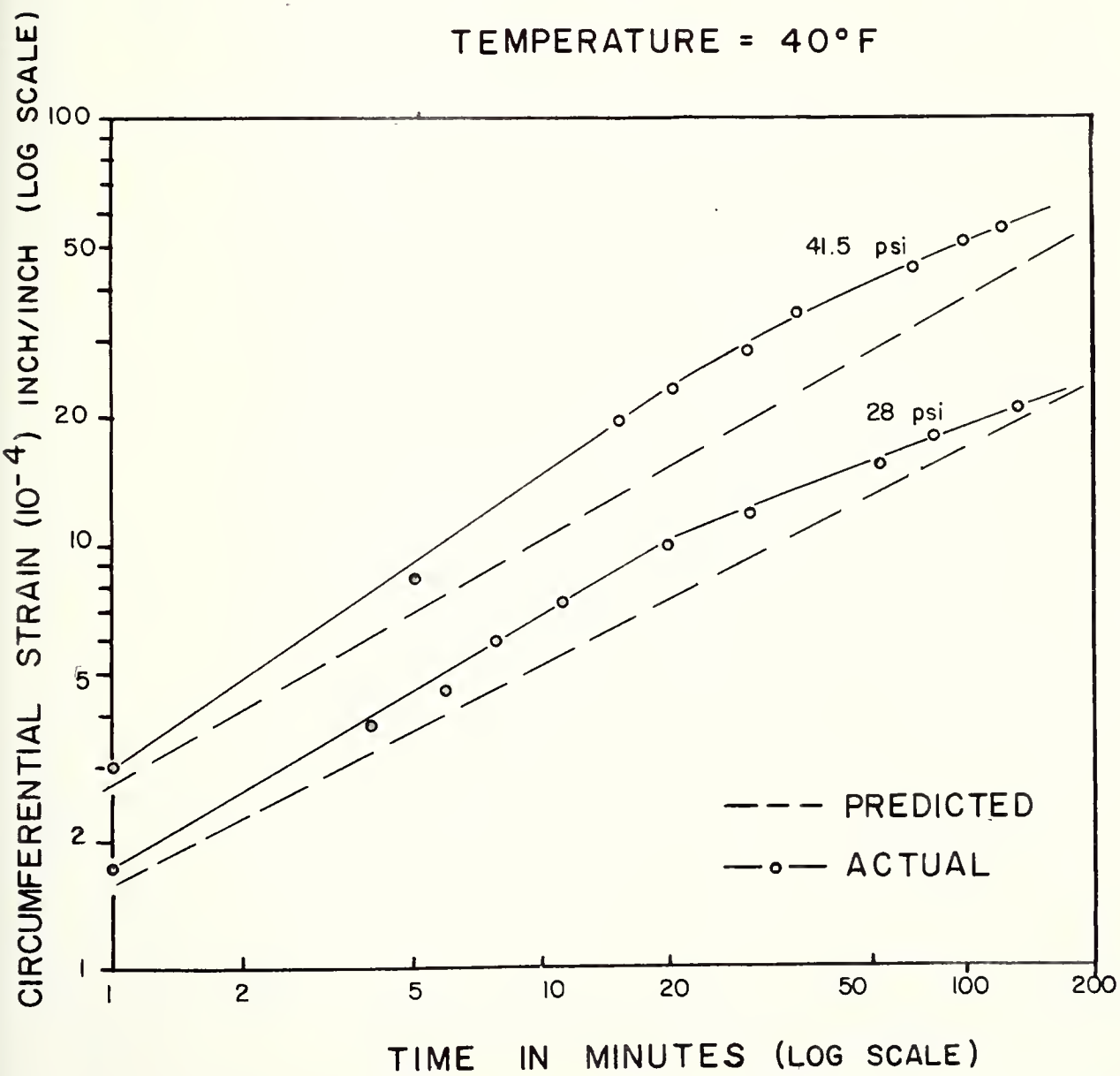

FIG. 33

AXIAL COMPRESSION TEST RESULTS

CIRCUMFERENTIAL STRAIN vs. TIME CURVES

TEMPERATURE = 77°F.

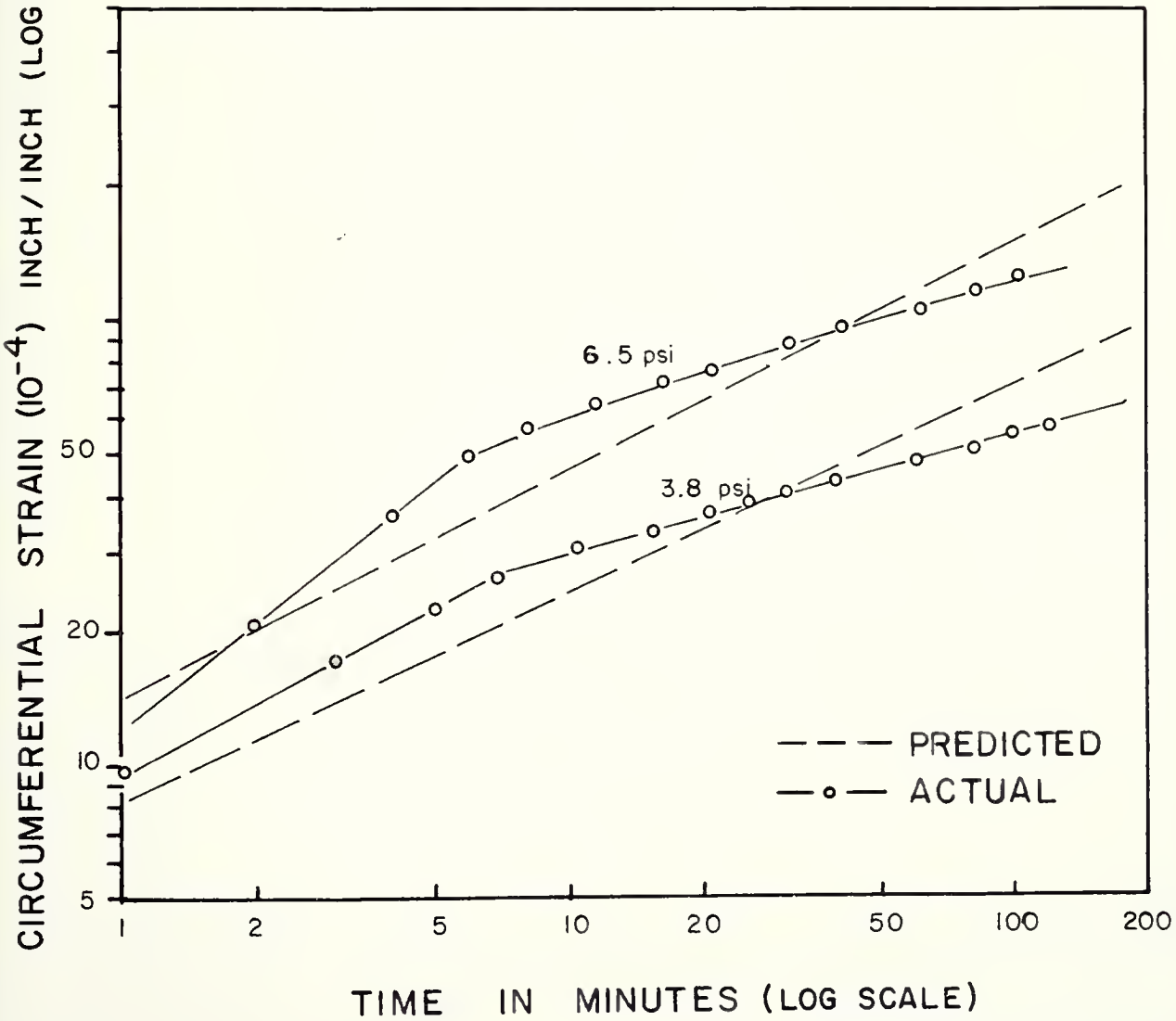

FIG. 34

AXIAL COMPRESSION TEST RESULTS

CIRCUMFERENTIAL STRAIN vs. TIME CURVES

TEMPERATURE = 100° F

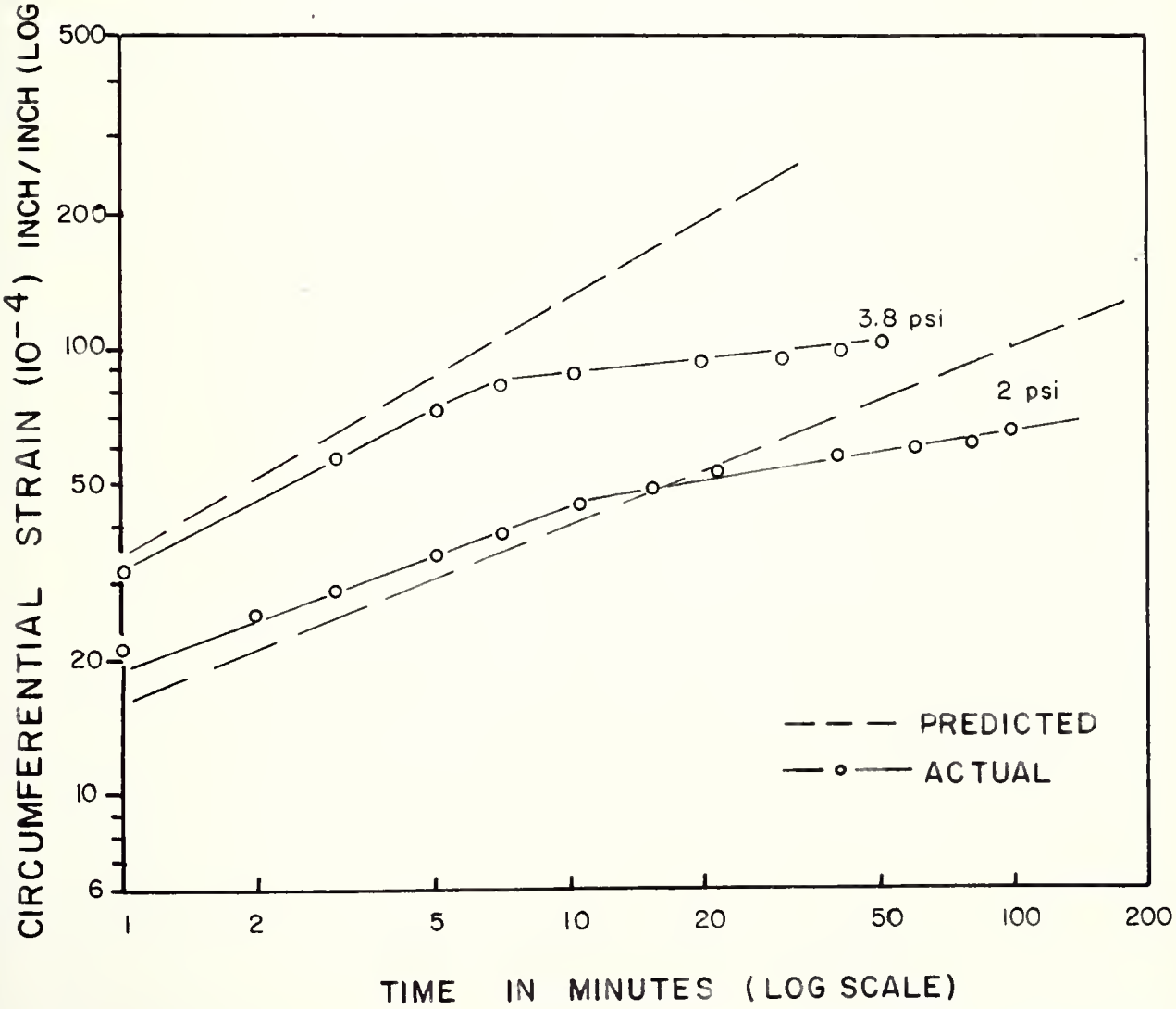

FIG. 35

It is interesting to note from the axial strain vs. time plots on log-log scale that, approximately at the time at which the straight-line portion of the curve tends to curve upward in the case of the axial strain-time plots (log-log) of Uniaxial Tension tests, the corresponding curve in case of compression tests tends to curve downward to lesser slopes. This goes to show that after this time, different mechanisms of deformation in the two tests might have taken over. However, it must be recognized that pure compression was probably not achieved in the test performed and that the measurements made were less than ideal.

It can be observed from the predicted and actual plots that the strains up to about 0.4 percent can be predicted quite well for the two tests.

It must be mentioned here that the compressive stress over the cross-section of specimen decreases with time, as the area of cross-section of the specimen increases with time, under the constant load. The decrease in compressive stress is, however, very small as the maximum compressive strain recorded in these results is only about 1 percent. Thus the stress can be assumed to be constant during the test.

Also, the discrepancy between the increased stress in Uniaxial Tension test specimens and the correspondingly decreased stress in Axial Compression test specimens is too small to warrant consideration for verification of results.

SUMMARY OF TEST RESULTS

To obtain the experimental data required for this study, three different types of laboratory tests, viz. Uniaxial Tension tests, Simple Shear tests and Axial Compression tests were performed. In this order, the results of these tests are summarized here.

For the Uniaxial Tension tests, the axial strain of specimens under constant stress and constant temperature, when plotted as ordinate against time on log-log scales gave a straight line relationship in the pre-failure region. As failure started to take place with the appearance of minute cracks in the middle portion of specimen, the straight line on the log-log plot tended to curve upward. It was found convenient to characterize the straight line portion of the plot by its slope and axial strain at one minute. Within the range of temperatures and stress-levels tested, the following points of interest were observed from the results:

At constant temperature, the axial strain at one minute did not vary proportionally with applied stress. The deviation from proportionality increased with increasing temperature as well as with increasing applied stress. The slopes of the straight-line portions of the log-log plots varied with the applied stress and temperature. The slopes became steeper with increase in applied stress at constant temperature. For an incremental change in stress, the corresponding change in slope was more significantly marked at higher temperatures.

The circumferential strain when plotted as ordinate against time on log-log scales also gave a straight-line relationship. The same trends as observed for axial strains were observed for circumferential strains.

A study of Poisson's ratio for the material as determined from the Uniaxial Tension test data showed it to be a function of applied stress, time and temperature. Using the theory of elasticity, however, the Poisson's ratio would have been taken as a constant at least for stress. Whereas at $40^{\circ}F$, its value was found almost independent of applied stress, at higher temperatures it decreased with increasing applied stress.

For the Simple Shear tests, the shearing strain in the specimen under constant shear stress and constant temperature, when plotted as ordinate against time on log-log scales, gave a straight-line relationship in the pre-failure region. The shearing strain-time relationships showed the same trends with regard to temperature and applied stress as were observed in the axial strain-time relationships in the Uniaxial Tension tests. This was an indication of the fact that the same basic material properties were being reflected in these two types of tests.

For the Axial Compression tests, the log-log plots of axial strain vs. time were not found to be continuous straight lines for the entire range. The plots were straight lines up to a certain percentage of deformation after which they curved downward to lesser slopes. The initial straight-line portions of the Axial Compression test plots showed the same trends with regard to applied stress and temperature as were observed in the axial strain-time plots from the Uniaxial Tension tests. It was also observed from the Axial Compression test results that strains up to about 0.4 percent can be quite satisfactorily predicted from the

Uniaxial Tension tests.

DISCUSSION OF STRESS-STRAIN EXPRESSIONS

Based on the Uniaxial Tension test and Simple Shear test results, as discussed in the preceding section, three stress-strain expressions were derived. These derivations are presented in Appendix C. In this section, the general forms of these expressions are given and discussed. From Uniaxial Tension test results, the expression relating the normal tensile stress (σ_z) to axial strain (ϵ_z) was found to be:

$$\sigma_z = \left(\frac{T}{c_1}\right)^{-c_2} - \left(\frac{T}{p_1}\right)^{-p_2} \frac{\epsilon_z}{t\,\frac{\partial \epsilon_z}{\partial t}}$$

where t stands for time, T for temperature and c_1, c_2, p_1, p_2 are material constants. An expression of the same form relating σ_z to circumferential strain (ϵ_y) was found viz.

$$\sigma_z = \left(\frac{T}{c_1'}\right)^{-c_2'} - \left(\frac{T}{p_1'}\right)^{-p_2'} \frac{\epsilon_y}{t\,\frac{\partial \epsilon_y}{\partial t}}$$

Assuming the material to be isotropic and homogeneous, the following equations can be written:

$$\sigma_y = \left(\frac{T}{c_1}\right)^{-c_2} - \left(\frac{T}{p_1}\right)^{-p_2} \frac{\epsilon_y}{t\,\frac{\partial \epsilon_y}{\partial t}} = \left(\frac{T}{c_1'}\right)^{-c_2'} - \left(\frac{T}{p_1'}\right)^{-p_2'} \frac{\epsilon_z}{t\,\frac{\partial \epsilon_z}{\partial t}}$$

From the Simple Shear test results, the expression relating the shear stress (τ_{yz}) to shear strain (γ_{yz}), was found to be of the same form, viz:

$$\tau_{yz} = \left(\frac{T}{c_1''}\right)^{-c_2''} - \left(\frac{T}{p_1''}\right)^{-p_2''} \frac{\gamma_{yz}}{t\,\frac{\partial \gamma_{yz}}{\partial t}}$$

where c_1'', c_2'', p_1'' and p_2'' are material constants. Noting the definitions that $\epsilon_z = \frac{\partial w}{\partial z}$, $\epsilon_y = \frac{\partial v}{\partial y}$ and $\gamma_{yz} = \frac{\partial w}{\partial y} + \frac{\partial v}{\partial z}$ where w and v are the displacements in the z and y directions respectively,

and that the term $\frac{\partial v}{\partial z}$ for γ_{yz} was found negligible relative to the method of measurement the material constants c_1, c_2, p_1, p_2 and c_1'', c_2'', p_1'', p_2'' from the two types of tests are comparable.

The values of the four material constants as determined from Uniaxial Tension test results are:

$$c_1 = 130 \qquad c_2 = 5.15$$

$$p_1 = 98 \qquad p_2 = 6.00$$

The corresponding material constants as determined from the Simple Shear test results are:

$$c_1'' = 150 \qquad c_2'' = 4.40$$

$$p_1'' = 108 \qquad p_2'' = 5.15$$

A comparison of these material constants as obtained from the two types of tests shows that they are quite close, considering the experimental limitations involved in the study. The stress-strain expressions from these two types of tests show that there are at least four material constants independent of time and temperature. These expressions when used to predict strains in an Axial Compression test gave reasonably good results for small strains up to 0.4 percent only as observed in the previous section. For strains greater than 0.4 percent, it appears that a different deformation mechanism is operating in compression as compared to tension tests. However, it must be recognized that pure compression was probably not achieved in the test performed and that the measurements made were less than ideal.

The existence of at least four material constants, independent of time and temperature, as obtained from two different types of tests in

this study, gives a promising line of approach to testing bituminous mixtures quantitatively.

As stated in the Outline of the Investigation, the purpose of the study was to derive the independent stress-strain relationships which are necessary to render a two-dimensional system of the sheet-asphalt mixture solvable. This has been achieved with the three independent stress-strain expressions obtained from relevant experimental data, which, with the two equations of motion in two dimensions give a set of five independent equations containing five unknowns as follows:

$$\frac{\partial \sigma_z}{\partial z} + \frac{\partial \tau_{yz}}{\partial y} = Z + m\frac{\partial^2 w}{\partial t^2} \quad \text{.....(i)}$$

$$\frac{\partial \tau_{yz}}{\partial z} + \frac{\partial \sigma_y}{\partial y} = m\frac{\partial^2 v}{\partial t^2} \quad \text{.....(ii)}$$

$$\sigma_z = \left(\frac{T}{c_1}\right)^{-c_2} - \left(\frac{T}{p_1}\right)^{-p_2} \frac{\frac{\partial w}{\partial z}}{t\frac{\partial^2 w}{\partial t\,\partial z}}$$

$$= \left(\frac{T}{c_1'}\right)^{-c_2'} - \left(\frac{T}{p_1'}\right)^{-p_2'} \frac{\frac{\partial v}{\partial y}}{t\frac{\partial^2 v}{\partial t\,\partial y}} \quad \text{.....(iii)}$$

$$\sigma_y = \left(\frac{T}{c_1}\right)^{-c_2} - \left(\frac{T}{p_1}\right)^{-p_2} \frac{\frac{\partial v}{\partial y}}{t\frac{\partial^2 v}{\partial t\,\partial y}}$$

$$= \left(\frac{T}{c_1'}\right)^{-c_2'} - \left(\frac{T}{p_1'}\right)^{-p_2'} \frac{\frac{\partial w}{\partial z}}{t\frac{\partial^2 w}{\partial t\,\partial z}} \quad \text{.....(iv)}$$

$$\tau_{yz} = \left(\frac{T}{c_1''}\right)^{-c_2''} - \left(\frac{T}{p_1''}\right)^{-p_2''} \frac{\frac{\partial w}{\partial y} + \frac{\partial v}{\partial z}}{t\left(\frac{\partial^2 w}{\partial t\,\partial y} + \frac{\partial^2 v}{\partial t\,\partial z}\right)} \quad \text{...(v)}$$

Knowing the boundary conditions imposed on the material, the above five equations may solve the two-dimensional deformable system mathematically. It has to be recognized, however, that the three stress-strain expressions obtained from experimental data are valid only for the range of temperatures and stress levels for which the material was tested in this study. Similar expressions can be found for wider application by extending the experimental work along lines suggested in "Suggestions for Further Research."

CONCLUSIONS

The following conclusions have been drawn from the experimental data obtained for the sheet-asphalt mixture, within the range of temperatures and stress-levels for which it was tested in this investigation:

1. Three independent stress-strain relationships exist as functions of time and temperature which together with the two-dimensional equations of motion give a system of five equations containing five unknowns.

2. There exist four basic material constants independent of time and temperature as opposed to the usual modulus of elasticity and Poisson's ratio constants assumed in elastic theory. These four basic material constants exist in the tensile stress-axial strain expression derived from Uniaxial Tension test results and also in the shear stress-shear strain expression derived from Simple Shear test results. From the fact that the magnitude of the material constants as determined from two different types of tests, performed for a number of different conditions of time and temperature, were quite close to each other, it can be concluded that these material constants are independent of the type of test. As the results from Axial Compression tests corresponded reasonably well with those predicted from Uniaxial Tension test results for strains less than about 0.4 percent, it can be concluded that the derived expressions hold for both tension and compression of the material for

very small strains.

SUGGESTIONS FOR FURTHER RESEARCH

This study was based on a new approach to the problem of understanding and predicting the deformation characteristics of bituminous mixtures, but was restricted only to a sheet-asphalt mixture tested within a limited range of temperatures and stress levels.

Since the investigation appears to be quite fruitful, it would be worthwhile investigating the effect of mixture variables on the material constants as evaluated in this study. Also, it would be interesting to test other bituminous mixtures which are not as homogeneous and isotropic in nature as the sheet-asphalt mixture selected for this study.

It is important to extend this study to a wider range of temperatures and stress levels. At very low temperatures and under very low stresses, the deformations being too small to be measured adequately with an accuracy of 0.00005 inches, the use of Tuckerman optical strain gages which can read up to 2×10^{-6} in. deformation and of base length 1 inch is recommended, both for longitudinal as well as lateral deformations. A rectangular cross-section of the specimen is more desirable for use with optical strain gages, compared to a circular cross-section as used in this study. For higher temperatures, more than 100°F or so, the Tuckerman optical strain gage has a tendency to penetrate into the specimen and its use therefore is not recommended for high temperatures. A suitable method for higher temperatures seems to be the "grid method". If a grid consisting of 100 lines or more per inch, at right angles, is

printed on a specimen, pictures of the deforming specimen can be taken at frequent intervals of time and deformations read from the pictures. Although the accuracy of the grid technique is not as high as that of the optical strain gage, it has the advantage of having an almost unlimited range of deformations. Also, the relative deformations of stone and the bituminous matrix may be studied by the grid technique.

The use of the expressions relating stress to strain as functions of time and temperature and material constants, as obtained from this laboratory study, can be extended to predicting and verifying the deformations of bituminous mixtures in the field.

LIST OF REFERENCES

1. Burmister, D. M., The Theory of Stresses and Displacements in Layered Systems and Applications to the Design of Airport Runways, Proceedings, Highway Research Board, Vol. 23, 1943.

2. van der Poel, C., Road Asphalt, Building Materials, Their Elasticity and Inelasticity, M. Reiner, Chapter IX, Part C, 1954.

3. Kuhn, S. H. and Rigden, P. J., Measurement of Visco-elastic Properties of Bitumens under Dynamic Loading, Proceedings, Highway Research Board, Vol. 38, 1959.

4. Brodnyan, J. G., Use of Rheological and other Data in Asphalt Engineering Problems, Rheological and Adhesion Characteristics of Asphalt, Highway Research Board Bulletin 192, 1958.

5. Love, A. E. H., A Treatise on the Mathematical Theory of Elasticity, Dover Publications, New York, P. 85, 1944.

6. Milburn, H. M., A Deformation Test for Asphaltic Mixtures, Proceedings, American Society for Testing Materials, Vol. 25, Part II, 1925.

7. Emmons, W. J. and Anderton, B. A., A Stability Test for Bituminous Paving Mixtures, Proceedings, American Society for Testing Materials, Vol. 25, Part II, 1925.

8. Kriege, H. F. and Gilbert, L. C., Some factors Affecting the Resistance of Bituminous Mixtures to Deformation under Moving Wheel Loads, Proceedings, Association of Asphalt Paving Technologists, Vol. 5, 1933.

9. Vokac, R., An Impact Test for Studying Characteristics of Asphalt Paving Mixtures, Proceedings, Association of Asphalt Paving Technologists, Vol. 6, 1935.

10. Vokac, R., Compression Testing of Asphalt Paving Mixtures, Proceedings, American Society for Testing Materials, Vol. 36, Part 2, 1936.

11. Lee, A. R. and Markwick, A. H. D., The Mechanical Properties of Bituminous Surfacing Materials Under Constant Stress, Journal, Society of Chemical Industry, London, Vol. 56, Part 1, 1937.

12. Lee, A. R., Warren, J. B. and Walters, D. B., The Flow Properties of Bituminous Materials, Journal, Institute of Petroleum, Vol. 26, No. 197, 1940.

13. Pfeiffer, J. Ph., Observations on the Mechanical Testing of Bituminous Road Materials, Journal, Society of Chemical Industry, Vol. 57, 1938.

14. Hillman, W. O. B., Bending Tests on Bituminous Mixtures, Public Roads, Vol. 21 (4), 1940.

15. Mack, C., Rheology of Bituminous Mixtures Relative to the Properties of Asphalts, Proceedings, Association of Asphalt Paving Technologists, Vol. 13, 1942.

16. Nijboer, L. W., The Determination of the Plastic Properties of Bitumen-Aggregate Mixtures and the Influence of Variations in the Composition of the Mix, Proceedings, Association of Asphalt Paving Technologists, Vol. 16, 1947.

17. Nijboer, L. W., Mechanical Stability of Bitumen-Aggregate Mixtures, Journal, Society of Chemical Industry, London, Vol. 67 (6), 1948.

18. Mack, C., A Quantitative Approach to the Measurement of the Bearing Strength of Road Surfaces, Proceedings, Association of Asphalt Paving Technologists, Vol. 17, 1947.

19. van der Poel, C., A General System Describing the Visco-elastic Properties of Bitumens and Its Relation to Routine Test Data, Journal of Applied Chemistry, No. 4, May, 1954.

20. Nijboer, L. W., Mechanical Properties of Asphalt Materials and Structural Design of Asphalt Roads, Proceedings, Highway Research Board, Vol. 33, 1954.

21. Mack, C., The Deformation Mechanism and Bearing Strength of Bituminous Pavements, Proceedings, Association of Asphalt Paving Technologists, Vol. 23, 1954.

22. Mack, C., Bearing Strength Determination on Bituminous Pavements by the Methods of Constant Rate of Loading or Deformation, Proceedings, Highway Research Board, Vol. 36, 1957.

23. Wood, L. E., The Stress-Deformation Characteristics of Asphaltic Mixtures under Various Conditions of Loading, Ph.D. Thesis, submitted to the Faculty of Purdue University, August, 1956.

24. McLaughlin, J. F., The Load-Carrying Characteristics of a Bituminous Concrete Resurfacing Mixture, Ph.D. Thesis, submitted to the Faculty of Purdue University, January, 1957.

25. Goetz, W. H., McLaughlin, J. F. and Wood, L. E., Load-Deformation Characteristics of Bituminous Mixtures Under Various Conditions of Loading, Proceedings, Association of Asphalt Paving Technologists, Vol. 26, 1957.

26. Wood, L. E. and Goetz, W. H., Rheological Characteristics of a

Sand-Asphalt Mixture, Proceedings, Association of Asphalt Paving Technologists, Vol. 28, 1959.

27. Secor, K. E. and Monismith, C. L., Analysis of Triaxial Test Data on Asphalt Concrete Using Visco-elastic Principles, Proceedings, Highway Research Board, Vol. 40, 1961.

28. Secor, K. E. and Monismith, C. L., Visco-elastic Properties of Asphalt Concrete, Proceedings, Highway Research Board, Vol. 41, 1962.

29. Hargett, E. R. and Johnson, E. E., Strength Properties of Bituminous Concrete Tested in Tension and Compression, Proceedings, Highway Research Board, 1961.

30. Krokosky, E. M., The Rheological Properties of Asphalt/Aggregate Compositions, Ph.D. Thesis, submitted at the Massachusetts Institute of Technology, August, 1962.

31. Pister, K. E. and Monismith, C. L., Analysis of Visco-elastic Flexible Pavements, Flexible Pavement Design Studies, Highway Research Board Bulletin 269, 1960.

32. Monismith, C. L. and Secor, K. E., Visco-elastic Behavior of Asphalt Concrete Pavements, International Conference on the Structural Design of Asphalt Pavements, University of Michigan, Ann Arbor, August, 1962.

33. Papazian, H. S., The Response of Linear Visco-elastic Materials in the Frequency Domain with Emphasis on Asphaltic Concrete, International Conference on the Structural Design of Asphalt Pavements, University of Michigan, Ann Arbor, August, 1962.

34. Davis, E. F., Krokosky, E. M. and Tons, E., Stress Relaxation of Bituminous Concrete in Tension, MIT Report R63-40, Massachusetts Institute of Technology, August, 1963.

35. Huang, Y. H., The Deformation Characteristics of Sand-Bitumen Mixtures Under Constant Compressive Stresses, Paper presented at the Annual Meeting of the Association of Asphalt Paving Technologists, February, 1965.

36. Monismith, C. L., Secor, G. A. and Secor, K. E., Temperature Induced Stresses and Deformations in Asphalt Concrete, Paper presented at the Annual Meeting of the Association of Asphalt Paving Technologists, February, 1965.

37. Hetenyi, Miklos Imre, Handbook of Experimental Stress Analysis, New York, Wiley, 1950.

APPENDIX A

APPENDIX A

Equations of Motion in Two Dimensions

The equations of motion of a two-dimensional deformable system (5) are derived as follows:

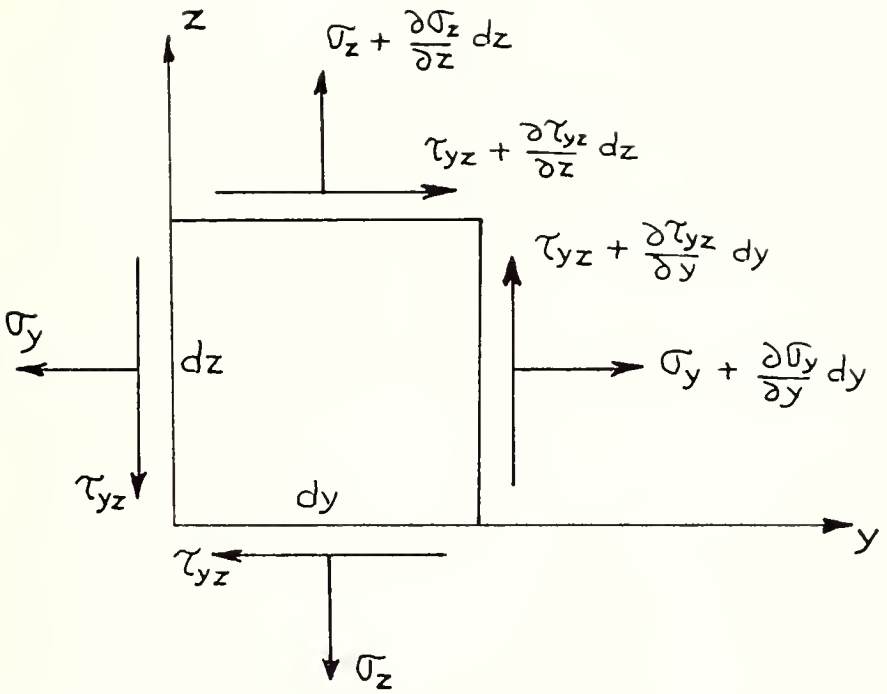

Consider a two-dimensional infinitesimal element of a homogeneous and isotropic body with dimensions dz and dy as shown in figure.

σ_z and σ_y are the normal stresses on this element in the yz plane passing through the origin, the variations in these stresses along the z and y directions being $\frac{\partial \sigma_z}{\partial z} dz$ and $\frac{\partial \sigma_y}{\partial y} dy$ respectively. Similarly τ_{yz} is the shear stress in the yz plane, its variations along the y and z directions being $\frac{\partial \tau_{yz}}{\partial y} dy$ and $\frac{\partial \tau_{yz}}{\partial z} dz$ respectively. Besides these stresses

acting on the element, consider the body forces like gravity and inertia forces Z and Y acting in the z and y directions respectively, per unit volume of material, taking unit dimension at right angles to paper.

If the element is in motion, having displacements w and v in the z and y directions respectively in time t, we have according to the Newton's second law of motion,

Sum of forces in z direction, $\Sigma F_z = m' \frac{\partial^2 w}{\partial t^2}$ = mass x acceleration

Sum of forces in y direction, $\Sigma F_y = m' \frac{\partial^2 v}{\partial t^2}$ = mass x acceleration

where m' is the mass of the material in element, with unit dimension at right angles to paper.

Resolving all forces acting on the element along the z and y directions respectively, we get:

$$\Sigma F_z = \frac{\partial \sigma_z}{\partial z} dz\,dy + \frac{\partial \tau_{zy}}{\partial y} dy\,dz - Z\,dy\,dz = m' \frac{\partial^2 w}{\partial t^2}$$

$$\Sigma F_y = \frac{\partial \tau_{zy}}{\partial z} dy\,dz + \frac{\partial \sigma_y}{\partial y} dy\,dz - Y\,dy\,dz = m' \frac{\partial^2 v}{\partial t^2}$$

Dividing both sides of the equations by dydz which is the volume of the element having unit dimension at right angles to the paper, we get:

$$\frac{\partial \sigma_z}{\partial z} + \frac{\partial \tau_{zy}}{\partial y} = Z + m \frac{\partial^2 w}{\partial t^2}$$

$$\frac{\partial \tau_{zy}}{\partial z} + \frac{\partial \sigma_y}{\partial y} = Y + m \frac{\partial^2 v}{\partial t^2}$$

where Z and Y are the body forces per unit volume of the material in z and y directions respectively, and m is the mass per unit volume of material.

Z = unit weight of the material acting vertically down.

$Y = 0$, there being no body forces in the y direction.

Hence the equations of motion for a two-dimensional deformable system reduce to:

$$\frac{\partial \sigma_z}{\partial z} + \frac{\partial \tau_{yz}}{\partial y} = Z + m \frac{\partial^2 w}{\partial t^2} \quad \ldots\ldots\ldots (i)$$

$$\frac{\partial \tau_{yz}}{\partial z} + \frac{\partial \sigma_y}{\partial y} = m \frac{\partial^2 v}{\partial t^2} \quad \ldots\ldots\ldots (ii)$$

APPENDIX B

APPENDIX B

Uniaxial Tension Tests

Preparation of Specimens

The procedure used for making cylindrical specimens, 2 inches in diameter and 4 inches high for the Uniaxial Tension tests was as follows:

The split mold was oiled inside with a very thin film of lubricating oil and assembled. This assembled mold together with the cylindrical plungers, mixing bowl, mixing spoon and tamping rod were placed in the upper shelf of the oven at a temperature of 400°F. The molds are shown in Figure 2.

The different fractions of aggregate were proportioned according to the gradation given in Table 4, Appendix D. The total quantity of aggregate taken was such that, together with the required asphalt cement, the resulting quantity of the mixture would give a specimen of the required size having a unit weight of 140 lbs./cft. or 2.24 gms./cc. The aggregate was put in a pan inside an oven and heated to a temperature of 350°F for about four hours before mixing it with asphalt.

More than the calculated quantity of 60-70 pen. asphalt cement required for a single specimen was taken out of the can of asphalt by means of hot spatula and placed in the oven at a temperature of 290°F for about 45 minutes. The exact calculated amount was then poured into the heated aggregate.

Mixing of the required quantities of heated aggregate and heated

asphalt cement was done by hand with a heated mixing spoon for a period of two minutes.

One of the heated plungers was removed from the oven, split rings placed around it, and the heated split mold placed over it. The hot bituminous mixture from the mixing bowl was put in the mold with a heated spoon in three layers and each layer was tamped or rodded with 50 blows by a one-half inch diameter rod. When rodding was complete, the second heated plunger was fitted into the mold and this assembly was then placed in a hydraulic compaction device, see Figure 3. With the split rings in position a small seating load was applied, after which the split rings were removed and the load applied gradually until the compacted length of specimen reached the desired 4 inches. This was indicated by a pre-positioned dial indicator. After the desired height was reached, the load was maintained for two minutes. On releasing the load, the assembled mold with plungers was taken out of the compaction device and placed on an adjoining table.

The mold, with the upper plunger in position, was lifted off the lower plunger and placed on a flat surface. The bolts were taken out and the upper plunger gently pushed so as to make the specimen move a little distance. The specimen was thus made to rest on the flat surface and the mold around it removed.

After the specimen had cooled, it was weighed and measured for its dimensions.

Curing of Specimens

To avoid the effects of variable aging on the test results, each specimen was kept at room temperature for 36 hours, after which it was

placed in the constant temperature room at the temperature of test for 12 hours before starting the test. The capping of test specimens was done after about 24 hours after compaction.

Capping of Specimens

For the Uniaxial Tension test, each specimen had to be cemented to caps at its ends, as shown in Figure 4. The cementing process had to be very carefully done in order to ensure the vertical and horizontal alignment of the axes of specimen with the caps so that a uniform application of stress on the specimen would be obtained under test.

To make sure that the ends of the specimen were at right angles to its vertical axis, a split aligning block specially machined to suit the dimensions of the specimen, was used. The specimen was held within the tightened split block so that its axis was coincident with the vertical axis of the block. The upper end was then adequately sandpapered to make it perpendicular to the specimen axis. The ends of the specimen were then reversed and the other end treated in the same way.

To withstand the range of test temperatures and stress levels for the Uniaxial Tension tests, the following formulation of epoxy resins, developed by Davis, Krokosky and Tons (34) was used:

Epon (shell) Resin 828	55% by weight
Epon (shell) Resin 871	36% by weight
Diethyl Tri-Amine Curing Agent	9% by weight

The above formulation was found to have desirable properties of flexibility, provided by Epon Resin 871, the required strength, provided by Epon Resin 828, and a reasonable period of about 2 hours for setting provided by the curing agent.

While the epoxy was still in a semi-liquid state, and viscous enough not to flow readily over the specimen, the caps were placed in position over the ends of the specimen. The two parts of the split block machined to correspond to the configurations of the caps and the specimen were tightened over the assembled specimen. After about two hours, the two parts of the split block were removed. The specimen was then found to be secured to the caps by the set epoxy with its axis appropriately aligned with the caps.

The lower cap of the specimen was threaded on the outside to fit into the base plate of test apparatus with a recess correspondingly threaded on the inside to hold the bottom of the specimen fixed. The upper cap of the specimen was provided with a hole, machined exactly in the center of the cap and threaded on the inside to receive the swivel joint arrangement having its bottom correspondingly threaded on the outside. This is shown in the diagrammatic sketch in Figure 5.

A typical specimen finished in the manner described above is shown in Figure 4.

Testing of Specimens

The Uniaxial Tension tests were performed to obtain longitudinal and circumferential strains as functions of time, under constant stress, for different temperatures and stress levels.

A diagrammatic sketch of the set-up for the measurement of longitudinal and circumferential strains is shown in Figure 5 and a test in progress is shown in Figure 6.

The specimen was subjected to constant stress by a dead load (steel plates) transmitted by a thin steel cable passing over two pulleys. The

point C in Figure 5, the center of the circular recess threaded on the inside to receive the capped specimen, was very carefully determined by a plumb bob. The steel plate with the recess with center C was bolted down to the base plate so that there was no eccentricity within measurable limits in the application of tensile load to the specimen through the cable.

The prepared specimen with its bottom cap threaded on the outside was screwed into the recess with center C, correspondingly threaded on the inside, so that the specimen bottom was now fixed. The cable passing over the pulleys was connected to the top cap of the specimen by a swivel as shown in Figure 5, in order to ensure that the load being applied to the specimen was always vertical and in line with the axis of the specimen. The other end of the cable passed over the pulleys and terminated in a hook from which the dead load of steel plates could be hung.

Various strain measuring devices were investigated, as detailed in the outline of investigation; however, a simple mechanical device, consisting of pointers supported by minimum-friction hinges and penetrating into the specimen, was found most effective and therefore was adopted. This device is shown in Figures 5 and 6. It consists of a vertical column mounted on a steel plate with two pointers hinged to it exactly 1-inch apart. The hinges were made as frictionless as possible by being machined very smooth and oiled with a light oil periodically. The two pointers were of different lengths in order to facilitate the placing of dial indicators over them. The upper pointer was 3 1/4 inches long, with its pointed end penetrating into the specimen exactly 2 inches from the center of the hinge. At a distance of 1 inch

from the hinge, and away from the specimen, the deformation would be equal and opposite to one-half the deformation of the pointed end. The lower pointer was 4 1/4 inches long with the center of the hinge exactly 2 inches from the pointed end so that at a distance exactly 2 inches from the hinge, and away from the specimen, the deformation would be equal and opposite to the deformation of the pointed end. Each of the pointers was made 1/4 inch longer than desired so as to have a clearly marked line 1 or 2 inches away from the hinge, as the case might be, on which to put the extension of the dial indicator.

The points of the dial indicators were placed on the marked lines over the pointers, as shown in sketch. These dial indicators were held in clamps attached to a separate steel rod coming out of the same bottom steel plate which held the column supporting the pointers. Since the extension ends of the dial indicators exerted some force on the pointers, small counter-weights capable of sliding over the pointer, as shown in the sketch were used between the hinge and specimen to exactly counteract the force exerted by the dial indicators. Another dial indicator held by a clamp attached to the same vertical rod which held the clamps of the other two indicators was used with its extension-end touching the top cap of the specimen.

To measure the circumferential strain, or the decrease in the radius of the specimen (originally 1 inch), a dial indicator also was used. In this case, however, the extension end of the dial indicator in contact with the specimen was carefully machined to have a curved shape corresponding exactly to the curved surface of the specimen in order to minimize any penetration of this end into the specimen. The dial indicator with the curved-end extension was put directly in contact

with the surface at mid-height of the specimen with its axis at right angles to the vertical axis of the specimen. Thus, four dial indicators were placed in position, as shown in Figure 2, on one side of the axis of specimen. To minimize the errors in the measurement of deformations due to any possible eccentricity in the application of load, etc. four corresponding dial indicators were placed in the same fashion as described above symmetrically about the axis of specimen as shown in Figure 5.

Before loading the specimen, the pointers on both sides of the specimen axis were adjusted so that they were horizontal in position. This was done by the use of small studs over the hinge, as shown in Figure 6 so that they were penetrating the specimen appropriately and the dial indicators were showing constant readings. Similarly, the dial indicators placed in position to measure the change in radius were checked for no change in the readings due to penetration, etc.

A stop watch was started as soon as load was put on the hook of the free end of the cable. The axial and lateral deformations of the stressed specimen were recorded with time by reading the dial indicators. The dial indicator readings as observed at different intervals of time are shown on a typical data sheet in Figure 7.

The readings of the dial indicators touching the top cap of the specimen gave the total axial deformation of the specimen. Readings of indicators placed on the upper pointer gave one-half of the deformation of the pointed end, whereas the readings of the dial indicators on the lower pointers gave the total deformation at this point, while the readings on the dial indicators placed laterally gave the reduction in radius. A typical plot of the deformations at four points along the

axis of the specimen, at different times, is given in Figure 7. The axial strain was determined by finding the difference between the deformations recorded by the two pointers vertically 1-inch apart.

Simple Shear Tests

Preparation of Specimens

The specimens for Simple Shear tests were 4 x 2 x 1/4 inches in size made of the same composition of sheet asphalt and compacted to the same density as that of Uniaxial Tension test specimens. The mold shown in Figure 9 was used.

The procedure for the preparation of these specimens was the same as that for Uniaxial Tension test specimens with the following exceptions. As the quantity of aggregate required for a specimen was too small to be mixed effectively with asphalt, double the required quantities of aggregate and asphalt were mixed together. After mixing, half the amount of mixture was used for forming the specimen.

The specimen was allowed to cool in a horizontal position with half of the mold removed.

Curing of Specimens

To have results comparable with Uniaxial Tension test results, each specimen was cured for the same length of time and in the same way as for Uniaxial Tension test specimens.

Cementing of Specimens

To subject the 4 x 2 x 1/4 inch test specimen to uniform shear, one 4 x 2 inch face had to be kept fixed and the other face subjected to constant load. For this purpose, these faces had to be cemented to steel

plates. The steel plate to be fixed in position was 4 x 2 3/4 x 1/4 inch in size and had three holes at its lower end for bolting to the base plate. The steel plate to be subjected to constant load was 4 x 2 1/4 x 1/4 inch in size.

The cementing material used for this purpose was of the same formulation of epoxies and curing agent as used for cementing the Uniaxial Tension test specimens to the caps.

Care was taken to see that a uniform thin layer of cementing material was applied between the surface of specimen roughened by sandpaper, and the surface of steel plate in contact with it. That the two steel plates were cemented parallel to each other was checked by a hand level.

Testing of Specimens

The Simple Shear tests were performed to obtain shear strain vs. time curves under constant shear stress for different temperatures and shear stresses.

The diagrammatic sketch in Figure 10 shows how the specimen, cemented to the steel plates, was placed for the test. One face of the specimen was fixed in position by bolting the steel plate to which it was cemented to the steel base plate. The steel base plate was adjusted such that the center C of the movable steel plate was exactly vertically below the groove of the pulley over which the cable transmitting the load was to pass.

The dead load (steel plates) was transmitted by a cable to the movable plate through a swivel provided in a small steel block adjusted horizontally by two screws symmetrical about the center of swivel and screwed into the movable plate, as shown in Figure 10. Two dial indicators capable of

being read to 0.00005 inch were attached to the movable plate.

A stop-watch was started as soon as dead load was applied, and the deformation of the movable plate as recorded by the two dial indicators was observed with time.

A typical observation sheet is shown in Figure 12.

Axial Compression Tests

Preparation of Specimens

The hollow cylindrical specimens 4 inches high having 2-inch external and 1-inch internal diameters were made of the same composition of sheet asphalt and compacted to the same density as that of Uniaxial Tension and Simple Shear test specimens. The procedure for the preparation of these specimens was the same as that for Uniaxial Tension test specimens with the following modifications. The lower plunger for the mold was fitted with a steel rod 1-inch in diameter and 4 3/4 inches long. The upper plunger was fitted with a 1-inch thick circular steel plate having a 1-inch diameter hole in the center to receive the steel rod of the lower plunger. The molds and plungers are shown in Figure 13.

After compaction, the specimen was left resting on the lower plunger with the 1-inch diameter rod passing through it. After the specimen had cooled, the plunger was removed.

Curing of Specimens

To have results comparable with those of Uniaxial Tension and Simple Shear tests, the curing was done for the same length of time and in the same way as for the Uniaxial Tension and Simple Shear test specimens.

Testing of Specimens

The Axial Compression tests were performed on the hollow cylindrical specimens by applying a constant dead load through a lever system. From these tests, axial and circumferential strains were obtained as functions of time, for different temperatures and stress levels.

The diagrammatic sketch in Figure 14 shows the lever system for loading the specimen. Load was transmitted to the specimen through a swivel in the circular plate resting directly on the specimen.

To ensure axial loading, the hollow steel cylinder with the specimen on it rested on a steel block with a ball and socket in the center. This can be seen in Figure 14.

The measurements of axial as well as circumferential deformations on the outside surface of the specimen were carried out exactly in the same way as in the Uniaxial Tension tests. The measurements of deformations on the inside of the specimen at its mid-height has been explained in detail in the text. A typical data sheet is given in Figure 17.

For each combination of variables, at least two identical specimens were tested in the three series of tests described in this Appendix.

APPENDIX C

APPENDIX C

Derivation of Stress-Strain Expressions

It has been observed from the test data developed that the axial strain-time and circumferential strain-time relationships from Uniaxial Tension test results, and shear strain-time curves from Simple Shear test results are straight lines on log-log plots. Further, it was observed that a study of the change in slope of these strain-time curves, as a function of applied tensile or shear stress and temperature, appeared to be useful in developing stress-strain relationships. The development of pertinent stress-strain expressions is presented in this Appendix.

Derivation of Normal Tensile Stress-Axial Strain Relationship as Function of Time and Temperature

The general expression for a straight line relating to time on a log-log plot is:

$$\log \epsilon_z = \log K_1 + K_2 \log t \quad \ldots\ldots (a)$$

where ϵ_z = the axial strain at time t

K_2 = slope of the straight line portion of curve

K_1 = a constant taken as the axial strain at one minute.

Differentiating the above expression with respect to time t, we get:

$$\frac{1}{\epsilon_z}\frac{\partial \epsilon_z}{\partial t} = K_2 \cdot \frac{1}{t}$$

$$\text{or} \quad \frac{\dot{\epsilon}_z}{\epsilon_z} = \frac{K_2}{t} \quad \ldots\ldots\ldots\ldots\ldots (b)$$

where $\dot{\epsilon}_z = \frac{\partial \epsilon_z}{\partial t}$ = rate of strain.

In Figure 36, the applied stress is plotted against the reciprocal of slope. It was found that, at least for the range of applied stresses tested, the variation was linear for each temperature although the slopes of straight lines at these three temperatures varied considerably. Linearity was not found to extend to stresses lower and higher than the ones shown here. This is due to the following reasons:

Under very low stresses, the deformations being very small, the observations estimated to 0.00005 inch tend to be erratic. This can be seen in the low stress portion of the plots at all temperatures, for example in the circumferential strain vs. time plot at 100°F for a tensile stress of 0.75 psi (Figure 23). Also, the errors due to friction in the mechanical parts of the set up for transmitting the dead load to the specimen become increasingly prominent at lower stresses.

Under very high stresses, the deformations being large, the specimen starts developing cracks within a very short time after being loaded. As a consequence, the axial strain-time plot starts curving upward. This leaves the length of the straight line portion of the plot too short to have its slope determined accurately. This can be seen in the axial strain-time plots at the highest stresses at all temperatures, for example at 100°F under a tensile stress of 2.45 psi, (Figure 20).

This development of stress-strain expressions, therefore, is limited only to the range of stresses applied at different temperatures in the investigation.

The equations of the straight lines, within the range, on the stress vs. reciprocal of slope plots are given as follows:

UNIAXIAL TENSION TEST RESULTS

$1/K_2$ vs. σ_z

$1/K_2$ = RECIPROCAL OF SLOPE OF AXIAL STRAIN vs. TIME LOG-LOG PLOT

σ_z = TENSILE STRESS IN PSI

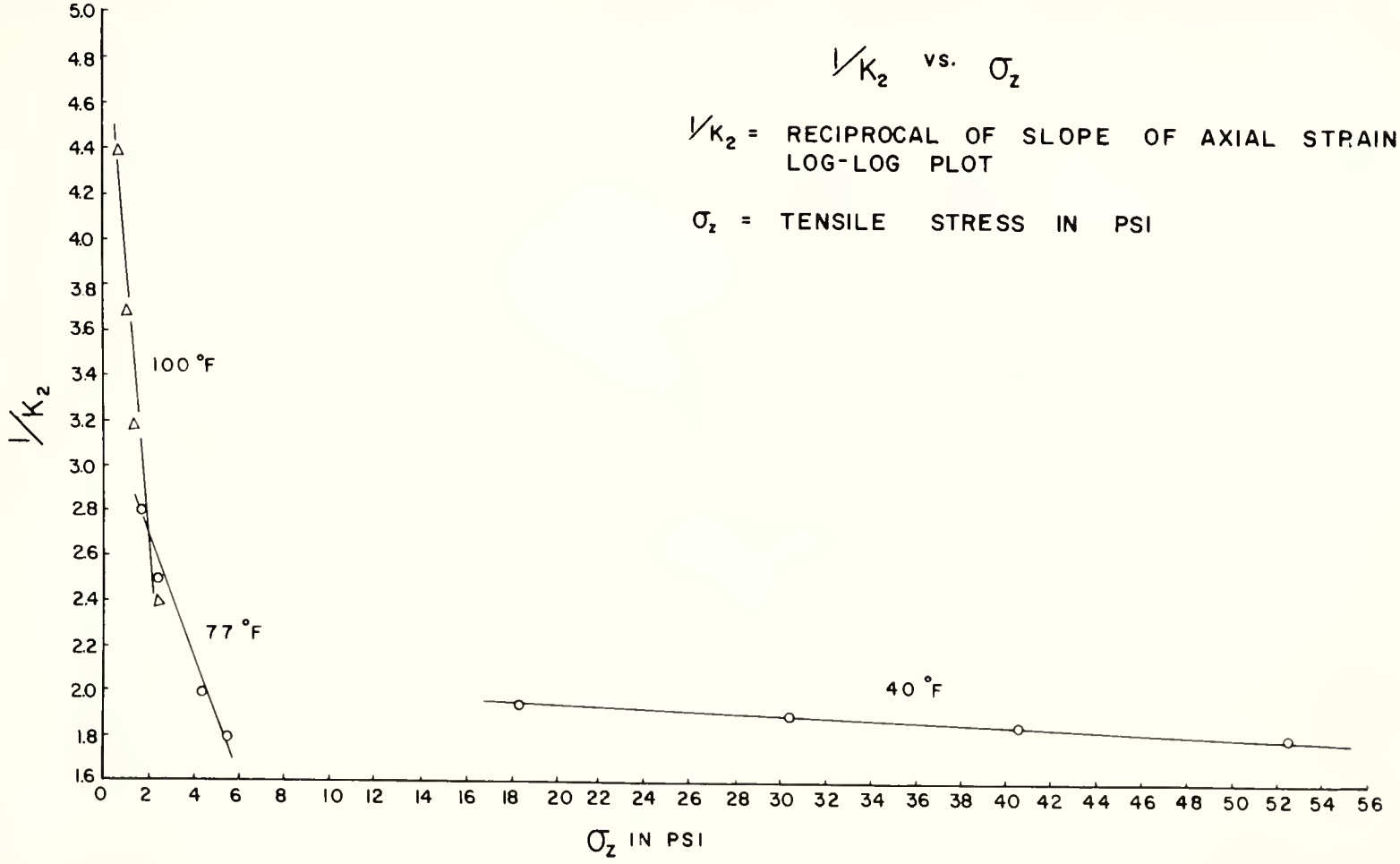

FIG. 36

$$\frac{1}{k_2} = I(T) - S(T)\sigma_z$$

or, $$\sigma_z = \frac{I(T)}{S(T)} - \frac{1}{S(T)} \cdot \frac{1}{k_2} \quad \ldots\ldots\ldots\ldots\ldots \quad (c)$$

where σ_z = applied tensile stress,

$I(T)$ = intercept, as a function of temperature (T) on the $1/k_2$ axis, and

$S(T)$ = slope, as a function of temperature (T) of the straight line.

The ratio $I(T)/S(T)$ of the straight lines for the temperatures $40^{\circ}F$, $77^{\circ}F$ and $100^{\circ}F$ are plotted against temperature on log-log scales (Figure 37). It was found that a straight line relationship existed on the log-log plots that could be expressed as:

$$T = c_1 [I(T)/S(T)]^{C_2} \quad \ldots\ldots\ldots \quad (d)$$

i.e., $$\log T = \log c_1 + C_2 \log [I(T)/S(T)]$$

For $I(T)/S(T) = 1$, we have

$$\log T = \log c_1 \text{ or } c_1 = T,$$

i.e., c_1 is a temperature in $^{\circ}F$ such that a constant tensile stress would satisfy the following expression:

$$\sigma_z = 1 - \frac{1}{[S(T)]_{T = c_1}} \times \frac{1}{k_2} .$$

C_2 is the slope of the straight line on the log-log plot of temperature T vs. $I(T)/S(T)$.

UNIAXIAL TENSION TEST RESULTS

LOG $[I(T)/S(T)]$ vs. LOG(T)

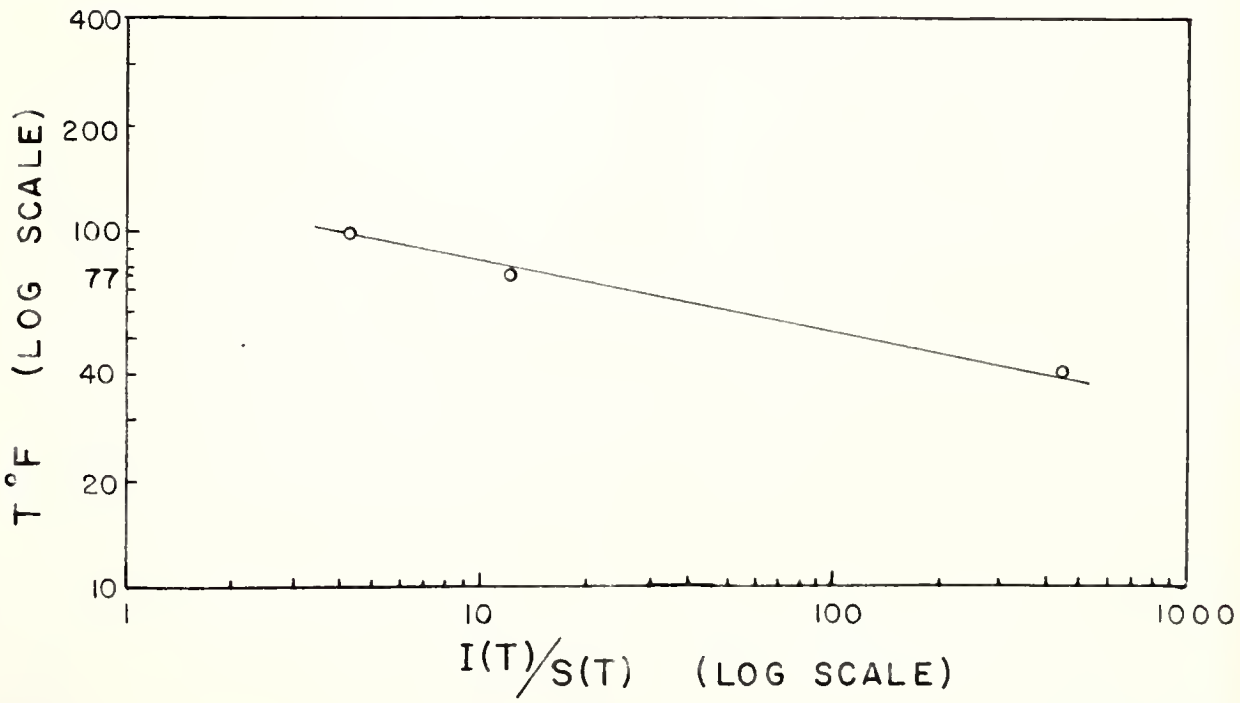

FIG. 37

The reciprocals of slopes of the straight lines 1/S(T) for the temperatures 40°F, 77°F and 100°F are plotted against temperature on log-log scales in Figure 38. It was found that a straight line relationship existed on the resulting log-log plot which could be expressed as:

$$T = p_1 \left[1/S(T)\right]^{P_2} \quad \ldots\ldots\ldots (e)$$

i.e., $\log T = \log p_1 - P_2 \log S(T)$

For $1/S(T) = 1.0$, we have $\log T = \log p_1$, therefore p_1 is the temperature T, at which the slope of the plot of $1/k_2$ vs. σ_z is 1 in 1 or 45°; i.e., $1/k_2 = \sigma_z$ in psi.

P_2 is the slope of the straight line on the log-log plot of temperature T vs. 1/S(T).

From equation (c), we have: $\sigma_z = \frac{I(T)}{S(T)} - \frac{1}{S(T)} \times \frac{1}{k_2}$

and from equation (b), $\frac{\dot{\epsilon}_z}{\epsilon_z} = \frac{k_2}{t}$

therefore, substituting the value of k_2 from (b) in (c), we get:

$$\sigma_z = \frac{I(T)}{S(T)} - \frac{1}{S(T)} \times \frac{\epsilon_z}{t\,\dot{\epsilon}_z} \quad \ldots\ldots\ldots (f)$$

From equation (d), $T = c_1 \left[\frac{I(T)}{S(T)}\right]^{C_2}$ or $\frac{I(T)}{S(T)} = \left[\frac{T}{c_1}\right]^{-c_2}$ where $c_2 = \frac{1}{C_2}$ and the negative sign given as the slope of the straight line is negative. From equation (e), $T = p_1 \left[\frac{1}{S(T)}\right]^{P_2}$ or $\frac{1}{S(T)} = \left[\frac{T}{p_1}\right]^{-P_2}$

where $p_2 = \frac{1}{P_2}$ and the negative sign given as the slope of the straight line is negative.

$$\therefore \quad \sigma_z = \left[\frac{T}{c_1}\right]^{-c_2} - \left[\frac{T}{p_1}\right]^{-P_2} \frac{\epsilon_z}{t\,\dot{\epsilon}_z}\,; \quad 40^\circ F \leq T \leq 100^\circ F. \quad \ldots\ldots\ldots (A)$$

UNIAXIAL TENSION TEST RESULTS

$\text{LOG}\left[1/S(T)\right]$ vs. LOG(T)

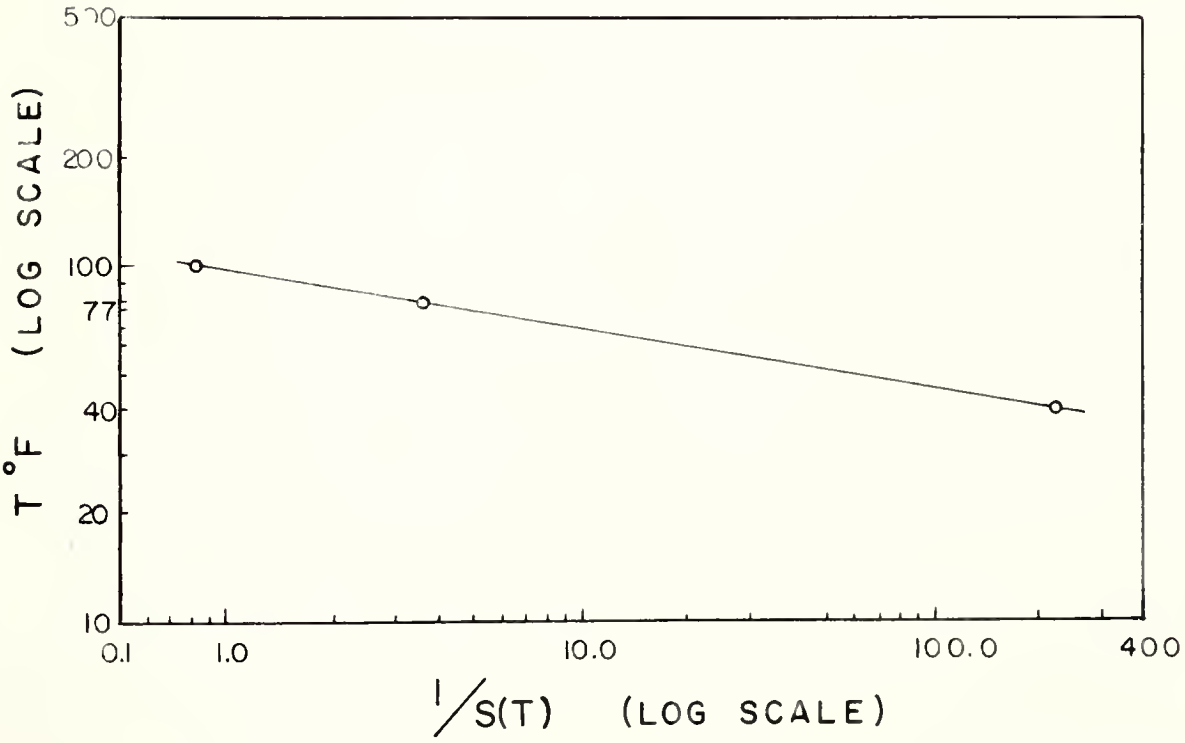

FIG. 38

The equation(A) gives a relationship between applied tensile stress and strain in the direction of applied stress, as a function of time, temperature, strain rate and the material constants c_1, c_2, p_1 and p_2. It is to be noted, however, that this relationship holds only for the range of test temperatures from $40^{\circ}F$ to $100^{\circ}F$ and for the range of deformations measured as discussed earlier.

The basic material constants c_1, c_2, p_1 and p_2 which are independent of time and temperature had numerical values for this mixture as explained below:

From Figure 36, $I(T)_{T = 40^{\circ}F} = 2.04$; $S(T)_{T = 40^{\circ}F} = \frac{1}{220}$

$I(T)_{T = 77^{\circ}F} = 3.25$; $S(T)_{T = 77^{\circ}F} = \frac{1}{3.7}$

$I(T)_{T = 100^{\circ}F} = 5.15$; $I(T)_{T = 100^{\circ}F} = \frac{1}{0.83}$

Thus the equation (c), viz. $\sigma_z = \frac{I(T)}{S(T)} - \frac{1}{S(T)} \times \frac{1}{K_2}$ for the three different temperatures is as follows:

At $40^{\circ}F$, $\sigma_z = 448.8 - 220 \times \frac{1}{k_2}$.

At $77^{\circ}F$, $\sigma_z = 11.925 - 3.7 \times \frac{1}{k_2}$.

At $100^{\circ}F$, $\sigma_z = 4.275 - 0.83 \times \frac{1}{k_2}$.

The log-log plot of T vs. $\frac{I(T)}{S(T)}$ and T vs. $1/S(T)$ are given in Figures 37 and 38, respectively; from these we find:

$c_1 = 130$, $c_2 = 5.15$

$p_1 = 98$, $p_2 = 6.00$ as the material constants,

giving the final stress-strain expression as:

$$\sigma_z = \left(\frac{T}{130}\right)^{-5.15} - \left(\frac{T}{98}\right)^{-6.00} \frac{\epsilon_z}{t\,\dot{\epsilon}_z} \quad ; \quad 40^\circ F \leq T \leq 100^\circ F$$

Derivation of Normal Tensile Stress--Circumferential Strain Relationship as Function of Time and Temperature

The derivations of expressions in this section follow exactly on the same lines as those for tensile stress and axial strain. Substituting circumferential strain ϵ_y for axial strain and replacing other symbols by their primes, the equations (a)' through (e)' corresponding to equations (a) through (e) and the determination of the numerical values of material constants follow:

$$\log \epsilon_y = \log K_1' + K_2' \log t \qquad \ldots (a)'$$

$$\frac{\dot{\epsilon}_y}{\epsilon_y} = \frac{K_2'}{t} \qquad \ldots (b)'$$

$$\sigma_z = \frac{I'(T)}{S'(T)} - \frac{1}{S'(T)} \cdot \frac{1}{K_2'} \qquad \ldots (c)'$$

$$T = C_1' \left[\frac{I'(T)}{S'(T)} \right]^{C_2'} \qquad \ldots (d)'$$

$$T = P_1' \left[S'(T) \right]^{-P_2'} \qquad \ldots (e)'$$

Substituting the expressions of K_2', $\frac{I'(T)}{S'(T)}$ and $S'(T)$ from (b)', (d)' and (e)' respectively, we get

$$\sigma_z = \left[\frac{T}{C_1'} \right]^{-C_2'} - \left[\frac{T}{P_1'} \right]^{-P_2'} \frac{\epsilon_y}{t\,\dot{\epsilon}_y}, \quad 40^\circ F \leq T \leq 100^\circ F$$

From Figure 39,

$$\left[I'(T) \right]_{T=40^\circ F} = 2.085 \; ; \; \left[S'(T) \right]_{T=40^\circ F} = \frac{1}{22.8}$$

$$\left[I'(T) \right]_{T=77^\circ F} = 2.435 \; ; \; \left[S'(T) \right]_{T=77^\circ F} = \frac{1}{19.2}$$

$$\left[I'(T) \right]_{T=100^\circ F} = 2.935 \; ; \; \left[S'(T) \right]_{T=100^\circ F} = \frac{1}{7.6}$$

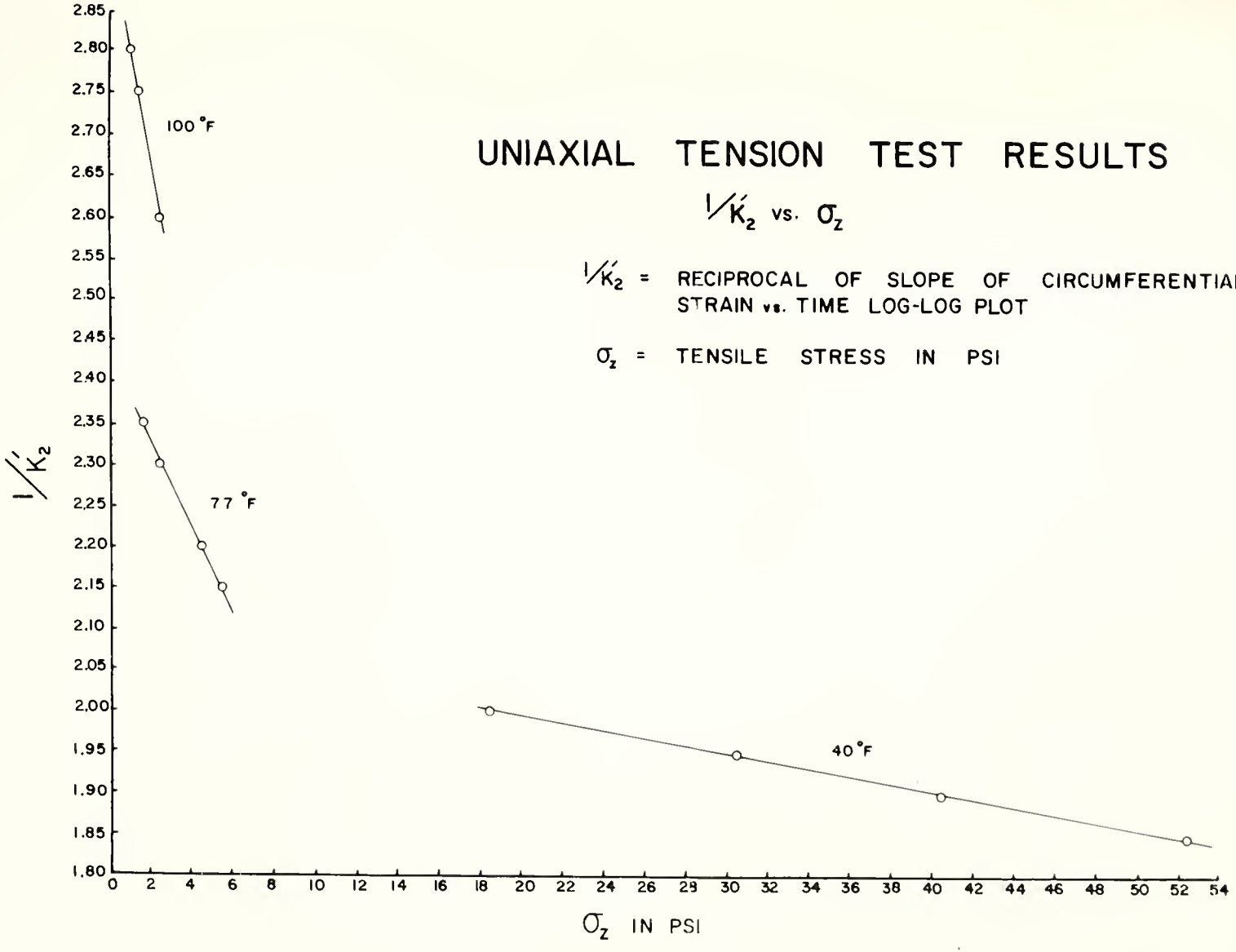
UNIAXIAL TENSION TEST RESULTS
1/K'2 vs. σz
1/K'2 = RECIPROCAL OF SLOPE OF CIRCUMFERENTIAL STRAIN vs. TIME LOG-LOG PLOT
σz = TENSILE STRESS IN PSI
100 °F
77 °F
40 °F
1/K'2
σz IN PSI
2.85
2.80
2.75
2.70
2.65
2.60
2.55
2.50
2.45
2.40
2.35
2.30
2.25
2.20
2.15
2.10
2.05
2.00
1.95
1.90
1.85
1.80
0 2 4 6 8 10 12 14 16 18 20 22 24 26 28 30 32 34 36 38 40 42 44 46 48 50 52 54

FIG. 39

UNIAXIAL TENSION TEST RESULTS

$$\text{LOG}\left[\dot{I}(T)/\dot{S}(T)\right] \text{ vs. } \text{LOG}(T)$$

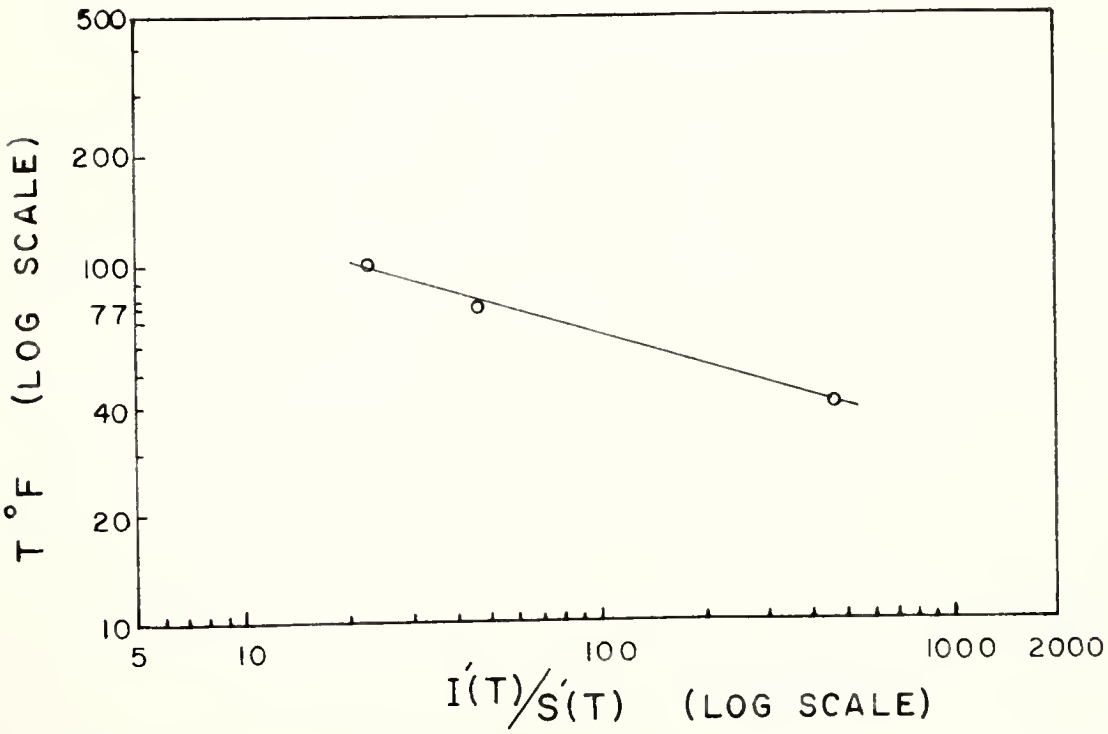

FIG. 40

UNIAXIAL TENSION TEST RESULTS

$$\text{LOG}\left[1/\acute{S}(T)\right] \quad \text{vs.} \quad \text{LOG}(T)$$

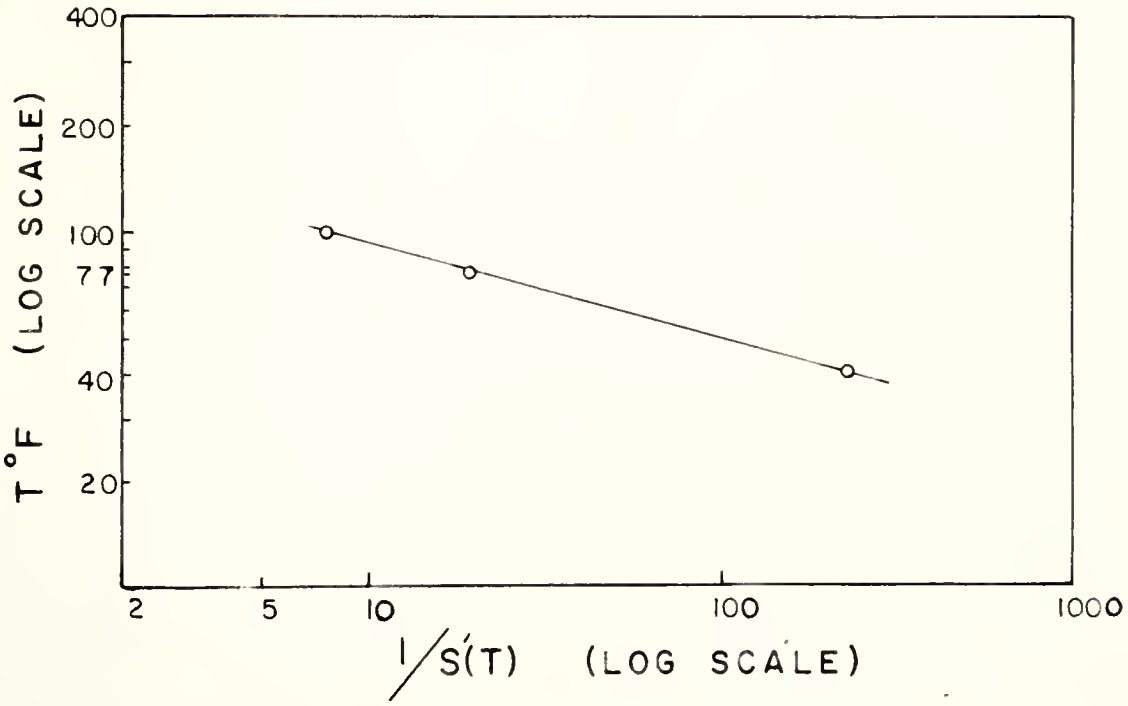

FIG. 41

Corresponding to equation (c)', we have the following equations at the three temperatures:

$$\sigma_z = 47.5 - 22.8 \frac{1}{K_2'} \qquad @ \ 40^\circ F$$

$$\sigma_z = 46.6 - 19.2 \cdot \frac{1}{K_2'} \qquad @ \ 77^\circ F$$

$$\sigma_z = 22.3 - 7.6 \cdot \frac{1}{K_2'} \qquad @ \ 100^\circ F$$

The log-log plots of T vs. $\frac{I'(T)}{S'(T)}$ and T vs. $\frac{1}{S'(T)}$ are given in Figures 40 and 41; from these we find:

$$c_1' = 250, \quad c_2' = 3.3$$

$$p_1' = 170, \quad p_2' = 3.6$$

as the material constants, giving the final stress-circumferential strain expression as:

$$\sigma_z = \left(\frac{T}{250}\right)^{-3.3} - \left(\frac{T}{170}\right)^{-3.6} \frac{\epsilon_y}{t\,\dot{\epsilon}_y} \; ; \; 40^\circ F \leq T \leq 100^\circ F$$

Derivation of Shear Stress--Shear Strain Relationship as Function of Time and Temperature

The derivations of expressions in this section also are based exactly on the same lines as those for tensile stress and axial strain. Substituting shear strain γ_{yz} for axial strain and replacing other symbols by their double primes having the same significance, the equations (a)'' through (e)'' corresponding to (a) through (e) and the determination of the numerical values of material constants follow:

$$\log \gamma_{yz} = \log K_1'' + K_2'' \log t$$

$$\frac{\gamma_{yz}}{\dot{\gamma}_{yz}} = \frac{t}{K_2''} \qquad \ldots\ldots\ldots\ldots (b)''$$

Applied shear stress $$\tau_{zy} = \frac{I''(T)}{S''(T)} - \frac{1}{S''(T)} \cdot \frac{1}{K_2''} \qquad \ldots (c)''$$

$$T = c_1'' \left[\frac{I''(T)}{S''(T)}\right]^{c_2''} \qquad \ldots\ldots (d)''$$

$$T = p_1'' \left[\frac{1}{S''(T)}\right]^{p_2''} \qquad \ldots\ldots (e)''$$

Substituting the expressions of K_2'', $\frac{I''(T)}{S''(T)}$ and $S''(T)$ from the equations (b)'', (d)'', and (e)'' respectively, we get

$$\tau_{zy} = \left[\frac{T}{c_1''}\right]^{-c_2''} - \left[\frac{T}{p_1''}\right]^{-p_2''} \frac{\gamma_{zy}}{t\,\dot{\gamma}_{zy}}\,; \quad 40^\circ F \leq T \leq 100^\circ F$$

From Figure 42,

$I''(T)_{T = 40^\circ F} = 2.58$ $\qquad$ $S''(T)_{T = 40^\circ F} = \frac{1}{135}$

$I''(T)_{T = 77^\circ F} = 3.20$ $\qquad$ $S''(T)_{T = 77^\circ F} = \frac{1}{9.3}$

$I''(T)_{T = 100^\circ F} = 4.85$ $\qquad$ $S''(T)_{T = 100^\circ F} = \frac{1}{1.15}$

Corresponding to equation (c)'', we have the following equations at the three temperatures:

$$\tau_{zy} = 34.8 - 135 \cdot \frac{1}{K_2''} \qquad @\ 40^\circ F$$

$$\tau_{zy} = 29.76 - 9.3 \frac{1}{K_2''} \qquad @\ 77^\circ F$$

$$\tau_{zy} = 5.58 - 1.15 \frac{1}{K_2''} \qquad @\ 100^\circ F$$

The log-log plots of T vs. $\frac{I''(T)}{S''(T)}$ and T vs. $\frac{1}{S''(T)}$ are given in Figures 43 and 44, and from these we find:

$c_1'' = 150$, $c_2'' = 4.40$, $p_1'' = 108$, $p_2'' = 5.00$ as the material

SIMPLE SHEAR TEST RESULTS

$1/K_2''$ vs. σ_z

$1/K_2''$ = RECIPROCAL OF SLOPE OF SHEAR STRAIN vs. TIME LOG-LOG PLOT

σ_z = SHEAR STRESS IN PSI

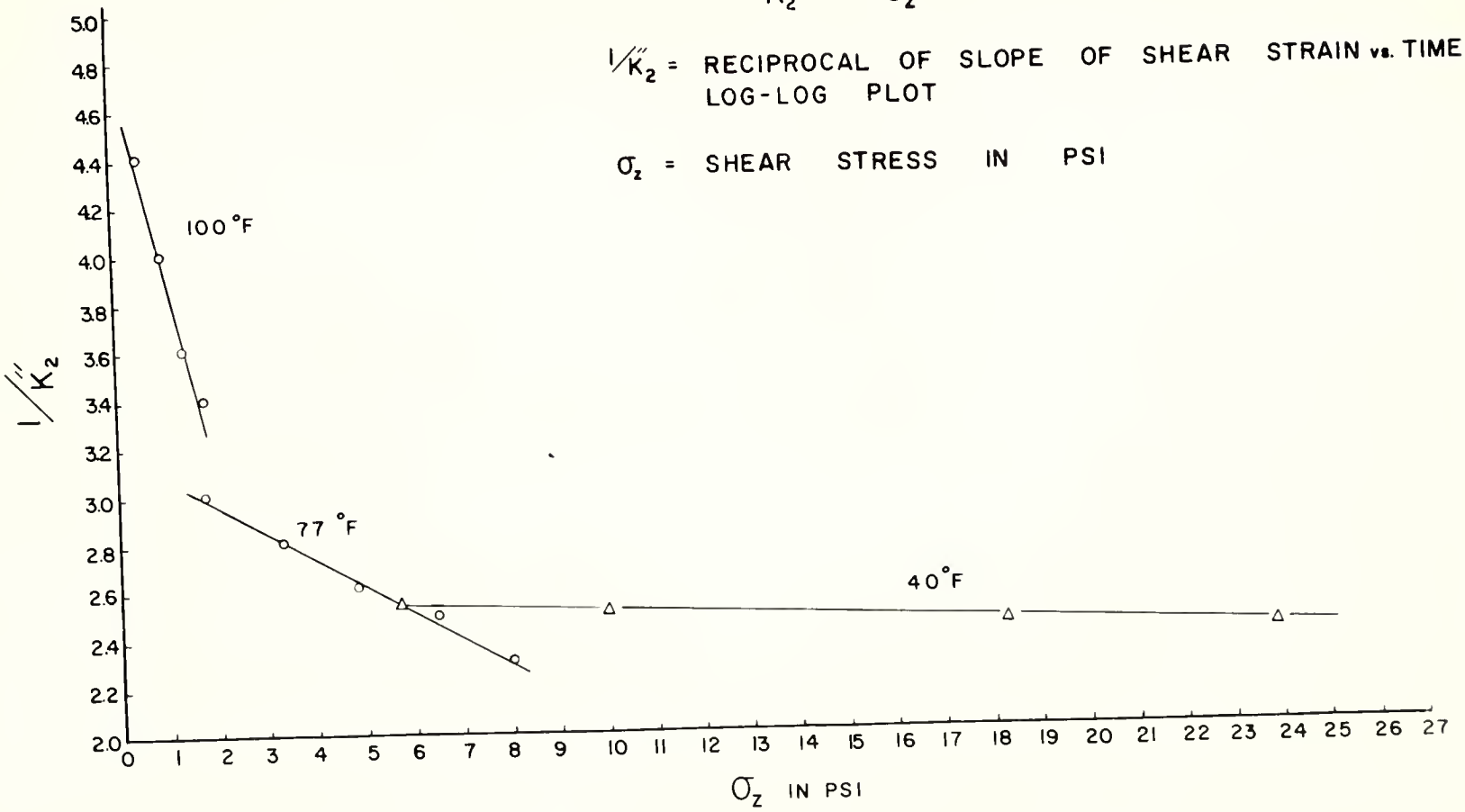

FIG. 42

SIMPLE SHEAR TEST RESULTS

$$\text{LOG}\left[\overline{I}''(T)/\overline{S}''(T)\right] \text{ vs. } \text{LOG}(T)$$

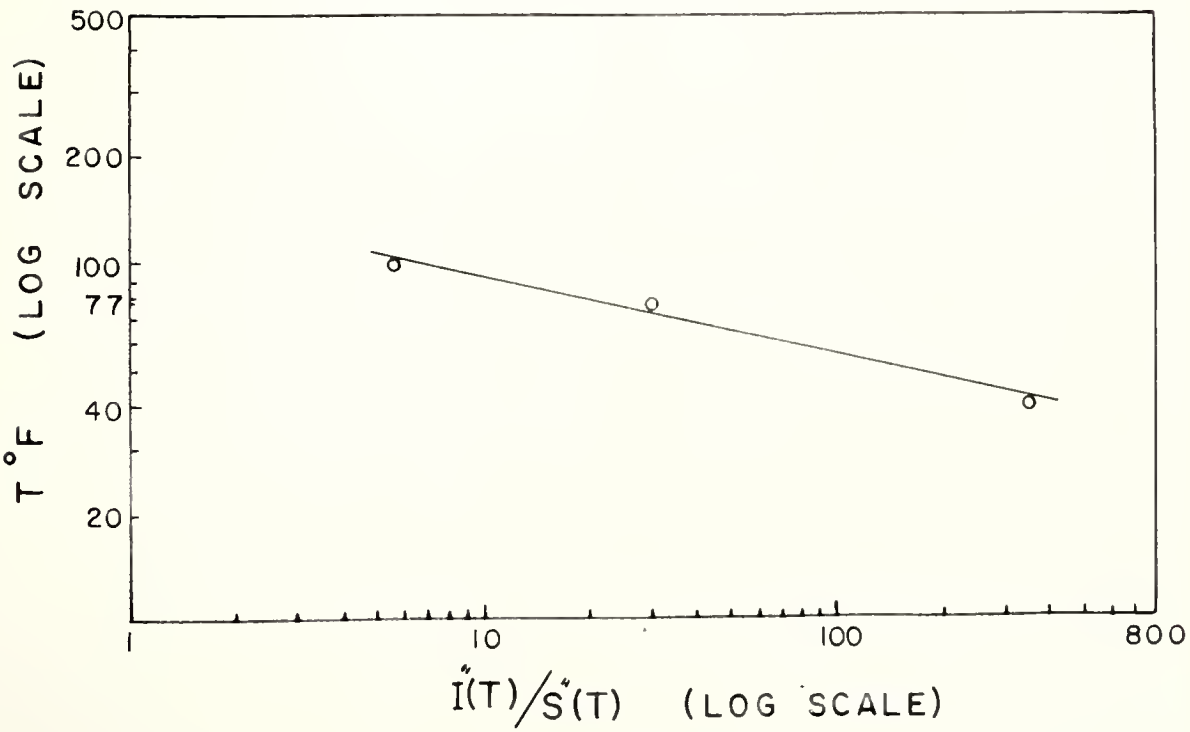

FIG. 43

SIMPLE SHEAR TEST RESULTS

$\text{LOG}\left[1/\bar{S}''(T)\right]$ vs. $\text{LOG}(T)$

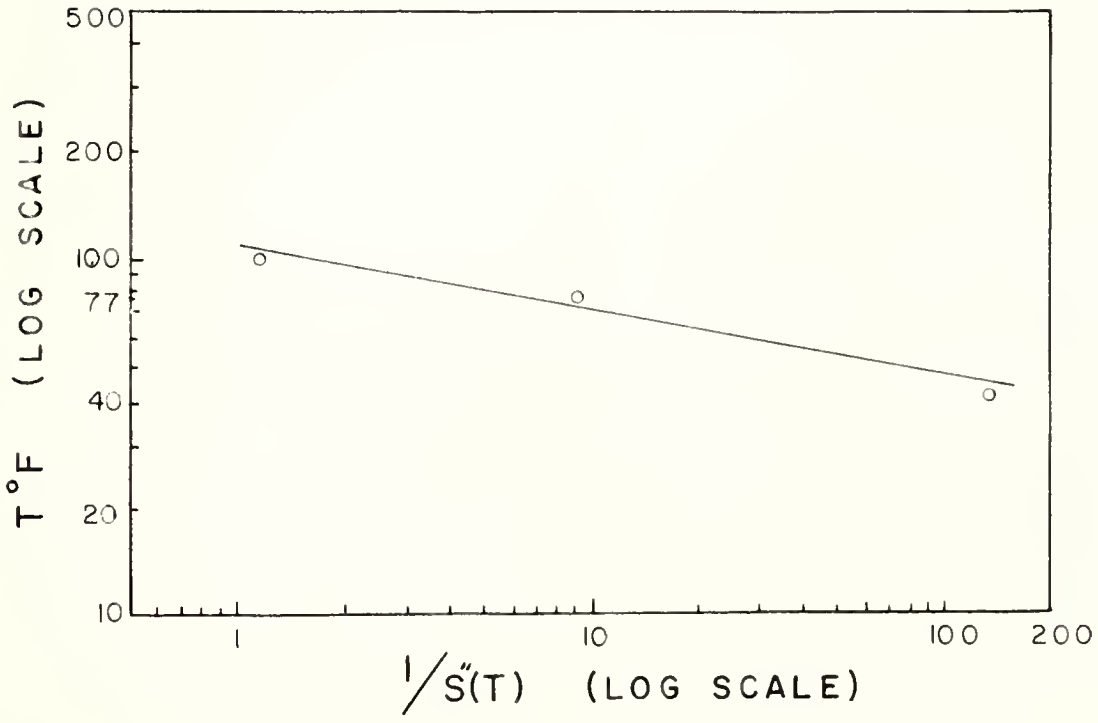

FIG. 44

constants, giving the final expression as:

$$\tau_{zy} = \left[\frac{T}{150}\right]^{-4.40} - \left[\frac{T}{108}\right]^{-5.00} \cdot \frac{\gamma_{zy}}{t\dot{\gamma}_{zy}}; \; 40^{\circ}F \leq T \leq 100^{\circ}F$$

APPENDIX D

APPENDIX D

Materials Used in the Study

A sheet-asphalt mixture was used for all the tests performed in this study. The test properties of the asphalt cement and aggregates used in the mixture are given in this Appendix.

Asphalt Cement

The asphalt cement used throughout the study was an asphalt cement of ASTM penetration grade 60-70 supplied by the Texas Co. Several standard ASTM tests were performed on this asphalt cement in the laboratory. The results of these tests are as follows:

Penetration (100 gms., 5 sec., 77°F)	64
Specific Gravity at 77°F	1.024
Ductility (77°F, 5 cm./sec.), cm.	100+
Softening Point, °F	122

The asphalt content used in the mixture was 9.0 percent by weight of aggregage as found optimum by Wood (23).

Aggregates

The sand used in the study was a local natural material obtained from a river terrace. The sieve analysis of the chosen gradation is given in Table 4 and graphically presented in Figure 45. This gradation meets the requirements of ASTM 1663-59T, tentative specifications for Hot-mixed, Hot-laid Asphalt Paving Mixtures. The physical properties of

the sand are as follows:

Bulk specific gravity	2.54
Apparent specific gravity	2.67
Percent absorption	2.04

Since the local sand was deficient in -200 material, a limestone filler with an apparent specific gravity of 2.73 was blended with the sand.

Table 4

Sieve Analysis of Sheet-Asphalt Mixture (Percent by Weight)

Sieve		Grading
Passing	Retained	
No. 8	No. 16	7
No. 16	No. 30	17
No. 30	No. 40	8
No. 40	No. 50	9
No. 50	No. 100	27
No. 100	No. 200	15
No. 200		17

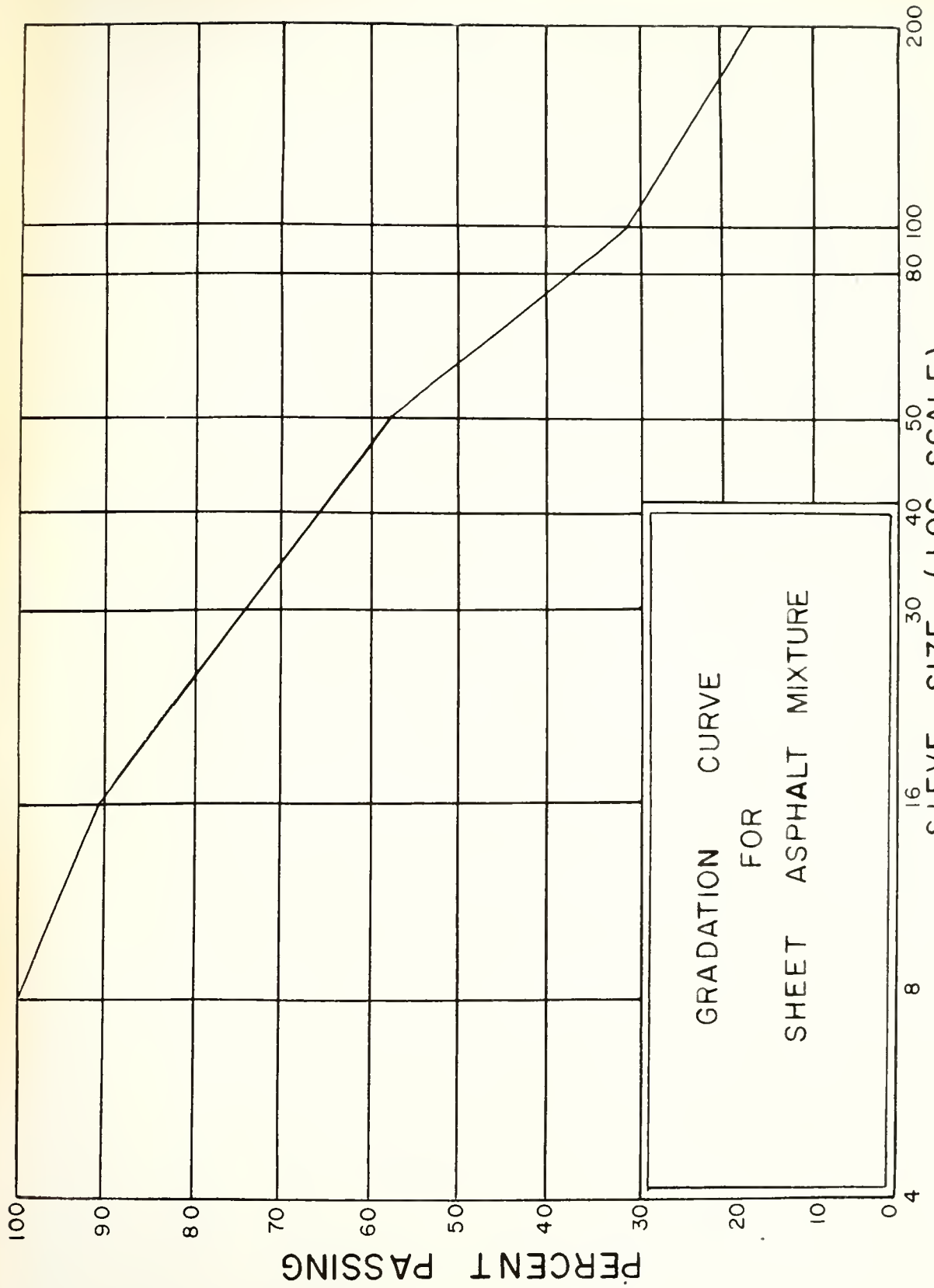
PERCENT PASSING
100
90
80
70
60
50
40
30
20
10
0
4
8
16
30
40
50
80
100
200
SIEVE SIZE (LOG SCALE)
GRADATION CURVE
FOR
SHEET ASPHALT MIXTURE

FIG. 45

V I T A

VITA

Narindra Bansi Lal was born November 21, 1933 at Simla, India. He had his early school and college education in New Delhi, India. After obtaining a Bachelor's Degree with honours in Mathematics from St. Stephen's College, Delhi, he joined the Indian Institute of Technology, Kharagpur, in 1955 to study Civil Engineering. He was awarded a Bachelor's Degree in Civil Engineering with first class honours in June 1959.

In September 1959, he joined the faculty of Punjab Engineering College Chandigarh, India teaching undergraduate Civil Engineering courses. Simultaneously, he took courses for a Master's Degree in Highway Engineering in the same college. He was declared to have passed his M. Sc. (Eng.) with distinction both in the course work and the thesis that he submitted to Punjab University in 1962. His Master's Degree Thesis was titled, " A Comparative Study of the Marshall and Hveem Methods of Design for Dense-Graded Bituminous Paving Mixtures."

It was in the capacity of an Assistant Professor of Civil Engineering that he was sanctioned leave of absence by Government of Punjab, India, to study for a Doctor's Degree at Purdue in September 1962. He worked as a part-time teaching assistant during his first academic year at Purdue, while taking graduate courses. Thereafter, he worked as a Graduate Research Assistant under the Joint Highway Research Project, Purdue University.

He is a bachelor and is a citizen of India.